SAHC

Structural Analysis of Historic Reinforced Concrete Building - Fuchs' Cafe in Prague.

Bradley John Scheuer

Czech Republic | 2020

ADVANCED MASTERS IN STRUCTURAL ANALYSIS OF MONUMENTS AND HISTORICAL CONSTRUCTIONS

Master's Thesis

Bradley John Scheuer

Structural Analysis of Historic Reinforced Concrete Building - Fuchs' Cafe in Prague.

University of Minho

Czech Republic | 2020

DECLARATION

Name: Bradley John Scheuer

Email: brad.scheuer@gmail.com

Title of the Msc Dissertation: Structural Analysis of Historic Reinforced Concrete Building - Fuchs' Cafe in Prague

Supervisor(s): Petr Kabele, Cristiana Lara Nuñes

Year: 2020

I hereby declare that all information in this document has been obtained and presented in accordance with academic rules and ethical conduct. I also declare that, as required by these rules and conduct, I have fully cited and referenced all material and results that are not original to this work.

I hereby declare that the MSc Consortium responsible for the Advanced Masters in Structural Analysis of Monuments and Historical Constructions is allowed to store and make available electronically the present MSc Dissertation.

University: CZECH TECHNICAL UNIVERSITY IN PRAGUE

Date: 12 July 2020

Signature: _____

This page is left blank on purpose.

To the memory of my sister Ella Scheuer

Whose passion for exploration and design is a constant inspiration

This page is left blank on purpose.

ACKNOWLEDGEMENTS

Thank you -

to my advisor Petr Kabele for your generosity, positive attitude and your ability to take a complex subject and make it seem easy.

to my advisor Cristiana Lara Nuñes for your support and quick reflexes whenever I needed an article or report.

to all consortium professors, lecturers and laboratory technicians for sharing your knowledge, passion and enthusiasm for conservation and personal growth.

to my fellow SAHC students, I have learned so much from all of you. You are all amazing.

to the consortium for the scholarship, which made is easier to quit my job and move a quarter of the way around the world responsibly.

to my aunt and uncle, Suzie and Walter, for always encouraging and backing my education.

to my in-laws, Julie, Stu and Mimi, for putting a roof over my head and putting up with me

to my sister, Kristian, who believed in my potential and never doubted my abilities.

to my parents, Diane and Jack, for the unwavering encouragement and push to be the best I could be.

to my wife, Katie, without you, none of this would have been possible. You make me want to become a better person every single day.

This page is left blank on purpose.

ABSTRACT

Fuchs Café, part of the Štvanice Island former winter stadium facility, in Prague, Czech Republic is an important cultural building woven into the fabric of the city. The Functionalist building represents a modern architectural style that was popular in Czechoslovakia when the building was built in the early 1930s. In a city with as rich a history as Prague, modern buildings are often overlooked for heritage conservation efforts as there is a perception that they do not possess the same value as ancient buildings. This building is worthy of conservation not just because of its architectural uniquity but because it has been a part of a sport culture identity of not just the city but the entire country.

In order to verify the condition and safety of the building, the structure has been inspected in recent years in various ways to identify its composition and material properties as well as damage. The information from these surveys has been used to create a 3D structural finite element model. From there, the current national building code, Eurocode, was used to determine the loads and perform the static evaluation on the structural elements of known composition. The results of the analysis prove that the level of safety of each member and the building as a whole is adequate.

Damage to the building does exist in some locations. The extent of the repairs depends on the severity of the damage, much of which is not known at this time. Therefore, different levels of repairs are detailed as well as testing methods for more information acquisition. Finally, a maintenance regime is discussed to minimize future deterioration, allowing for many more generations to enjoy and appreciate this distinct building.

This page is left blank on purpose.

Obsah

Fuchsova kavárna, která je součástí bývalého zimního stadionu na pražské Štvanici, je významnou kulturní stavbou začleněnou do struktury metropole. Tato funkcionalistická budova je představitelem moderního architektonického stylu, který se v Československu hojně užíval ve 30. letech 20. století, tedy v době, kdy byla budova postavena. Ve městě s tak bohatou historií, jako má Praha, jsou při úsilí o zachování kulturního dědictví moderní budovy často přehlíženy v důsledku dojmu, že jejich hodnota nedosahuje významu historických staveb. Tato budova si však zasluhuje, aby byla zachována nejen pro svou architektonickou výjimečnost, ale i proto, že tvoří součást sportovně kulturní identity města Prahy i celé země.

Za účelem ověření stavu a bezpečnosti proběhly na budově v nedávných letech různé průzkumné práce, při kterých byla zaměřena její kompozice, byly určeny vlastnosti použitých stavebních materiálů a bylo popsáno poškození konstrukcí. Informace z těchto průzkumů byly použity pro vytvoření 3D modelu budovy pro statickou analýzu metodou konečných prvků. Současné stavební normy, Eurocode, byly použity pro určení zatížení a provedení statického posouzení vybraných konstrukčních prvků, jejichž skladba byla známa. Výsledky analýzy ukazují, že jednotlivé prvky i budova jako celek mají dostatečnou úroveň bezpečnosti.

Na některých místech je konstrukce budovy porušená. Rozsah oprav závisí na závažnosti poruch, která však aktuálně v mnoha případech není známa. Proto jsou navrženy různé úrovně oprav i experimentální metody pro získání více informací. V závěru je diskutován režim údržby, jehož cílem je minimalizace další degradace tak, aby tato význačná budova mohla být zdrojem potěšení a předmětem obdivu pro mnoho budoucích generací.

This page is left blank on purpose.

TABLE OF CONTENTS

TABLE OF FIGURES AND TABLES

CZECH TECHNICAL UNIVERSITY IN PRAGUE
Faculty of Civil Engineering
Thákurova 7, 166 29 Prague 6, Czech Republic

DIPLOMA THESIS ASSIGNMENT FORM

I. PERSONAL AND STUDY DATA

Surname: Scheuer Name: Bradley Personal number: 497051

Assigning Department: Department of Mechanics

Study programme: Civil Engineering

Branch of study: Advanced Masters in Structural Analysis of Monuments and Historical Construction

II. DIPLOMA THESIS DATA

Diploma Thesis (DT) title: Structural Analysis of Historic Reinforced Concrete Building - Fuchs' Cafe in Prague

Diploma Thesis title in English: see above

Instructions for writing the thesis:
Perform a review of available documents describing the history, present state and future use of the building. Construct a structural computational model of the building using a suitable finite element software. Using the model, clarify the concept of the bearing system and identify critical locations and members which should be subjected to further inspection and probing. For members where sufficient information is available, evaluate the structural capacity.
Note: The thesis work will likely have to be carried out remotely due to travel restrictions arising frm the COVID-19 pandemic situation.

List of recommended literature:
Plans, historical documentation, and material parameters about the case study
- C. Croft, S. Macdonald, Eds. (2019) Concrete: Case Studies in Conservation Practice, Los Angeles: The Getty Conservation Institute
- H.A. Heinemann (2013) Historic Concrete: From Concrete Repair to Concrete Conservation. PhD thesis, Delft: TUD
- ICOMOS (2014) Madrid document: Approaches for the Conservation of 20th-cent. Architectural Heritage, 2nd Ed., ISC20C

Name of Diploma Thesis Supervisor: Petr Kabele, Cristiana Lara Nuñes

DT assignment date: April 6, 2020 DT submission date: July 12, 2020

DT Supervisor's signature Head of Department's signature

III. ASSIGNMENT RECEIPT

I declare that I am obliged to write the Diploma Thesis on my own, without anyone's assistance, except for provided consultations. The list of references, other sources and consultants' names must be stated in the Diploma Thesis and in referencing I must abide by the CTU methodological manual "How to Write University Final Theses" and the CTU methodological instruction "On the Observation of Ethical Principles in the Preparation of University Final Theses".

Assignment receipt date Student's name

1. INTRODUCTION

1.1. Outline and Motivation

Fuchs Cafe Building is a structure situated on Štvanice Island on the Vltava River in central Prague, Czech Republic. Built in 1932, the cafe was part of a larger national winter stadium complex, since demolished. It was conceptualized in the then en vogue Functionalist architectural style. It holds a special place in the city's history with the sports and architectural roots that run through it. In its current state, it is a shadow of its former self with years of neglect and damage. In a city with a deep architectural history, modern structures do not have the same societal appreciation as the medieval ones, but that does not make modern buildings any less valuable. The purpose of this discussion is to provide an analysis to verify the viability of the reuse of the building.

Historic conservation is a nuanced science. A deep understanding of the building is necessary, not just the dimensions. It begins with the method of design used in the era in which the building was built. What understanding of building mechanics did the designer have and what approaches were used to detail it? It is also important to understand the how the building was constructed. This entails the technology available at the time and the skill level of the laborer. The materials used on the building must be identified, which relates to strength and reliability of the materials along with the compatibility of possible interventions. It is vital to create and understanding of the structure in terms of its original intended behavior and possible damage within it.

Finally, any interventions conducted on the historic structure must be respectful to the authenticity of the of the building. Contemporary designers must not leave their mark on the building. This also includes creating solutions compatible with the building. Any interventions performed must use materials and techniques that are as similar to the original as possible. The key is to provide the least invasive method for any work done on the building.

1.2. Background

This Structural Analysis of Monuments and Historical Constructions thesis was developed as a joint project between the Czech Technical University and the Institute of Theoretical and Applied Mechanics of the Czech Academy of Sciences. The subject matter was developed within the scope of the CONSECH20 international project, meaning CONSErvation of 20th-century concrete Cultural Heritage in urban changing environments which is supported by the Joint Programme Initiative on Cultural Heritage. The project aims at raising awareness of the modern concrete structures while providing new approaches to conservation.

1.3. Objectives

The objectives of this thesis are to provide a complete structural analytical assessment of the building. This will be done in terms of the main structural bearing system stability and safety, capacity assessment of individual members and damage assessment of the building in its current state. This will be achieved by reviewing existing documentation available, building a structural analytical finite element model and reviewing modern code requirements.

The results will include safety levels of the structure and its elements, strengthening techniques to remediate any insufficient capacity, repair techniques for any damage or deterioration of the building.

2. HISTORY

2.1. History of the Area

The Vltava River has helped shape Prague since prehistory. Much of daily life centered around the river, with trade and transportation. As Prague grew in population and importance, people from all over the area would travel to the town to share in its prosperity [1]. As a path across the hydrological impediment was sought, a ford was used in the area of Štvanice Island (figure 2.1). Many people traveled across this island in the outlying area of the town but few spent time there. This changed in the 16th century when it began its recreational existence with the increased popularity of a shooting range [2]. The name of the island, Štvanice, meaning the hunt or chase, came into being in later centuries with the increased popularity of animal flights taking place for the pleasure of spectators.

Figure 2.1 - Map of Prague in 1923 [3]

Later during the industrial revolution, Prague began to expand in area and population [1]. Suburbs began to form, and a transit network developed. With this growth, new neighborhoods enveloped the island on each side of the river, and free space became a premium. During this time, inns, dance halls and theaters were built on the island though none lasted too long [2]. Many of the developments and infrastructure were in precarious positions with the frequent floods occurring seemingly every few years. New major infrastructure took root on the island starting with the Negrelli, then Karlin, Viaduct, built between 1846 and 1849 (figure 2.2). This was the first rail bridge over the Vltava river, connecting Prague to other European cities like Dresden. Later between 1908 and 1910 the Hlávek Bridge opened the island to an increasing amount of vehicular and pedestrian traffic. At the same time, locks and weirs were installed on the river to regulate level and flow.

Figure 2.2: Negrelli Viaduct [4]

During this time of tangible growth of the city and economy, a Czech character was also forming and strengthening. Control of the region constantly changed over the preceding centuries, between Germany, Austria and Bohemia. Each of these changes brought about outside cultural, political and language influences. However, with the increasing significance of the working class and the economic industrial power of Prague, the Czech identity started to shape life. In the early 19th century the Czech National Revival began pushing for autonomy and independence, specifically with the Czech language [1]. This revolutionary movement peaked in the 1848 rebellion, however, within 20 years, due to surrounding European revolutions, the Austro-Hungarian empire took hold of the city and region. This once again took control of the region away from Prague and to Vienna. This reign concluded with World War I and the formation of Czechoslovakia in 1918 at the Treaty of Saint-Germain-en-Laye. The interwar was a time of relative prosperity in Prague.

Figure 2.3 - 1920 Czechoslovakia Olympic Bronze Medal Winning Team [5]

The growth of the Czech identity coincided with the rebirth of organized international sport in the form of the Olympics. The Kingdom of Bohemia, with which Prague was a part of until 1918, first participated in the Olympics in 1900 and won four Olympic medals between 1900 and 1912, then Czechoslovakia went on to win 22 medals between 1920 and 1928 [6]. Bohemia and Czechoslovakia flourished in many of the games but the sport that caught the national interest was ice hockey. In the 1910's and 1920's the national teams won six gold medals in the European Championship while Czechoslovakia won a noteworthy bronze medal in the 1920 Summer Olympics the first time hockey was played in the Olympics (figure 2.3). This success and growth of the sport led to a need for a permanent home for the team with artificial ice so that play could occur irrespective of the weather [2]. Prague as the capital and largest city in Czechoslovakia was the natural choice. To spur the development of the stadium, in a meeting in 1923 it was decided that two years later, Prague would host the European Championships. However, this plan did not materialize in the allotted time and a natural ice surface was planned for the tournament. The week of the games, the weather warmed unexpectedly and the rink in Prague became unplayable, forcing a move to the town of Starý Smokovec in Slovakia [7]. Even in the colder area of the country the playing surface was melting so one final move was made to a picturesque resort lake in the mountains, Štrbské Pleso (see figure 2.4). The Czechoslovakian team went on to win the tournament.

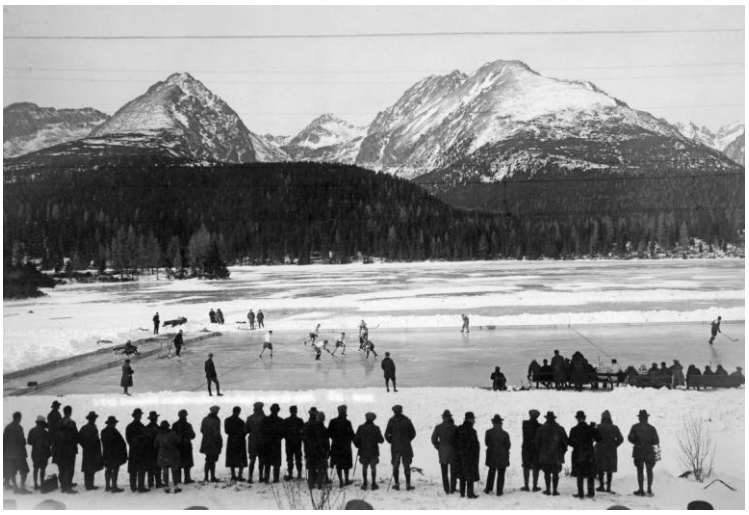

Figure 2.4: 1925 European Championship [7]

After the war, a new way of thinking affected many countries across Europe, involving philosophy, art and architecture. Different variations of Modernist movements occurred everywhere, embodied in the Functionalist movement in Czechoslovakia. This style was seen all over the country with architects commingling and influencing each other. One of the earliest and largest functionalist buildings in Prague was the Veletržní palác or Fair-Trade Palace (figure 2.5) conceived in 1924 and completed in 1928 for the Czechoslovak decennial [8]. A young architect named Josef Fuchs won the tender and created the eight story white plaster and glass facade, notable for its open airy interior and long sharp lines. This helped launch Fuchs into the forefront of the fledgling architectural movement. Fuchs was in his early thirties when he won this major project, so it led to a young architect, in a new style, creating an impact on the budding republic.

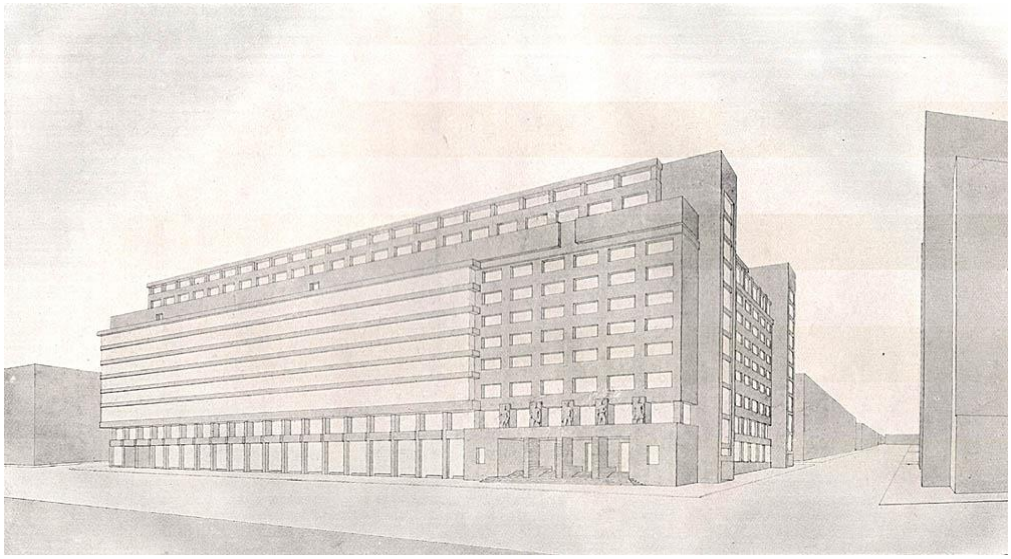

Figure 2.5 - Veletržní palác [8]

2.2. Conception and Construction of the Café Building

In 1927, Josef Fuchs was commissioned to start work on the new stadium, including the ice rink, wooden grandstands and a main building that would function as a restaurant and locker rooms [2]. The funding for the endeavor came from the city and from Prague Sample Fair (PVV). During this time, Prague had agreed to host the 1932 European Championships, and not wanting more embarrassment, pushed progress forward. By early 1929 the exact site on Štvanice Island was selected and the PVV's role increased, becoming responsible for construction. Fuchs' design progressed and by early 1930 construction began on the building. The design of the building contained many of the Functionalist attributes that were popular at the time. Large and long windows were planned, similar to contemporary curtain walls (figure 2.6).

Figure 2.6: Original Fuchs Design [9]

Reinforced concrete was the nature material choice for the new building style. The use of concrete was steadily increasing throughout the era with higher material reliability. Cementitious materials were first used in Crete around 2000 B.C. [10] The material was further developed by the Romans who added pozzolans to the concrete to increase its durability. The next major development arrived in 1854 with the patent of a metal reinforced concrete, by W. B. Wilkinson of England who patented a concrete floor system that utilized steel rope reinforcement in ribs between plaster forms. In France shortly after, François Coignet gained recognition for publishing a book with illustrative details of reinforced concrete [10]. This culminated with Coignet building the first all reinforced concrete house in Paris in 1862 (see figure 2.7) [11]. This new system expanded the ways concrete could be used, pushing the capabilities of the material. Many of the early developments centered around the geometry of the reinforcing bars, creatively using different shaped bars and bends. The first widely distributed concrete code was developed at the University of Stuttgart, distributed to the Kingdom of Prussia in 1904 [10]. By the 1930s, concrete was a common building material in Czechoslovakia ever increasing material reliability.

Figure 2.7 – First Reinforced Concrete House in Paris, Home of François Coignet [12]

By November of that year, Fuchs predicted that the ice rink would be operational within a few months. Soon after, disaster struck as the great depression impacted the PVV economic viability; construction halted and Fuchs went unpaid. At that moment, the foundations and core structural elements were completed, including columns, beams and some floor slabs (figure 2.8). For a brief time, no progress on the building was made.

Figure 2.8: Construction Progress after Shutdown [9]

After months of inactivity, the city felt an urgency to continue construction since the European Championships were still scheduled to occur and the city didn't want to be embarrassed again. A new company was formed to take over responsibility for the project, Brno Engineering Works. With this new organization going forward, a new architect was brought on, Bohumil Steigenhofer [2]. Stiegenhofer was no stranger to Czechoslovak hockey, he was a player on the national team from 1926 through 1931 (figure 2.9) [13]. During his time he participated in the 1928 Olympics and won two medals, silver and gold, in European championships during that time. He was a young budding architect with a focus in economical design and connections to the hockey community. He took responsibility for the stadium from this point until the last game was played at the stadium.

Figure 2.9: Bohumil Steigenhofer at a young age [13]

Since there were many new financial restrictions on the construction, changes to the design had to be made [2]. This was to reduce the cost of labor, materials and certain details. There are minimal drawings available from the original design, but it is known that some of the defining Functionalist features had to be compromised and adapted to the new economical limitations. Since much of the core structural elements of the building were already completed or underway, most of the changes involved the shell of the building and interior. In all, the quality of the materials was diminished, and the skilled labor was withdrawn to fit within the confines of the new budget.

With construction of the rink itself completed, the first game was played in 1931, even though the surrounding infrastructure was incomplete. However, by January 1932 construction lagged behind schedule enough that it was clear that the city could not host the tournament two months later. Berlin Germany was selected as the alternate location. Later that year, construction was finally completed, and a ceremonial first match was played against France in November. At long last, in March of 1933, the city was able to show off its revolutionary new stadium to Europe, on the first artificial ice rink in central Europe (figure 2.10). From then on, the cafe and Štvanice Island were an integral part of life in Prague and Czechoslovakia.

Figure 2.10: Latvian Team at the 1933 World Hockey Championship at Štvanice Stadium, Café in background [14]

2.3. Lifespan of the Building

For the next 30 years, the site hosted events of all types including hockey, figure skating, basketball, volleyball games among other local events [2]. The highlight of these was the 1947 Ice Hockey world Championships (figure 2.11), where the host country finally won the tournament in front of the home crowd on its home ice, beating the United States to clinch the title in the round robin tournament [15]. In 1956 a roof over the rink was built to protect the game and fans from the elements (figure 2.12). During these years, many superficial changes were made to the building such as the addition of awnings, railings and plaster. This did not change the usability of the structure, but it greatly affected the functionalist character.

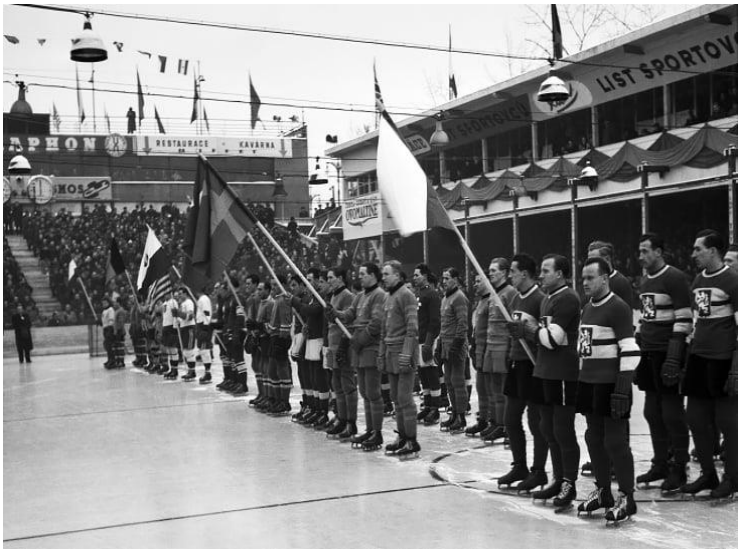

Figure 2.11: 1947 World Championship Ceremony at Štvanice [9]

Figure 2.12: Stadium Roof [9]

In 1962 a new larger modern stadium opened less than one and a half kilometers away from Štvanice Stadium. All major sporting events transferred to the Holesovice location which spelled the beginning of the end of Štvanice Stadium. The rink was still used for recreational community and routine maintenance was not conducted as thoroughly [2]. The stadium was repaired in 1968 while the cafe building was renovated in the 1970s. This work involved replacing plaster and infilling holes. By the late 1980s, the stadium was closed due to lack of use. The cafe building was declared a cultural monument in 1991 and placed on the cultural heritage list in 2000. The rink and surrounding area were damaged in a flood in 2002 but later that year, the rink reopened. Finally, in 2011 the stadium was demolished.

Figure 2.13: Current Exterior and Interior of Building, view from the northeast

Figure 2.13: Current Interior of Building from level 1NP

Not until 1997 did a new use come to the cafe building as a disco and bar. Since the area had an abandoned vibe, the disco became a hotspot for alternative culture. To further this idea, in 2007, major renovations were conducted. An additional balcony was added to mirror the original configuration, so that the performance space could be viewed from above from all angles (figure 2.13). Many of the long iconic windows were filled in to close off space behind the bar. Many of the original materials were covered and painted to create specific textures and an industrial atmosphere. In 2015 an extensive survey of the building where material samples were taken and concrete members were probed.

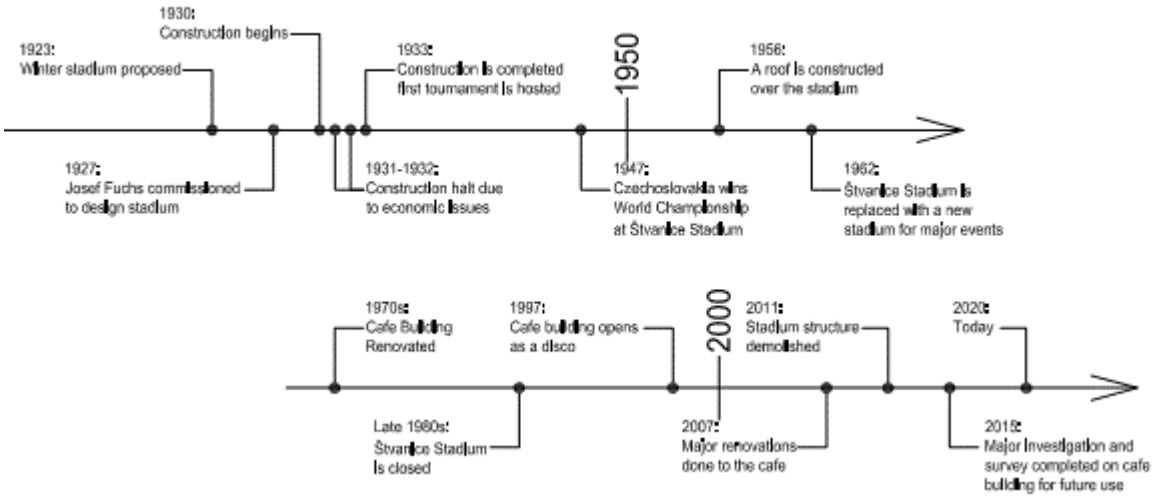

Figure 2.14: Graphical historical timeline

2.4. Future Use of the Building

The city of Prague has expressed interest in redeveloping the building back to its original state and function, a café and restaurant. The myriad of reports done in 2015 had a similar purpose, to investigate this return (figure 2.15). The idea is to embrace the modern architecture of the original building.

This work would include removing many of the added elements of the building that are not original. This includes major elements like the new balcony at level 2NP. Other structural elements to be removed include many of the window infills of various materials that have been added along the way. Then all décor and furniture currently in the building would be disposed of. The concept is to have just the original structure and architectural features left.

Figure 2.15: Rendering of the new café/restaurant concept [9]

3. DESCRIPTION AND CONDITION ASSESSMENT OF BUILDING

The building consists of three main levels with the addition of a roof terrace and partial basement (figure 3.1). The basement (2PP) is only in the northeast corner of the building and contains utility and mechanical areas. The ground level (1PP) is at the elevation of grade on the west side of the building, where the stadium and rink once stood. In its original configuration, this level had locker rooms and is currently used as a bar and bicycle rental and repair shop. The main level (1NP) is directly accessible to the east of the building via Hlavkuv Bridge, roadway and transit. This area has a smaller footprint than the level below, this creates terraces over the ground level to the north, south and east. There is also a walkway on the west side of the building that extends above the floor below. This level was the primary restaurant space that overlooked the stadium throughout its history. This space is currently occupied by the dance floor of the disco, occupying the building. The balcony or gallery level (2NP), is a partial level with only a narrow strip of floor along the west side of the building. This level expands to the full width of the building on the north side of the building. In 2007 a mirrored balcony was added on the east side of the level, creating an open space only along the center of the building [2]. This level was used as additional restaurant space overlooking the stadium. It is currently used as part of the disco venue. The roof level (3NP) is occupied by a terrace that was used as a viewing area for the stadium and café.

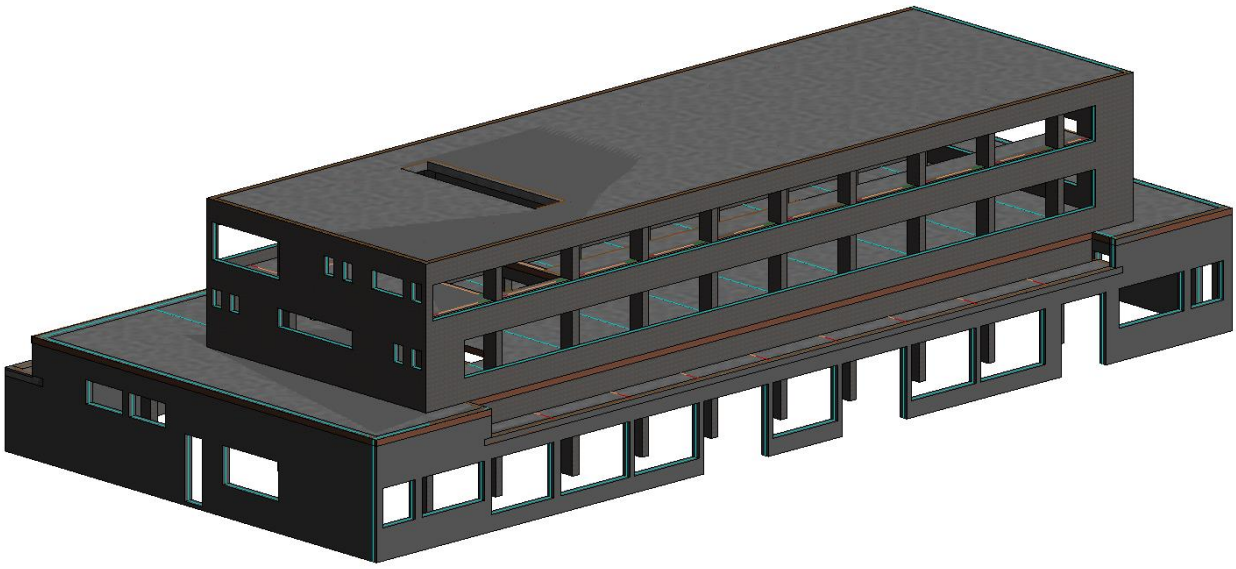

Figure 3.1: Isometric View of Revit Building Model (View from Northwest)

For the purposes of this report, all terminology regarding vertical location within the building will follow the pattern set in figure 3.2. To simplify matters, all structural elements will be coupled to the level with which they are associated. Instead of using the labels “floor” or “ceiling”, everything will be referred to by the level of the building they are supporting, see the green dotted squares in figure 3.2.

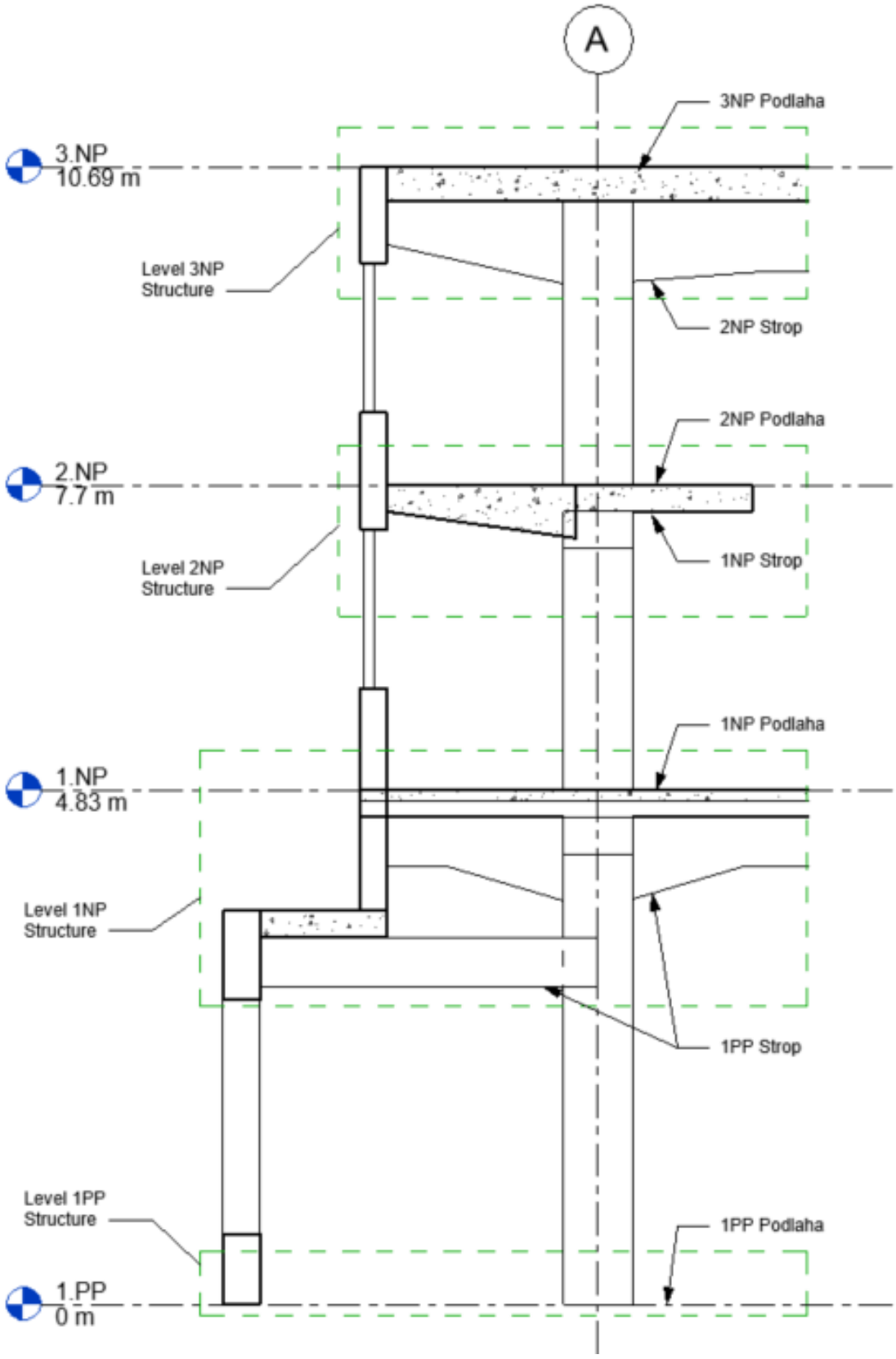

Figure 3.2: Section View with Elevation Level Labels

It was impossible to conduct a direct inspection with the full project team due to COVID-19 restrictions so various alternative methods were used. The team of Petr Kabele and Christiana Lara Nunes was able to conduct a visual inspection of the site but no destructive testing or minor destructive testing was performed. The visit occurred on 12 May 2020 at 14:00. However, a more comprehensive survey was conducted in 2015 by Diagnostika Staveb, with results provided in the report titled *Report on the Construction Technical Survey of Fuchs Cafe Building* [16]. Material samples were tested, and concrete probes were performed to identify the composition of various structural elements. The information from that report is used in this section for the description of the elements of the building.

3.1. Main Building Framing Systems

The foundation system is unknown due to lack of documentation and access. Certain assumptions can be made based on the type of construction and methods of the era. Concrete spread footings likely support the main structural elements of the building. It is unknown what depth and what bearing surface exists, whether bedrock or compacted soil. The exterior walls likely have continuous concrete footings that support the self-weight and occasional live load on bearing portions of the wall.

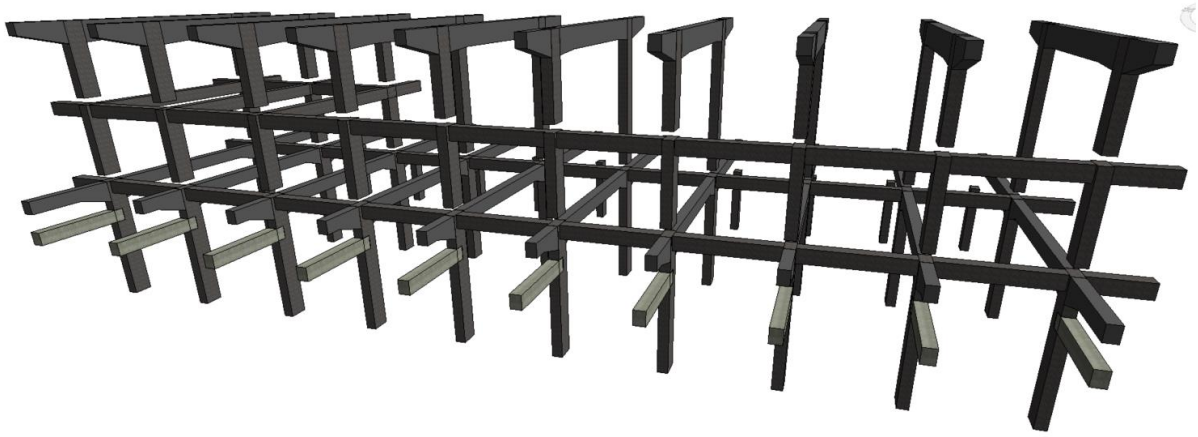

Figure 3.3: Isometric View of Internal Frame Structure (from the Southwest)

The main vertical and lateral supporting structure consists of monolithic concrete frames (figure 3.3). These frames act in the transverse direction of the building (figure 3.4). There are two rows of columns that extend the full building height, identified as such as column lines A and B. Additionally, one row of columns reaches level 1NP, column line C. From there, there are concrete beams between these columns at levels 1NP and 3NP. There are also beams on level 2NP on the north side of the building. The frames are typically spaced at 3.6 meters. Spanning between the frame beams on each level are concrete slabs, described later.

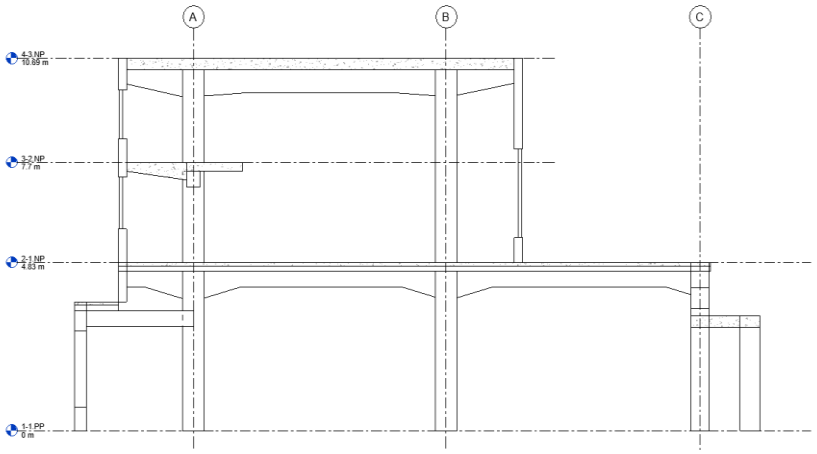

Figure 3.4: Transverse Frame Cross Section looking North

In the longitudinal direction the full height columns create continuous frames (see figure 3.5). At level 1NP, the beams of the frame occur at both full height columns, lines A and B, while at level 2NP, there is only one line of beams creating framing action at column line A. There are no frame beams at level 3NP so the columns cantilever above the frame beams to resist longitudinal lateral loads at the roof level.

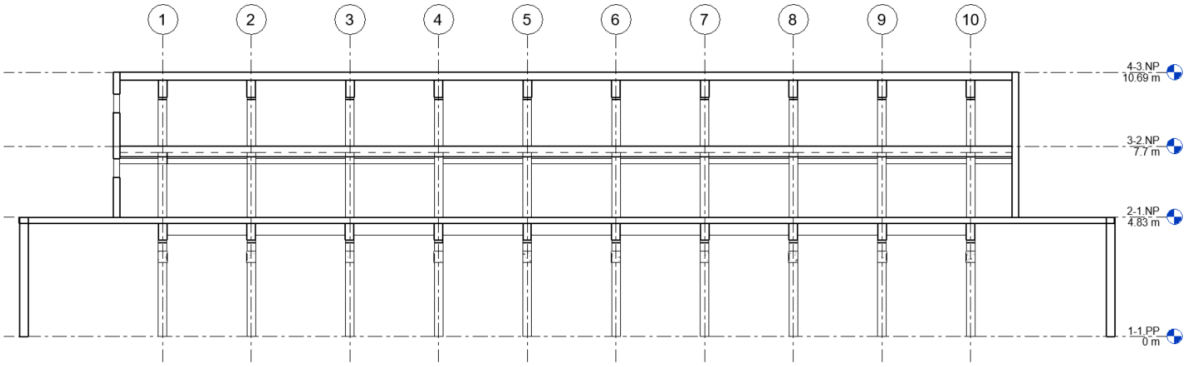

Figure 3.5: Longitudinal Frame Cross Section looking East – Frame Beams Exist at Levels 1NP and 2NP

3.2. Structural Element Composition

The columns are monolithically cast-in-place with continuous vertical reinforcement and stirrups (figure 3.6). The full height columns are 35 cm by 65 cm, while the single-story columns are 35 cm by 55 cm. All columns have the strong axis in the transverse direction of the building. Many of the columns have coverings, making it difficult to inspect the current condition. Where the structure is exposed, the concrete is in adequate shape with minor cracking and minimal spalling. In the locations of the previous probe testing, the outer layers of concrete were removed and never repaired, leaving the steel reinforcing exposed (figure 3.7).

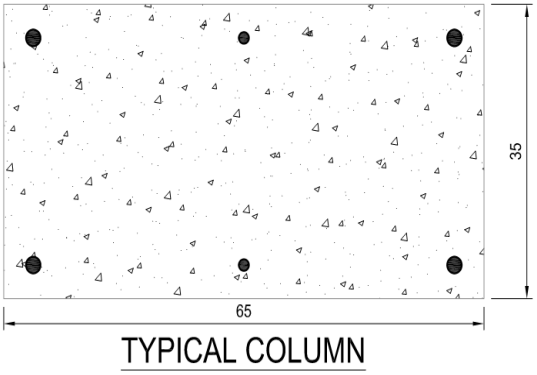

Figure 3.6: Typical column cross-section dimensions in centimeters [16]

Figure 3.7: Column damage from 2015 above Level 1PP at column lines A-4

The transverse beams spanning between the columns and cantilevering vary in depth along the span. The width of the beam is the same as the columns, 35 cm, while the depth at midspan is 46 cm (figure 3.6). Like the columns, most of this framing is covered with cladding, making visual investigation difficult. Also, the concrete is damaged in the locations where the probes were performed (figure 3.9). This framing provides lateral stability as well as support of the gravity loads.

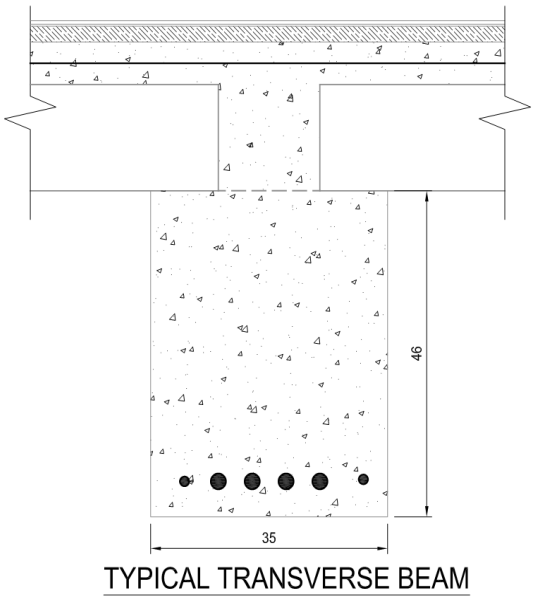

Figure 3.8: Typical Transverse Beam Cross-Section Dimensions in Centimeters [16]

a)  b) 

Figure 3.9: a) 3NP transverse beams at column line A looking south
b) Damage at 2015 probe location (Beam at Level 3NP, Column Line 5)

The longitudinal beams at the balcony level run continuously along the longitudinal length of the building. These beams are approximately the same width as the depth of the columns, 64 cm (figure 3.10). In the area of the balcony, on the south side of Level 2NP, the beams provide torsional restraint to the floor because the slab cantilevers on each side of the beam (figure 6.1). The framing provides lateral stability to the building as it is the highest lateral resistance frame in elevation in the building. Above level 2NP, the columns cantilever to resist lateral loads in the longitudinal direction, as there are no frame beams at level 3NP.

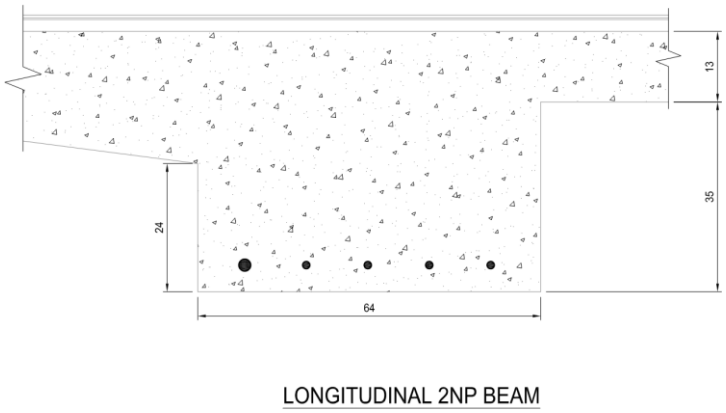

Figure 3.10: Typical 2NP Longitudinal Beam Cross-Section Dimensions in Centimeters [16]

Figure 3.11: Longitudinal Beam Damage from 2015 at Level 2NP, Column Line A, Between 8 and 9

The slabs of levels 1NP and 2NP consist of a ceramic and concrete composite slab system, while level 3NP consists of solid reinforced concrete several layers thick. The composite slabs utilize a series of ceramic inserts that are 15 cm tall and 30 cm wide (figure 3.12). They act as formwork for the concrete placed within and above. The amount of concrete above the ceramic is between 6 cm thick at the level 2NP slab and 10 cm thick at the level 1NP slab. The spaces between the ceramic inserts create rows of T-shaped concrete beams with reinforcement at the bottom of the T only in the longitudinal direction, causing the slab to behave as a one-way slab. The slab at level 3NP contains several distinct layers. The bottom concrete layer is 13 cm thick, reinforced with steel bars, which provides the flexural strength of the slab. Above that layer, is a 5 cm layer of slag then a 10 cm thick unreinforced concrete slab topped with another layer of slag, this one 3 cm thick. Due to the slab construction method and reinforcing, this slab could behave as a two-way slab but there are no longitudinal beams at the roof level, providing orthogonal support to the slab. All suspended floor slabs span between transverse beams, typically 3.6 meters. The end spans of level 2NP and 3NP are solid reinforced concrete cantilevering to the exterior wall, 1.75 meters.

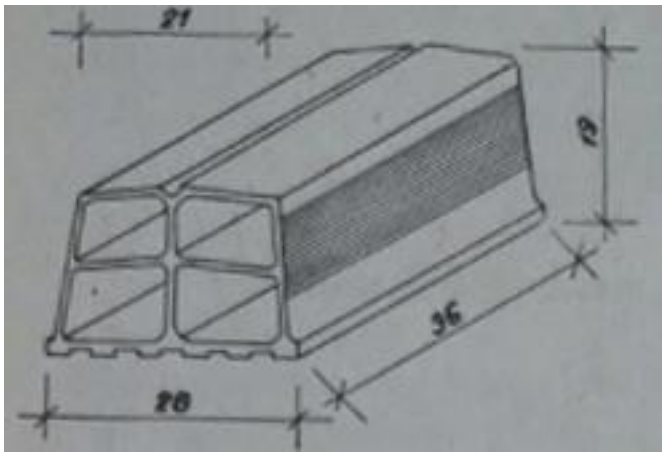

Figure 3.12: Typical Shape of 30 cm wide by 15 cm tall ceramic inserts [17]

The top of the concrete slab is rarely exposed in the building as there are many architectural coverings including wood and carpet. On level 1NP, the floor is built up in areas to provide different levels, especially at the bar (figure 3.13). This has been accomplished using blocking or other structural systems. The top of the slab at level 3NP is completely covered by roofing materials and is concealed (figure 3.14). Additionally, there are various slab penetrations on each level of the building for stairs. The main stair is between column lines 2 and 3. Additionally, in the area of level 2PP, the floor structure above on level 1PP is elevated approximately one meter.

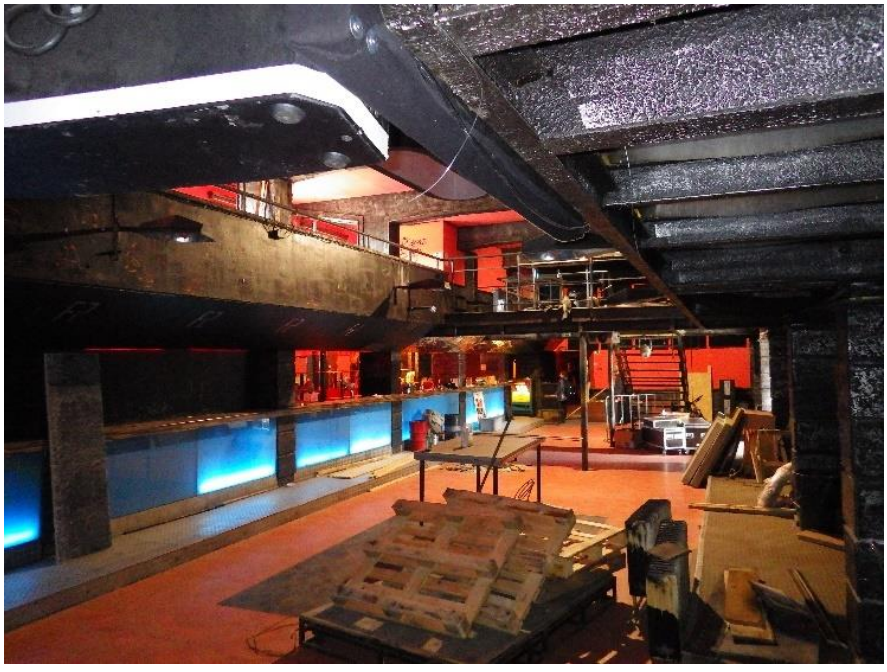

Figure 3.13: Elevated floor areas at the bar on level 1NP

Figure 3.14: Roofing above the level 3NP slab looking south

There are signs of deterioration of the slab in the terrace area of level 1NP north of column line 1. This is likely since the top of the slab is exposed to the exterior of the building and inherent water and moisture. Additionally, this slab spans further than the typical interior bay, over 5.5 meters, which could cause more substantial deflection and ponding of water above. There is clearly damage to the concrete, steel reinforcing, ceramic inserts and ceiling material. The area is currently shored with wood posts and beams (figure 15). The steel reinforcing is visible between the ceramic from below, showing signs of corrosion. Adjacent to the temporary shoring, there is an area of the ceiling that has been repaired, possible using a textile reinforced mortar or a steel reinforced grout system.

a)  b) 

Figure 3.15: a) Repair of composite slab damage due to water infiltration, level 1NP north of column line 1 b) Temporary shoring of damaged composite slab system, level 1NP north of column line 1

The typical exterior wall structure is concrete. There was no testing done on the walls so only visual observations were made. The wall is 25 cm thick with plaster on both sides of the concrete structure (figure 3.16). The concrete is likely reinforced in two layers but that was not directly confirmed (see figure 3.17).

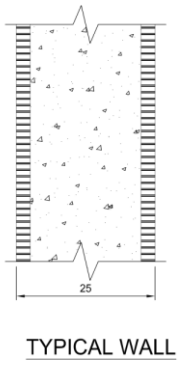

Figure 3.16: Exterior wall composition thickness in centimeters [16]

Figure 3.17: Exterior wall penetration at northeast corner of level 2NP

The exterior walls have been altered significantly throughout the history of the building. Some window and door penetrations in the wall have been infilled. Various materials have been used to achieve this purpose, including masonry and timber. New coverings and cladding have been installed as well. There are many areas where the exterior cladding surfaces are cracking and detaching, exposing the substructure (figure 3.18). This damage occurs on all the exterior walls, the extent of which is difficult to quantify. With all these alterations, the condition of the walls is poor, however, the extent of the damage is unknown until more extensive testing and inspections are performed.

Figure 3.17: Exterior wall surface condition on western side of building

The load path of the walls is unknown. The two possibilities are that the walls are supported or hung from the slabs at each level, acting like a curtain wall. The alternative is that the walls act in a load bearing manner with the total self-weight of the wall bearing at the base of the wall. Many of the windows on the east, west and south are very large and apparently lack any interior support. The window above level 2NP on the west exterior wall is over 34 meters long. This condition makes the bearing wall load path unlikely. However, if the exterior walls are supported by the slab on each level, this means that the ceramic composite slabs are supporting the wall self-weight, which also seems like a flawed method, but the lesser of two evils. Additionally, with the intention to reopen all the original windows that have been infilled, it is possible that the original load path has changed through all the alterations. Additionally, at the intersection of the south wall and east wall, the windows extend to almost all the way to the corner leaving a 24 cm by 32 cm post (figure 3.18). The function of the post is unknown, whether is it loaded and behaves like a post or whether it acts as a mullion tor which the windows attach.

Figure 3.18: South east corner of the building with corner post

The balcony area of level 2NP was originally constructed with a concrete parapet railing between the balcony and level 1NP below. However, during one of the renovations, possibly in 2007, where the mirrored balcony was installed, a small section of the parapet was demolished. It is probable that the reinforcing bars in the slab bent up within the parapet to provide bending strength for lateral railing loads. If this reinforcing was removed with the parapet, it likely removed the bent bar development capacity that was allowing the slab to function properly. This would mean that the slab might not have any tensile resistance from the steel. The exact reinforcement position will have to be investigated.

4. MATERIALS

The original structural elements of the building consist of steel reinforced concrete. Other materials can be found but they will either be considered architectural/non-structural or coming from later renovations or repairs. Since the intention of the project is to convert the building back to its original configuration, only the material of the original structural elements will be analyzed here.

No documentation from the original building design was available so the intended concrete strength or mix design is unknown. Furthermore, no record of the construction process exists in terms of manufacturer of the concrete, material logs or testing results. What is known is that construction and erection stopped for a period of time while the building was only partially finished. Since the reason for the stoppage was due to the economy, the budget of the project come into question. At that time, significant changes were made to the entire project. A new contractor came on the project to replace the bankrupt PCC and cheaper materials were used. The result of this is that there are two distinct portions of the building that likely have different material and mechanical characteristics. Unfortunately, it has not been documented what structural elements were completed in the first construction phase and what was completed in the second. In spite of this, from pictures taken during the stoppage (figure 2.8) it appears that the columns and beams were complete while many of the slabs and walls were completed later. It must be assumed that before and after the stoppage, both designers completed fully adequate designs. With the changes made, the safety of the building is not in doubt, just the quality of the materials and craftsmanship.

The exact changes made during this transition are not known. However, with cheaper concrete inevitably comes lower material qualities. Chiefly among these lower qualities would be the concrete strength, as high strength concrete is more expensive. When Steigenhofer was brought on to redesign the project more economically, it is expected that a lower material strength would have been accounted for in his design. The durability of the concrete could also be reduced with cheaper concrete. A lower durability concrete increases the risk of degradations such as reinforcement corrosion, freeze-thaw breakdown and chemical attach breakdown [10]. Considering the usage of the building as a winter stadium, the structure was at high risk for these types of damage.

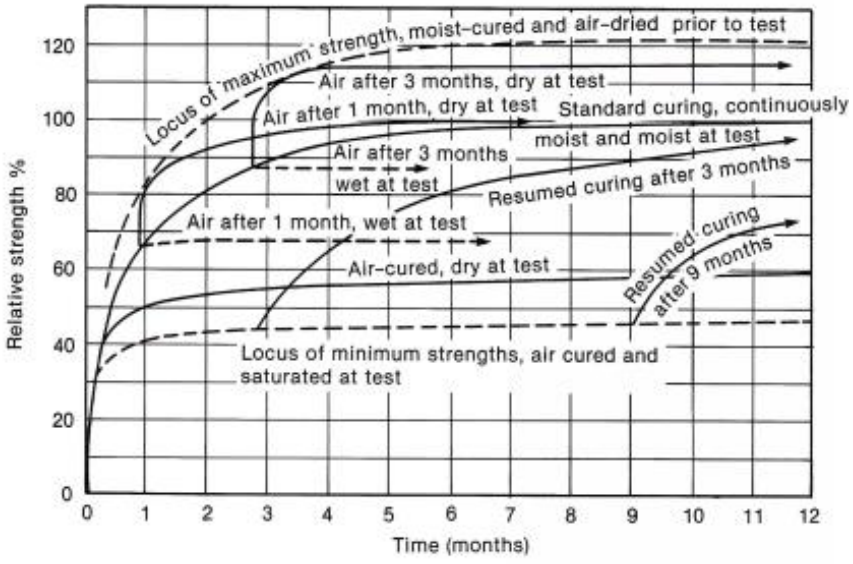

Figure 4.1: Effect of Moist-Curing Conditions on Compressive Strength [18]

A new contractor was brought on at the transition to reduce costs, which could have led to lower craftsmanship during the construction of the structure. Once again, the qualifications of the new contractor are not known, but if they came in with less expertise or concrete specialization, there are inherent risks to the materials. The long-term viability of concrete depends greatly on the procedure used during the mixing and placement of that concrete. In the 1920s and 1030s concrete was typically mixed in small batches [9]. This could lead to high variability and inconsistent mixes throughout the entire building and even possibly within individual elements. Concrete also needs to be properly consolidated as it is placed in the formwork. The aggregate must be uniformly distributed within the concrete as it is placed to prevent weak spots. If this consolidation was not achieved, this could also cause high inconsistency within areas where each batch of concrete was poured.

Like the mixing of the concrete, the curing procedure plays a large role in the final concrete product as well. Important factors that affect the strength of the concrete are water/cement ratio and moisture and temperature conditions during cuing [10]. All of these parameters affect how the concrete will hydrate, the important process that allows concrete to achieve its strength. When a batch of fresh concrete is being prepared for use at a jobsite, the water/cement ratio and workability of the mixture is estimated by laborers and if they are inexperienced, the concrete will not achieve the maximum possible strength. Similarly, the conditions of the concrete are very important during curing. The moisture must be controlled so that the concrete hydrates at a constant rate, if it is not, it will not reach the intended strength and possibly crack due to shrinkage. Improper curing moisture can reduce the concrete strength up to 40% from standard curing techniques after 28 days (see figure 4.1). The temperature of the specimen during curing is of critical importance as well. If the environment is too hot or too cold, the compressive strength will also be reduced. High temperatures can reduce the strength by up to 25% while low temperatures can reduce it 10% at 28 days (see figure 4.2).

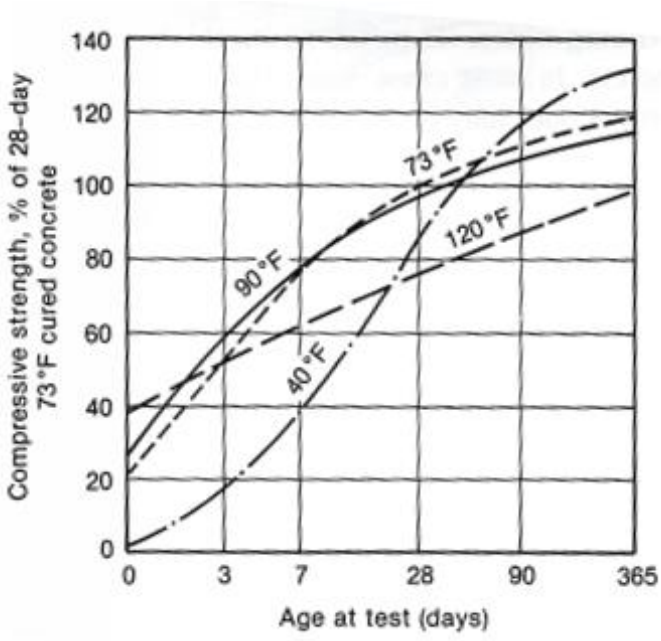

Figure 4.2: Effect of Temperature on Compressive Strength [19]

No on-site testing was performed for this report. However, testing was done during the preparation of the 2015 report *Usability Study of Fuchs' Café* by Javurek et al. [9]. Schmidt hardness tests were performed in various locations throughout the building to determine the compressive strength. Four elements were tested, the results and locations of which are not shared. Within these tests, there was a high amount of variability in the results, however, all tests have a minimum concrete quality of C12/15. C12/15 is not typically used for structural applications, as the minimum is C16/20. Since the strength was verified through testing and knowing that the building is historic and material quality was low, this is an acceptable conclusion. For the purposes of this report, all concrete elements are assumed to be this grade (Table 4.1). However, this is conservative as some element strengths may be underrepresented. It is recommended that more extensive material testing is done to identify patterns of concrete quality and identify elements that a higher compressive strength, considering the two distinct phases of construction.

Similarly, the steel reinforcement was tested for material characteristics. There is no record of the sample locations, the number of tests performed, or the type of test performed. The result of this testing is that the tensile strength of the steel is 180 MPa.

Strength classes for concrete															Analytical relation / Explanation
f_{ck} (MPa)	12	16	20	25	30	35	40	45	50	55	60	70	80	90	
$f_{ck,cube}$ (MPa)	15	20	25	30	37	45	50	55	60	67	75	85	95	105	2.8
f_{cm} (MPa)	20	24	28	33	38	43	48	53	58	63	68	78	88	98	$f_{cm} = f_{ck}+8$(MPa)
f_{ctm} (MPa)	1,6	1,9	2,2	2,6	2,9	3,2	3,5	3,8	4,1	4,2	4,4	4,6	4,8	5,0	$f_{ctm}=0,30\times f_{ck}^{(2/3)} \leq$C50/60 $f_{ctm}=2,12\cdot\ln(1+(f_{cm}/10))$ > C50/60
$f_{ctk,\ 0.05}$ (MPa)	1,1	1,3	1,5	1,8	2,0	2,2	2,5	2,7	2,9	3,0	3,1	3,2	3,4	3,5	$f_{ctk,0.05} = 0,7\times f_{ctm}$ 5% fractile
$f_{ctk,0.95}$ (MPa)	2,0	2,5	2,9	3,3	3,8	4,2	4,6	4,9	5,3	5,5	5,7	6,0	6,3	6,6	$f_{ctk,0.95} = 1,3\times f_{ctm}$ 95% fractile
E_{cm} (GPa)	27	29	30	31	33	34	35	36	37	38	39	41	42	44	$E_{cm} = 22[(f_{cm})/10]^{0.3}$ (f_{cm} in MPa)
ε_{c1} (‰)	1,8	1,9	2,0	2,1	2,2	2,25	2,3	2,4	2,45	2,5	2,6	2,7	2,8	2,8	see Figure 3.2 $\varepsilon_{c1}(^0/_{00}) = 0,7\ f_{cm}^{0,31} \leq 2,8$
ε_{cu1} (‰)	3,5									3,2	3,0	2,8	2,8	2,8	see Figure 3.2 for $f_{ck} \geq 50$ Mpa $\varepsilon_{cu1}(^0/_{00})=2,8+27[(98-f_{cm})/100]^4$
ε_{c2} (‰)	2,0									2,2	2,3	2,4	2, 5	2,6	see Figure 3.3 for $f_{ck} \geq 50$ Mpa $\varepsilon_{c2}(^0/_{00})=2,0+0,085(f_{ck}-50)^{0.53}$
ε_{cu2} (‰)	3,5									3,1	2,9	2,7	2,6	2,6	see Figure 3.3 for $f_{ck} \geq 50$ Mpa $\varepsilon_{cu2}(^0/_{00})=2,6+35[(90-f_{ck})/100]^4$
n	2,0									1,75	1,6	1,45	1,4	1,4	for $f_{ck} \geq 50$ Mpa $n=1,4+23,4[(90-f_{ck})/100]^4$
ε_{c3} (‰)	1,75									1,8	1,9	2,0	2,2	2,3	see Figure 3.4 for $f_{ck} \geq 50$ Mpa $\varepsilon_{c3}(^0/_{00})=1,75+0,55[(f_{ck}-50)/40]$
ε_{cu3} (‰)	3,5									3,1	2,9	2,7	2,6	2,6	see Figure 3.4 for $f_{ck} \geq 50$ Mpa $\varepsilon_{cu3}(^0/_{00})=2,6+35[(90-f_{ck})/100]^4$

Table 4.1: Table 3.1 from Eurocode 1992-1-1 showing Material Properties of C12/15 in Yellow [20]

5. BUILDING CODE AND DESIGN LOADS

The governing structural design code used today in the Czech Republic is the Eurocode. The code is intended for new construction but can be adapted to existing structures as well. There is currently no code specifically intended for existing structures adopted by the Czech Republic, as there are in other countries like Switzerland with the SIA 269/2 “A New Swiss Code for the Conservation of Concrete Structures”. So, for the purposes of this report, Eurocode will be used as the basis for all structural evaluation.

5.1. Eurocode Load Definitions and Combinations

Eurocode 1990 [21] establishes what loads are applied to a structure and how they are combined to maximize the effect of the loads on the structure. The applicable vertical loads for the building include dead load, live load and snow load. Laterally, wind load is applied to the building. These loads are factored, either favorably or unfavorably, based on the likelihood of them occurring simultaneously (Table 5.1). For the purposes of this investigation, all load combinations will be considered but only one combination will be used in the final analysis:

1.35 * Dead Load + 1.5 * Live Load + 0.75 * Snow Load

In this scenario the dead load is maximized as the live load is treated as the leading variable action and snow load treated as the accompanying variable action. The live load, as will be shown later, is five time larger than the snow load. Therefore, the maximum effect of the load is to make the live load the leading action.

Persistent and transient design situations	Permanent actions		Leading variable action	Accompanying variable actions (*)	
	Unfavourable	Favourable		Main (if any)	Others
(Eq. 6.10)	$\gamma_{Gj,sup}G_{kj,sup}$	$\gamma_{Gj,inf}G_{kj,inf}$	$\gamma_{Q,1}Q_{k,1}$		$\gamma_{Q,i}\psi_{0,i}Q_{k,i}$

Persistent and transient design situations	Permanent actions		Leading variable action (*)	Accompanying variable actions (*)	
	Unfavourable	Favourable	Action	Main	Others
(Eq. 6.10a)	$\gamma_{Gj,sup}G_{kj,sup}$	$\gamma_{Gj,inf}G_{kj,inf}$		$\gamma_{Q,1}\psi_{0,1}Q_{k,1}$	$\gamma_{Q,i}\psi_{0,i}Q_{k,i}$
(Eq. 6.10b)	$\xi\gamma_{Gj,sup}G_{kj,sup}$	$\gamma_{Gj,inf}G_{kj,inf}$	$\gamma_{Q,1}Q_{k,1}$		$\gamma_{Q,i}\psi_{0,i}Q_{k,i}$

(*) Variable actions are those considered in Table A1.1

NOTE 1 The choice between 6.10, or 6.10a and 6.10b will be in the National annex. In case of 6.10a and 6.10b, the National annex may in addition modify 6.10a to include permanent actions only.

NOTE 2 The γ and ξ values may be set by the National annex. The following values for γ and ξ are recommended when using expressions 6.10, or 6.10a and 6.10b.
$\gamma_{Gj,sup} = 1,35$
$\gamma_{Gj,inf} = 1,00$
$\gamma_{Q,1} = 1,50$ where unfavourable (0 where favourable)
$\gamma_{Q,i} = 1,50$ where unfavourable (0 where favourable)
$\xi = 0,85$ (so that $\xi\gamma_{Gj,sup} = 0,85 \times 1,35 \cong 1,15$).
See also EN 1991 to EN 1999 for γ values to be used for imposed deformations.

NOTE 3 The characteristic values of all permanent actions from one source are multiplied by $\gamma_{G,sup}$ if the total resulting action effect is unfavourable and $\gamma_{G,inf}$ if the total resulting action effect is favourable. For example, all actions originating from the self weight of the structure may be considered as coming from one source ; this also applies if different materials are involved.

NOTE 4 For particular verifications, the values for γ_G and γ_Q may be subdivided into γ_g and γ_q and the model uncertainty factor γ_{Sd}. A value of γ_{Sd} in the range 1,05 to 1,15 can be used in most common cases and can be modified in the National annex.

Table 5.1: Table A1.2(B) from Eurocode 1990 Ultimate Limit States Combination of Loads [21]

The Czech Republic benefits from being in a region with very low seismicity. It is close to the middle of the Eurasian Plate, distant from any boundary regions. This makes the country vulnerable to far field earthquakes but not the more severe near field earthquakes. The outlying earthquakes provide only minimal peak ground motion in Prague and very small magnitudes (figure 5.1) [22]. Because of this, seismic loads typically do not govern design as wind loads created a higher lateral loading.Therefore seismic load will not be included in this investigation.

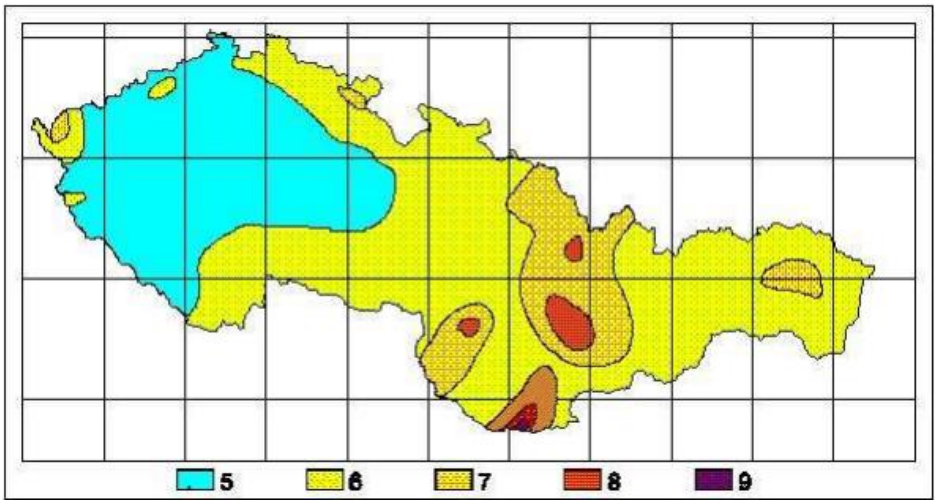

Figure 5.1: Maximum Estimated Earthquake Intensity in Czech Republic and Slovakia [22]

5.2. Dead Loads

The dead loads are addressed in Eurocode 1991-1-1 and consist of the self-weight of all the structural material and architectural finishes. The 2015 Report by Diagnostika Staveb, titled *Report on the Construction Technical Survey of Fuchs Cafe Building* [16] shows the in-situ composition of different structural elements tested with probes. In the final configuration of the building, the architectural finishes that will be used are unknown. The assumption made hereafter is that any future configuration will be similar in weight to the current, including flooring, ceilings and plaster. If the decision Is made in the future that a substantial new covering system will be used, then the building must be reevaluated. The makeup of the slabs as determined from the probes are shown in figures 5.2 and 5.3. The slabs are made up of many layers of different non-structural materials, such as rubber, wood and slag. The probes were conducted in limited locations, so it is assumed that the composition is uniform for all the slabs. Table 5.2 shows the arrangement of the individual layers of the slabs and the resulting dead load of the system in kN/m^2.

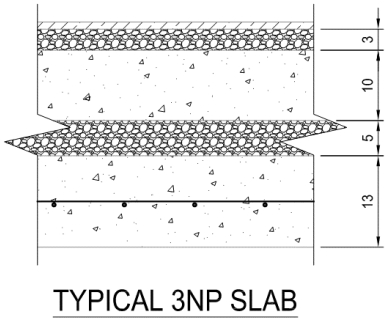

Figure 5.2: Composition of 3NP Slab [16]

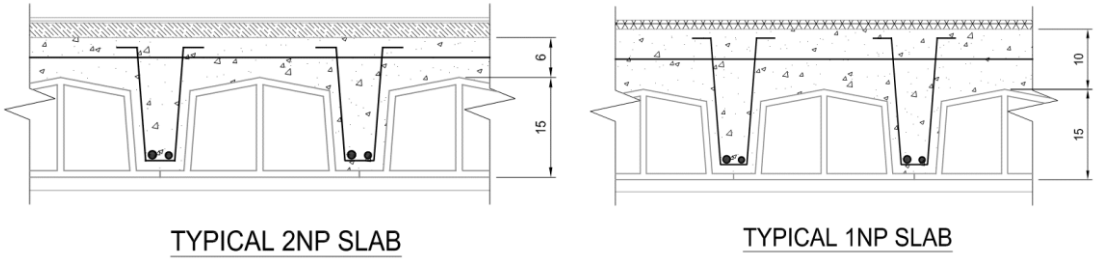

Figure 5.3: Composition of 2NP & 1NP Ceramic Composite Slab [16]

	Element	Thickness (m)	Unit Weight (kN/m3)	Weight (kN/m2)
1NP Floor Slab	Ceramic Tile	0.015	23	0.345
	Concrete	0.1	24	2.4
	Ceramic	0.15	10	1.5
	Ceiling	0.02	4	0.08
			Total Weight	**4.33**

	Element	Thickness (m)	Unit Weight (kN/m3)	Weight (kN/m2)
2NP Floor Slab	Rubber	0.005	10	0.05
	Carpet	0.003	0.2	0.0006
	Wood	0.022	5	0.11
	Concrete	0.06	24	1.44
	Ceramic	0.15	10	1.5
	Ceiling	0.02	4	0.08
			Total Weight	**3.18**

	Element	Thickness (m)	Unit Weight (kN/m3)	Weight (kN/m2)
3NP Floor Slab	Cardboard	0.01	0.07	0.0007
	Slag	0.03	20	0.6
	Concrete	0.1	24	2.4
	Slag	0.05	20	1
	Reinf Conc	0.13	24	3.12
			Total Weight	**7.12**

Table 5.2: Dead Loads of Floor Slab System by Level

The dead load of the beams and columns are solely based on the cross section of each element. They vary in size throughout the building and have limited architectural cladding so the dead load of each element will not be displayed here and will be determined on a case by case basis. The original exterior walls consist of concrete and plaster. They are of considerable thickness so the load must not be neglected (table 5.3).

	Material	Thickness (m)	Unit Weight (kN/m3)	Weight (kN/m2)
Ext Wall	Concrete	0.2	24	**4.8**

Table 5.3: Dead Loads of Exterior Walls

5.3. Live Loads

The live loads applied to the building are dictated by the usage. In the building's current usage as a bar, disco and concert venue, a load of up to 7.5 kN/m^2 needs to be accounted for due to the large crowds. In the building's original configuration and the new one, as a restauant, outlined in this report, a live load of 3.0 kN/m^2 is used (Table 5.4)

			Uniform	Point	Railing
Category of Use	Description	Time	qk (kN/mm2)	Qk (kN)	qk (kN/m)
C1	Areas with tables (Café, Restaurant)	NEW	2.0 to **3.0**	3.0 to **4.0**	0.2 to 1.0
C5	Areas Suseptable to Large Crowds	EXISTING	5.0 to **7.5**	3.5 to **4.5**	3.0 to 5.0

Table 5.4: Live Loads

5.4. Snow Load

Snow loads are calculated using the Eurocode 1991-1-3 [23]. Snowfall is common all-over the Czech Republic and the severity of the snowfall varies by location as indicated on the ground snow load map of Czech Republic (Figure 5.4). In addition to the ground snow load, coefficients like thermal effects, exposure effects and roof pitch factor the roof snow load based on the location and usage of the building. In this situation, the building has a float roof, is heated and has a normal exposure topography. The adjusted roof snow load value is shown in Table 5.5 as 0.6 kN/m^2.

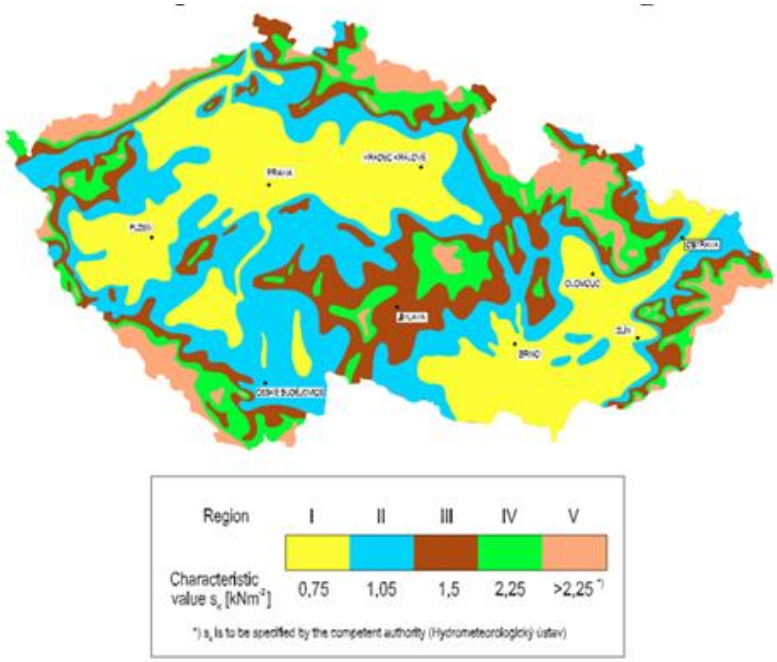

Figure 5.4: Figure C11 from Eurocode 1991-1-3 - Czech Republic ground snow load map [23]

Roof Snow Load			
Unit Weight	γ	2	kg/m3
Altitude	A	180	m
Roof Pitch	α	0	degrees
Exposure Coeff	**Ce**	1	
Thermal Coeff	**Ct**	1	
Snow Load Shape	**μ**	0.8	
Ground Snow Load	**sk**	0.75	kN/m2
Roof Snow Load	**s**	**0.6**	**kN/m2**

Table 5.5: Snow Load Calculation Table

5.5. Wind Loads

The wind load for the building is calculated using the Eurocode 1991-1-4. Many factors contribute to the loads including the wind speed, building height, surrounding terrain and topography. Friction along the ground slows the wind closer to the surface, while higher above, the wind will unimpeded, creating higher pressures. Natural and manmade obstructions around the site will reduce the wind load on the building as these objects disperse the wind. Major topographical features impact the wind by increasing the pressure as the wind approaches a tall hill or escarpment. The wind becomes focused in the smaller area. The reverse is true on the leeward side of a hill, the pressure will drop.

Factor	Variable	Value	Unit
Fund Basic Wind Velocity	$v_{b,0}$	22.5	m/s
Directional Factor	c_{dir}	1	
Seasonal Factor	c_{season}	1	
Basic Wind Velocity	v_b	22.5	m/s
Height Above Ground	z	10.7	m
Roughness Length	z_0	0.05	m
Roughness Length Cat II	z_{0II}	0.05	m
Minimum Height	z_{min}	2	m
Maximum Hight	z_{max}	200	m
Terrain Factor	k_r	0.19	
Roughness Factor	$c_r(z)$	1.02	
Orography Factor	$c_o(z)$	1	
Mean Wind Velocity	$v_m(z)$	22.9	m/s
Turbulance Factor	k_I	1	
Turbulance Intensity	$I_v(z)$	0.186	
Air Density	ρ	1.25	kg/m3
Peak Velocity Pressure	**$q_p(z)$**	**0.758**	kN/m2
External Pressure Coeff	cpe1	1	
External Pressure Coeff	cpe10	0.8	
External Wind Pressure	**w_e**	**0.758**	kN/m2
Size Factor	$c_s c_d$	1	
Force Coef w/o Free Flow	$c_{f.0}$	2	
Red Fact for Square Sec	ψ_r	1	
Red Fact for Struct El	ψ_λ	0.66	
Force Coefficient	c_f	1.32	
Reference Area	A_{ref}	210	m2
Wind Force	**F_w**	**210.1**	kN

Table 5.6: Wind Load Calculation Table

6. BIM MODEL

A three-dimensional model was created to visualize the structure. As was noted before, in person access to the building and site was not available during the preparation of this report. In lieu of this, the program Revit by Autodesk was used to create a graphical model of the building. The purpose of the model is twofold, to assist in spatially understanding the composition of the building and to then to convey the results and recommendations in the form of drawings.

An ample amount of information was available to create the model. The previous reports completed in 2015 articulated the different building systems and components. Included in this data are the sizes of specific beams and columns, thicknesses of main floor slabs and other nonstructural segments of those elements. In addition to the reports, CAD files were available showing plan layouts and cross sections of the building in various locations. These CAD files were prepared in the as built condition, therefore showing the reality of the current condition, including non-square corners and sloped slabs. This indicates that they were possibly created using photogrammetry or laser scanning. As previously stated, photos of the structure were provided by Kabele and Nunes from a site visit with the specific intention of identifying and documenting areas of interest. Their firsthand knowledge and observations were integral in interpreting and discussing any missing information about the site.

Creating a model, essentially constructing the building from scratch digitally, was incredibly helpful in understanding the connectivity and load path of the structural elements. The perspective and thought process of the original designer was taken into account during the model construction in order to recognize how all the individual elements function. The layout of the main structural frames is clear from pictures and drawings, however the load path from different elements is less clear. Specifically, the support and bearing conditions of the exterior walls difficult to ascertain. Additionally, longitudinal beams are not clearly shown on drawings and are often obscured in pictures especially on level 2NP, therefore the existence and size needed to be assumed (figure 6.1). All these issues, raised while the model was being created, helped initiate discussion within the project team to understand how the building was functioning.

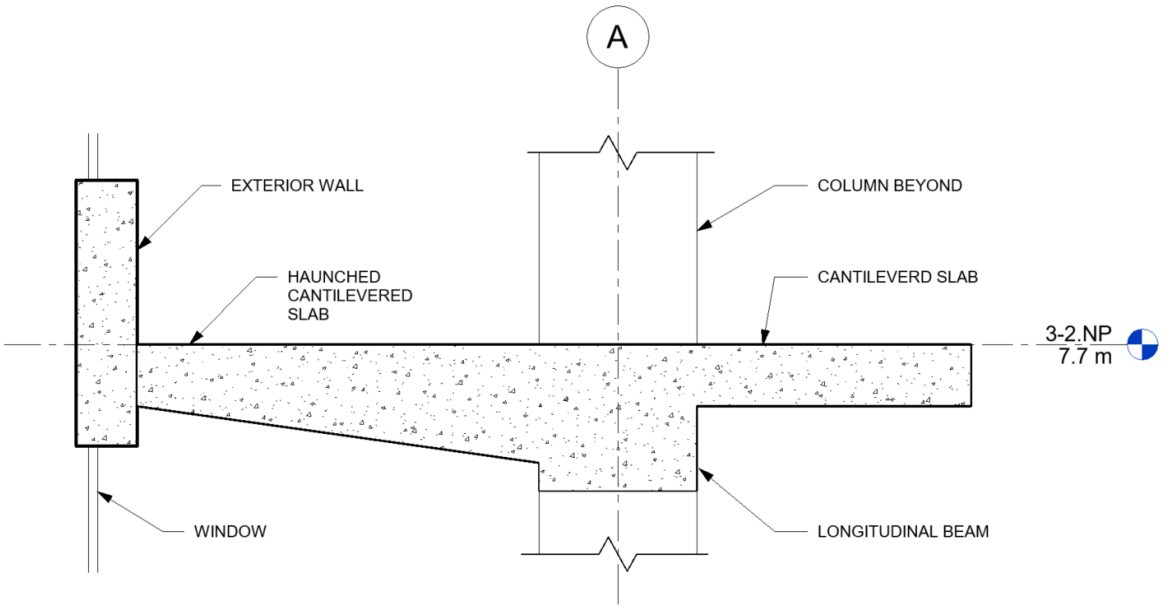

Figure 6.1: Revit Detail of Balcony Area of Level 2NP

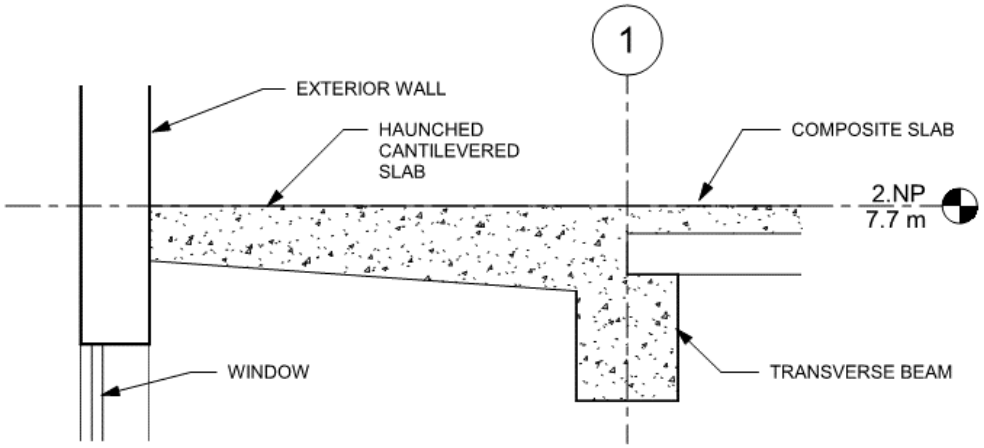

Figure 6.2: Revit detail of cantilevered area on north side of Level 2NP

7. STRUCTURAL MODEL CREATION

To perform the static analysis of the building, RAM Elements, by Bentley Systems, was used. It is a 3D finite element analysis program popular program in the United States and other locations. It is an easy to use program with powerful capabilities. It provides highly customizable materials and shapes. The user interface is simple and intuitive to use (figure 7.1).

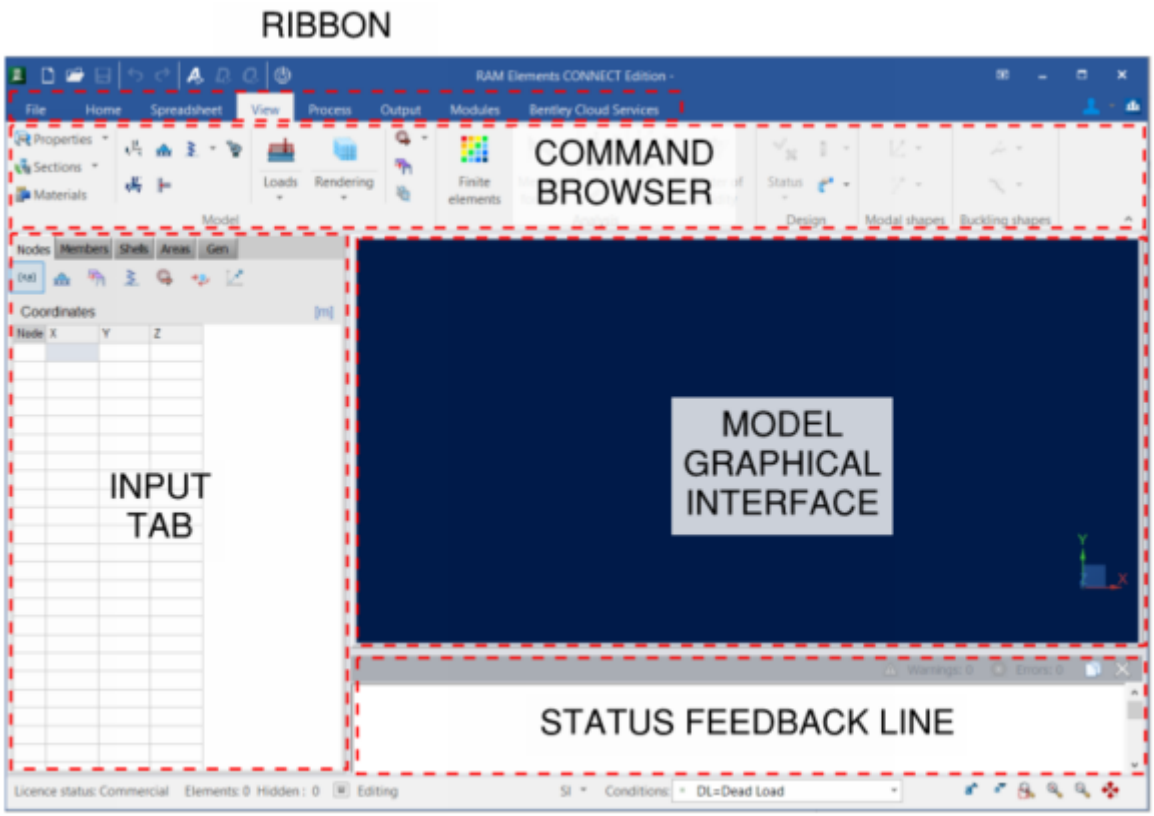

Figure 7.1: RAM Elements User Interface

7.1. Project Parameters

The first step was to set up the project parameters in the file. This included setting the Unit System to metric and establishing the units for how different parameters would be input or displayed. For example, lengths and coordinates would be input in meters while deflections would be presented in millimeters. Area distributed loads would be input as kilonewton per square meter, while moments shown as kilonewton meters and stresses as kilonewton per square meter. RAM Elements has a material property library containing various commonly used materials with parameters created from the codes from around the world. Due to the uniquity and quality of the concrete used in the present structure, a fully customized reinforced concrete material database was created. The data was adopted from previous tests mentioned earlier (figure 7.2).

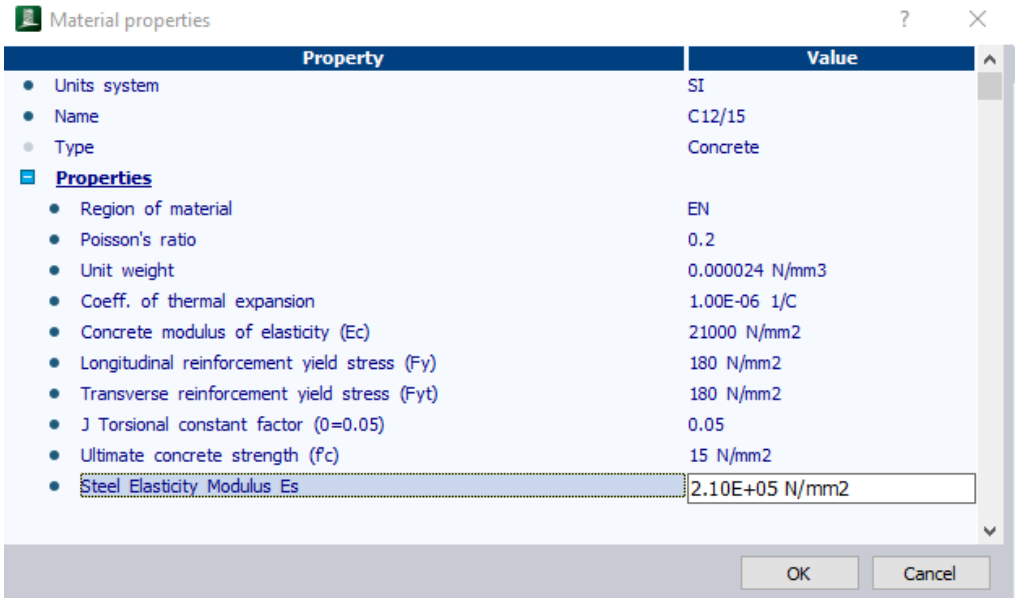

Figure 7.2: Customized Historic Concrete Material Properties

7.2. Loads Cases and Combinations

Next the load cases were created to the model. Included are the three vertical gravity loads of dead, live and snow load. Additionally, the wind loads were specified in four distinct cases, to be applied in the four cardinal directions (figure 7.6). RAM Elements has load combination library including the Eurocode ultimate limit state and serviceability limit states. The program automatically generates combinations including only the load cases for the project (figure 7.3). The four wind cases are applied separately in the load combinations, adding a separate combination for each case, not applying them cumulatively. In all 34 ULS combinations were used and ten SLS. The dead load case is set as the self-weight of the materials modeled.

As discussed earlier, analysis will be run using all possible load combinations, but one specific combination will be used in the detailed member analysis:

1.35 * Dead Load + 1.5 * Live Load + 0.75 * Snow Load

This combination provides the highest load effect to most of the elements in the model.

Load conditions

Cases:

Num	ID	Description	Category
1	DL	Dead Load	DL
2	LL	Live Load	LL
3	SL	Snow Load	SNOW
4	WL1	Wind Load 1	WIND
5	WL2	Wind Load 2	WIND
6	WL3	Wind Load 3	WIND
7	WL4	Wind Load 4	WIND

Combinations:

Formula: D1 = 1.35DL

Num	ID	DL	LL	SL	WL1	WL2	WL3	WL4	Type
1	D1	1.35	0	0	0	0	0	0	Design
2	D2	1.35	1.5	0	0	0	0	0	Design
3	D3	1.35	1.5	0	0.75	0	0	0	Design
4	D4	1.35	1.5	0	0	0.75	0	0	Design
5	D5	1.35	1.5	0	0	0	0.75	0	Design
6	D6	1.35	1.5	0	0	0	0	0.75	Design
7	D7	1.35	1.05	0	1.5	0	0	0	Design
8	D8	1.35	1.05	0	0	1.5	0	0	Design
9	D9	1.35	1.05	0	0	0	1.5	0	Design
10	D10	1.35	1.05	0	0	0	0	1.5	Design
11	D11	1.35	1.5	0.75	0	0	0	0	Design
12	D12	1.35	1.05	1.5	0	0	0	0	Design
13	D13	1.35	1.05	0	0	0	0	0	Design
14	D14	1.35	1.05	0	0.75	0	0	0	Design
15	D15	1.35	1.05	0	0	0.75	0	0	Design
16	D16	1.35	1.05	0	0	0	0.75	0	Design
17	D17	1.35	1.05	0	0	0	0	0.75	Design
18	D18	1.35	1.05	0.75	0	0	0	0	Design
19	D19	1.35	1.05	0.75	0.75	0	0	0	Design
20	D20	1.35	1.05	0.75	0	0.75	0	0	Design
21	D21	1.35	1.05	0.75	0	0	0.75	0	Design
22	D22	1.35	1.05	0.75	0	0	0	0.75	Design
23	D23	1.25	1.5	0	0	0	0	0	Design
24	D24	1.25	1.5	0	0.75	0	0	0	Design
25	D25	1.25	1.5	0	0	0.75	0	0	Design
26	D26	1.25	1.5	0	0	0	0.75	0	Design
27	D27	1.25	1.5	0	0	0	0	0.75	Design
28	D28	1.25	1.05	0	1.5	0	0	0	Design
29	D29	1.25	1.05	0	0	1.5	0	0	Design
30	D30	1.25	1.05	0	0	0	1.5	0	Design
31	D31	1.25	1.05	0	0	0	0	1.5	Design
32	D32	1.25	1.5	0.75	0	0	0	0	Design
33	D33	1.25	1.05	1.5	0	0	0	0	Design
34	D34	1.25	1.5	0.75	0	0	0	0	Design
35	S1	1	0	0	0	0	0	0	Service
36	S2	1	0.7	0	0	0	0	0	Service
37	S3	1	0	0	0.2	0	0	0	Service
38	S4	1	0	0	0	0.2	0	0	Service
39	S5	1	0	0	0	0	0.2	0	Service
40	S6	1	0	0	0	0	0	0.2	Service
41	S7	1	0.6	0	0.2	0	0	0	Service
42	S8	1	0.6	0	0	0.2	0	0	Service
43	S9	1	0.6	0	0	0	0.2	0	Service
44	S10	1	0.6	0	0	0	0	0.2	Service

OK Cancel

Figure 7.3: Load Case and Load Combination Table

7.3. Vertices – Members – Shells

To start building the model, vertices are input in the form of coordinates. All dimensions and vertex locations were determined using the Revit model. In total, over 300 vertices make up the model. Individual vertices were selected as restraints at the base level of the model to provide boundary conditions. Displacement and rotation can be restricted in all three coordinate axes. All boundary conditions were assumed to be pinned so they are free to rotate but displacement was restricted in all directions.

The different vertices are then connected using members. Once again, the structural concept comes from the Revit model. All members are assigned properties, size, material and boundary conditions. For the cross-section size, RAM Elements contains a library of different concrete beam sizes. The material, created earlier, is set for each member. The member boundary conditions are essential to an accurately functioning model. Since the concrete structural elements are monolithically cast, all member connections are modelled as fixed. This enables the transverse beams to transfer moment to the columns creating frame. Once all the parameters are established in the model, the members are shown in the rendering mode where the geometry of the model is verified (figure 7.4). Also, the orientation of the beams and columns are confirmed.

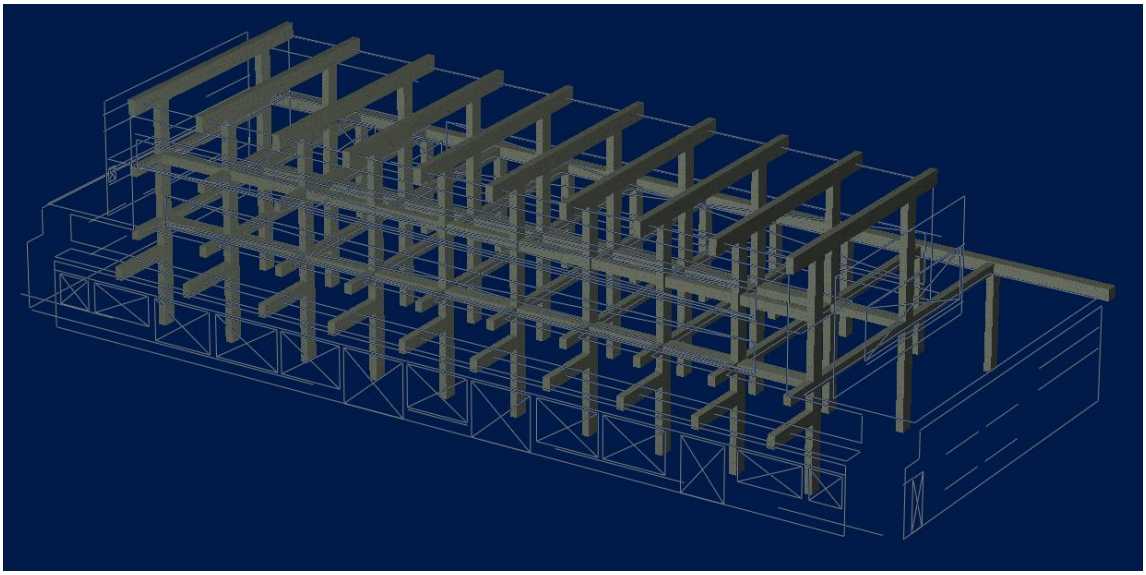

Figure 7.4: Beam and Column Members in RAM Elements Model

Finally, the walls and slabs are modelled in the form of shell elements. Shell elements are created by connecting at least four coplanar vertices. The thickness of the shell is assigned as well as the material properties. The exterior wall elements are modeled as 20 cm thick. The thickness of the Level 3NP slab is set as 13 cm, the thickness of the reinforced concrete portion of the slab system. For the composite ceramic floor slabs, the effective thickness of the slabs is determined using the bending stiffness of the

slab. This means finding the equivalent moment of inertia of a rectangular section from the T-shaped configuration. The boundary conditions for the shell elements are established as pinned along the length of the walls at level 1PP. Finally, openings, windows and doors, are modeled within the shells. In RAM Elements, the releases on the edges of all shell elements is are fixed, therefore the connections of the shells resist rotation. Typically, this is not a problem because the connections of the elements in real life involve continuous reinforcement, transferring the forces through a connection. However, in certain instances if the connections are not handled that way, then the model would be considered invalid. Therefore, all reinforcing assumptions made at the edge of shell elements will need to be confirmed in the field. This is particularly true of the reinforcing for the composite slabs, as will be discussed later. The walls are modeled to bear directly on the slab shell at each level.

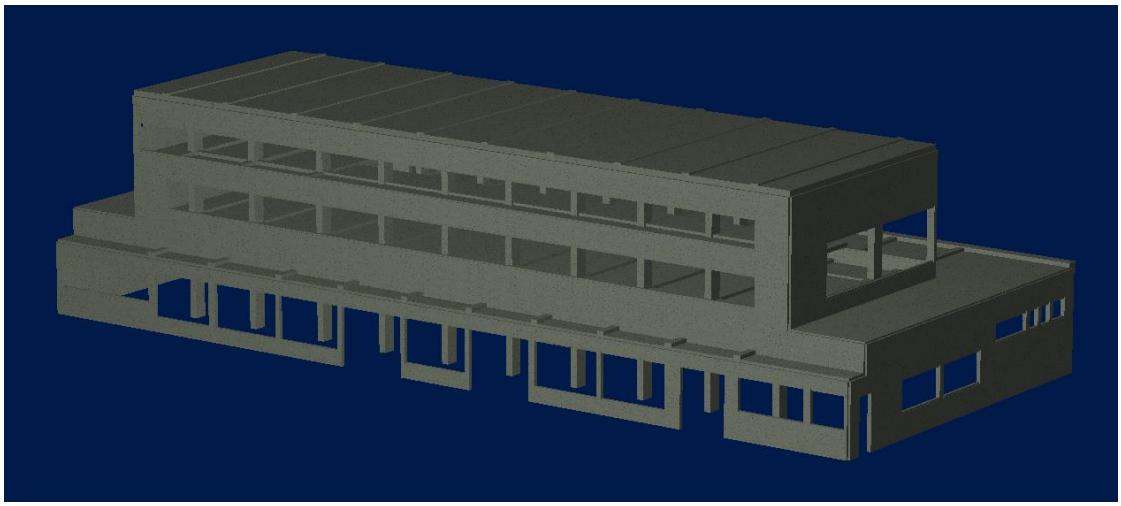

Figure 7.5: Shell Elements in RAM Elements Model

7.4. Application of Loads

The loads in the model are applied as pressures to the shell elements. For the dead load, the self weight is calculated automatically from the model. However, for some elements that have additional architectural finishes, additional superimposed dead loads must be added. The Level 3NP has alternating layers of concrete and slag, which were added. The live load and snow load were similarly applied to the slab shells.

For the lateral load, the main wind load pressures were applied to the wall shells (figure 7.6). However, at the openings, the pressure is not distributed automatically to the edges of the opening, so that had to be done automatically. Very small members were added within the wall shells at the top and bottom edges of the openings. Line loads were then applied to those members proportional to the distribution of the load from the window (figure 7.7). Since the members were modeled as very small members, self-weight and bending stiffness is minimal.

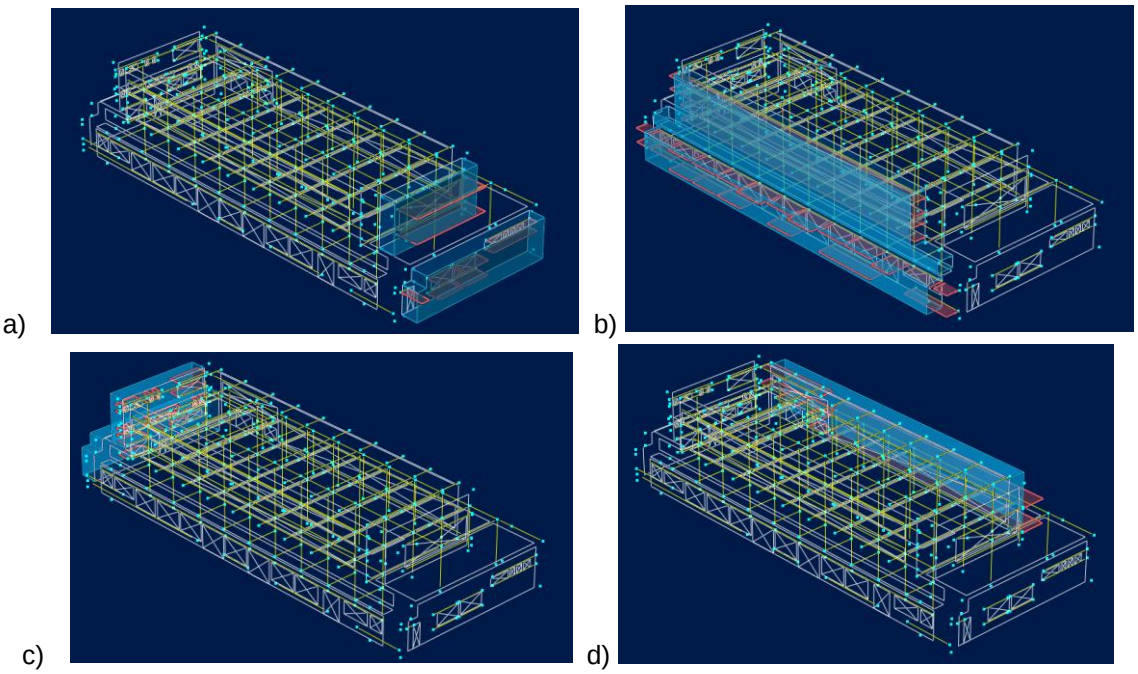

Figure 7.6: a) Northward Wind Loads b) Westward Wind Loads
c) Southward Wind Loads d) Westward Wind Loads

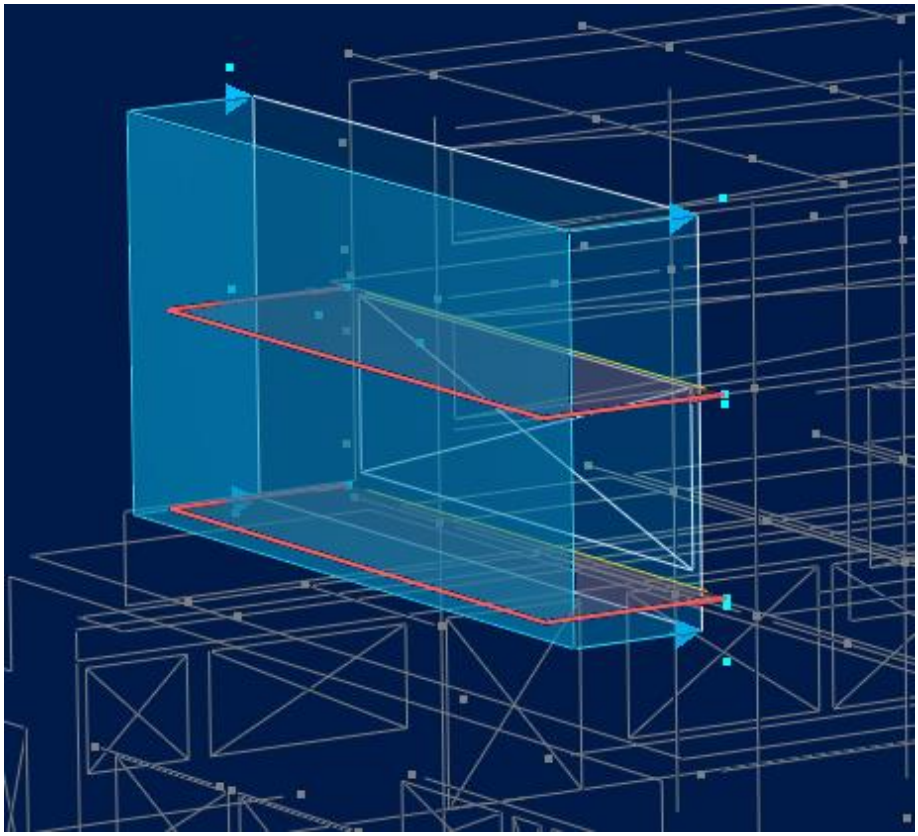

Figure 7.7: Line loads applied to window edges, south wall

7.5. Finite Element Discretization and Analysis Settings

Prior to running the analysis, the finite elements were discretized. Quadratic elements were used to create a more refined analysis. Various sizes were meshed to create a balance between realistic behavior and model computing size and time. In the end, a maximum note spacing of 50 cm was used (figure 7.8). This size fit well with the size of the wall shells and opening interfaces (figure 7.9).

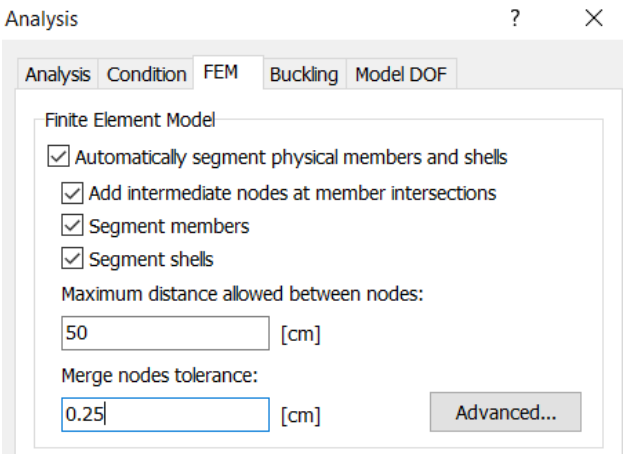

Figure 7.8: Finite Element input table from RAM Elements

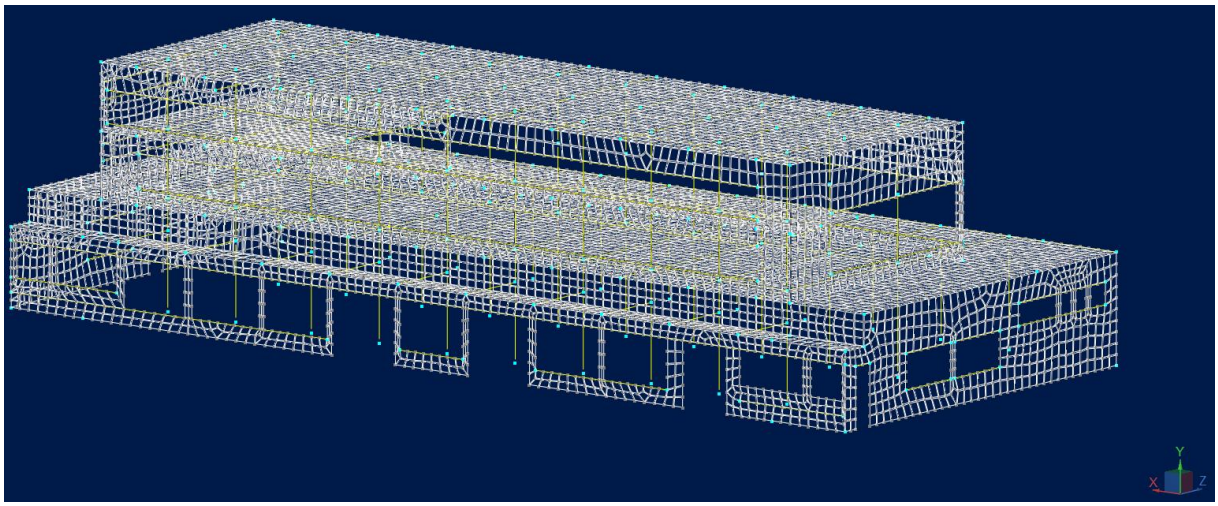

Figure 7.9: Finite elements in RAM Elements from the southwest

The analysis was then performed using a linear elastic analysis. The settings are shown in figure 7.10.

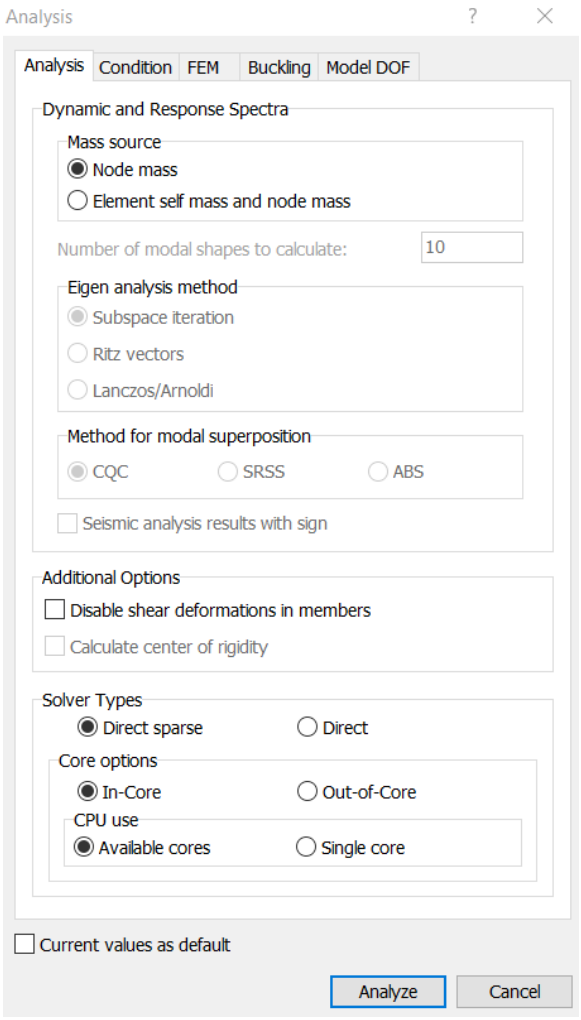

Figure 7.10: Analysis settings in RAM Elements

7.6. Analysis Results

The analysis provides reasonable and expected results. Upon performing verification procedures to confirm that the model is behaving properly. All loads are accounted for and hand checked moments and shears provided confirmation. Deflections of the members seemed reasonable.

Looking at the deflected shape, it is clear how the load from the wall affects the behavior of the entire structure (Figure 7.11). The most significant behavior relates to how the balcony area on level 2NP supports the wall on the western wall while that support does not exist at the eastern wall. Therefore, significant weigh of the wall on the eastern side of the building is concentrated on the roof framing, while it is distributed more evenly on the west side. This disproportionate loading causes the entire building to rotate. The maximum deflection of the center of the roof edge due to this rotation is less than 5 mm.

a)

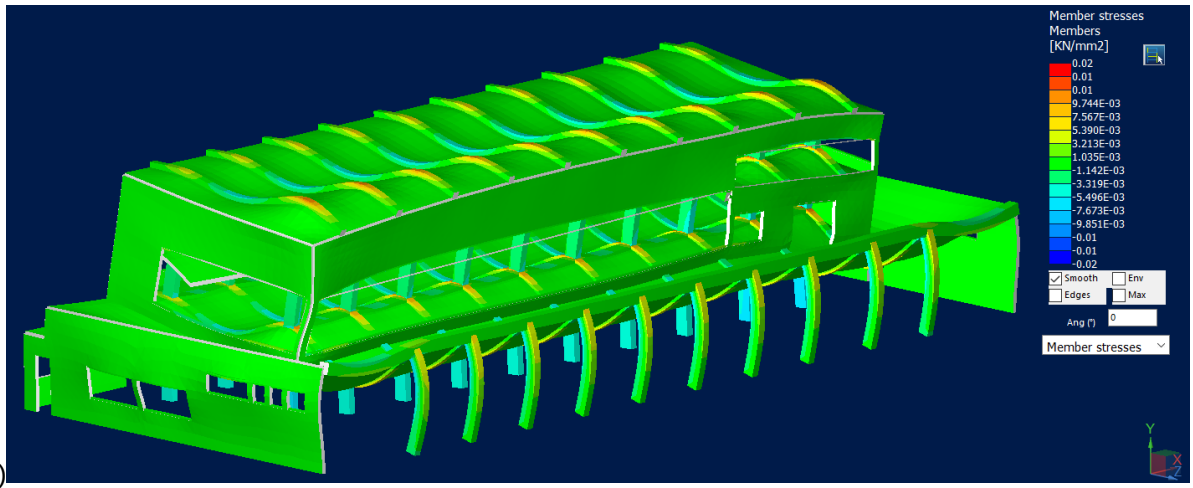

b)

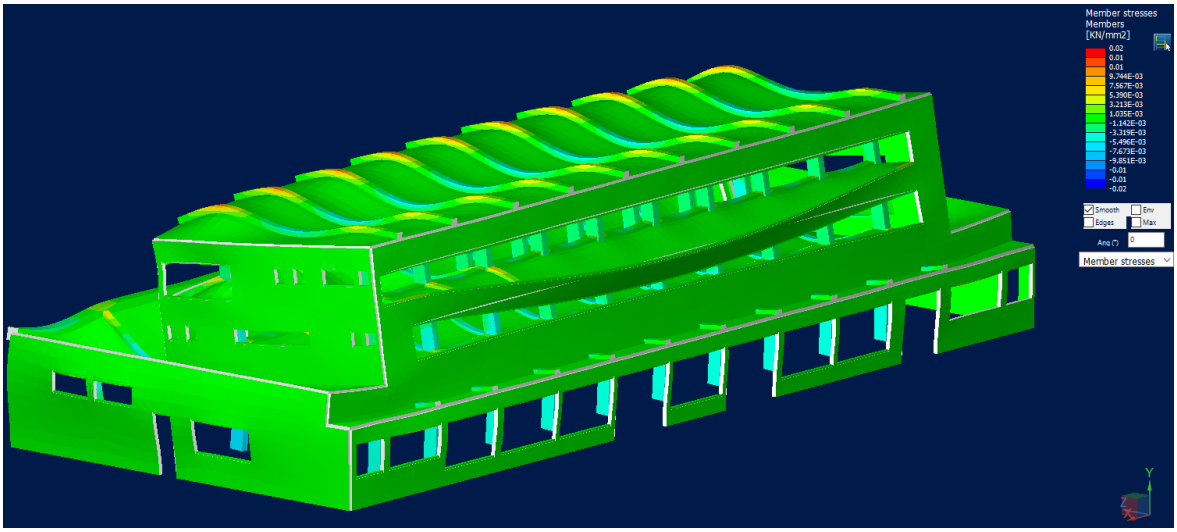

Figure 7.11: a) Member stresses for controlling load combination in the deformed shape from the southeast b) Member stresses for controlling load combination in the deformed shape from the northwest

Since the window openings are so long, it allows the walls at each level of the building to behave independently of the other wall areas. The downside of this is that the elements that connect the different wall areas are typically slender and transfer a large amount of load. This is most obvious example of this is the post between windows at the southeast corner of the building between levels 1NP and 3NP (figure 7.12). These concentration of force and stresses could cause cracking and damage. This is something that should be inspected in greater detail and would also be a candidate for more in-depth non-linear analysis. The other result of this load transfer is that the slab below has to support all the load. There is no beam directly below the wall in this area, so the slab is supporting it. This cause a significant amount of relative deflection at about 6 mm. The bearing conditions and reinforcement of this slab should be examined further to verify the adequacy of this condition.

a)

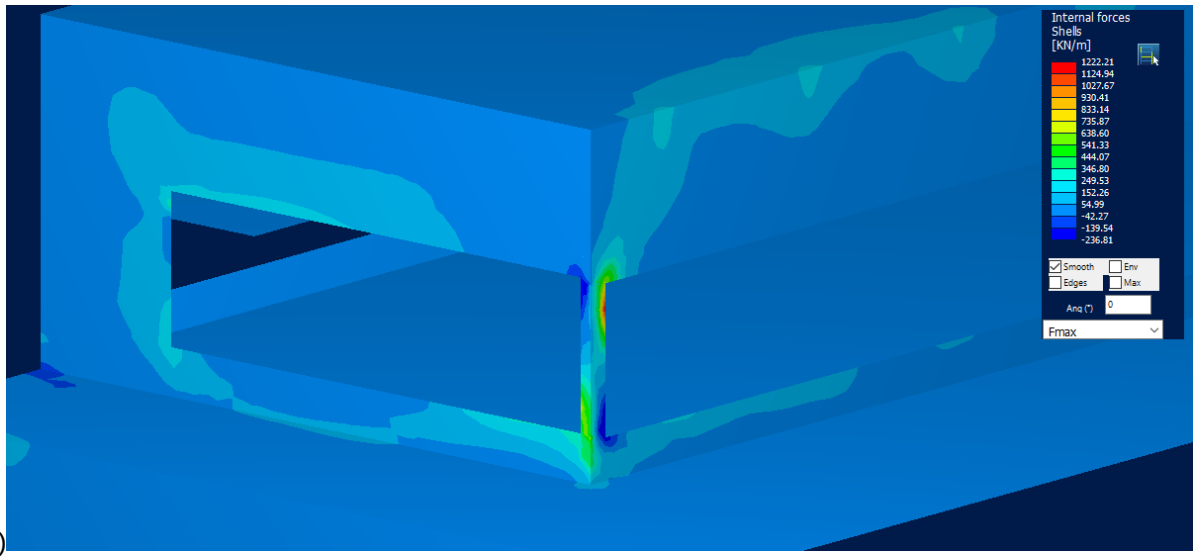

b)

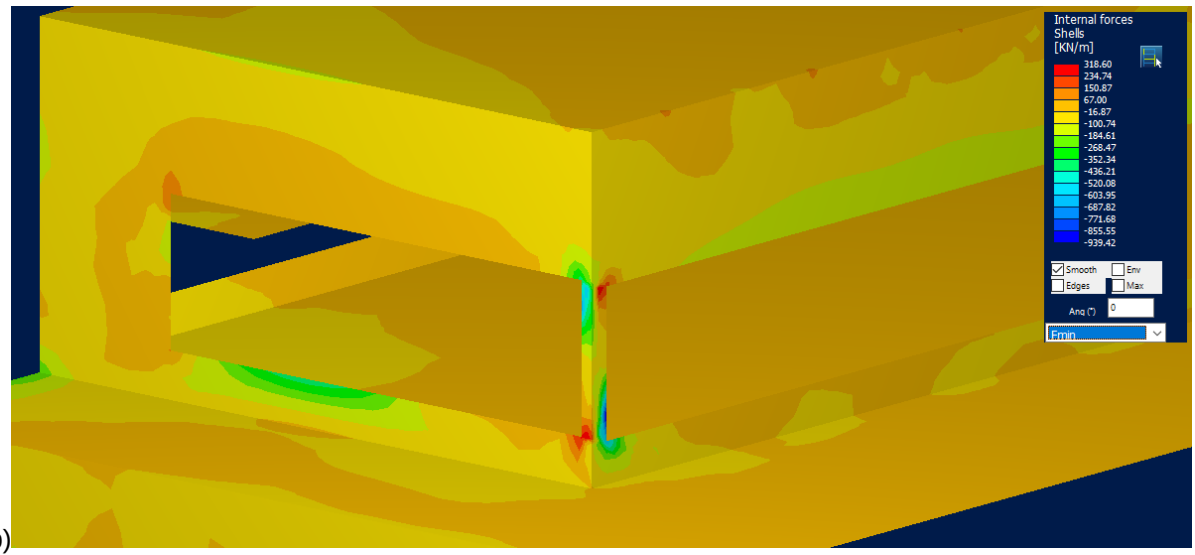

Figure 7.12: a) Maximum internal force envelope of southeast corner post b) Minimum internal force envelope of southeast corner post

In the area of the balcony on level 2NP where it is the torsional resistance of the longitudinal beams that stabilize the level, the entire wall and slab rotate, though the maximum deflection there is only 5 mm, which is below the limit. This further shows that the walls are likely supported at each level as the slabs have the capacity to resist it.

Additional results from the model will be investigated in more detail in chapters 8.

8. MEMBER ANALYSIS BASED ON EUROCODE

For a structural member to be completely verified a minimum amount of information must be known about the member. These attributes include material parameters, dimensions and reinforcement. In the survey of this building, the material properties have been tested and assumed. The cross-sectional dimensions have been measured. The exact reinforcement is known only in minimal member locations. That is the limitation for this part of the investigation, only a small number of members will be analyzed for their full bearing capacity due to lack of comprehensive information. In the slab locations, certain assumptions about the reinforcement will be made based on period literature for the sake of coming to a basic understanding of capacity.

8.1. Eurocode Analysis Parameters

The Eurocode 1992-1-1 - Design of Concrete Structures governs all design and analysis done on concrete buildings [20]. As with all design, the code sets failure mechanisms that must be checked if they apply to the assessed condition. These modes either fall under ultimate limit states (ULS) and serviceability limit states (SLS). ULS determine the safety of the building from a structural failure perspective, therefore ensuring the structure has enough capacity for its intended occupancy using safety factors. SLS deals with how the building functions during normal use.

For ultimate limit states, the failure mechanisms of bending, shear and torsion apply to Fuchs Café. Another ULS that would typically be checked is reinforcement anchorage and lapping, however there is simply not enough information about the reinforcing bar detailing to do this. The other ULS conditions that do not apply to this assessment are punching shear and fatigue. Punching shears is typically checked on flat slabs supported directly by columns or on columns bearing on a foundation system. The foundation system of this building is not known and will not be investigated. Fatigue occurs when a building is subjected to cyclical loading throughout its entire lifespan, upwards of 100,000 cycles, which commonly occurs on bridges.

Deflection control is the serviceability limit state that will be investigated here. Other SLS are crack control and stress limitations. Crack control in intended to set limits on the amount of crack expected from a member for a variety of reasons such as durability and cosmetic reasons. Stress limitations seek to set parameters to minimize the stress in certain locations for the purpose on increasing durability among other reasons.

Bending analysis occurs in the element locations with maximum moment. In the case of moment frame beams discussed here, midspan and the supports are typically the locations of the maximum positive bending moment and maximum negative bending moment, respectively. Only the locations of maximum positive bending will be investigated because only the bottom reinforcement is known. When a beam is subjected to bending, the tensile region of the beam will begin to crack, engaging the steel reinforcing

bars within. The concrete will be in compression on the other side of the neutral axis (figure 8.1). Within the bending check, there are three possible outcomes, a tension-controlled failure, compression-controlled failure or a balanced failure. Tension controlled failure occurs when the steel reinforcing bar begins to yield prior to the concrete reaching its maximum stress. This creates a slow ductile failure as the yielding steel allows a high amount of strain before rupture. Compression controlled failure occurs when the concrete compression interface is loaded beyond its maximum stress, causing a brittle, sudden failure. A balanced failure occurs when the concrete reaches its maximum stress at the same time the steel reaches its yield stress. This creates the most economic situation as all material is used to the fullest potential. In the beams check hereafter, they are all tension controlled, therefore the maximum steel strain ($\varepsilon_{ud} = 2.25$) is reached before the maximum allowable concrete strain is reached ($\varepsilon_{cu3} = 3.5$).

The equations that govern internal equilibrium are as follows:

$Fc = \eta * f_{cd} * \lambda * x * b_w$

$Ft = A_s * f_{yd}$

The moment capacity is then calculated as follows using the force and moment arm:

$M_{Rd} = F_c * [d - (\lambda * x) / 2]$

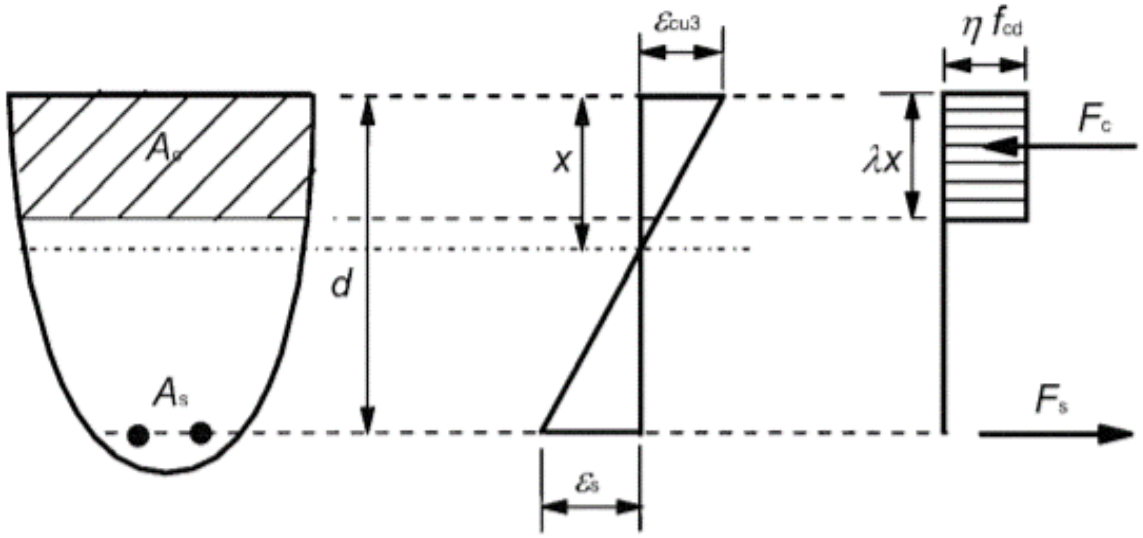

Figure 8.1: Concrete Beam Stress and Strain Distribution [20]

Resistance to shear forces in concrete beams is provided by the concrete strength and shear reinforcement also known as stirrups. The concrete acting without stirrups is verified first, using the equation given in the Eurocode as:

$V_{Rd,c} = [C_{Rd,c} * k (100 * \rho_1 * f_{ck})^{1/3} + k1 * \sigma_{cp}] b_w * d$ (equation 6.2a) [20]

greater than: $V_{Rd,c} = (vmin + k1 * \sigma_{cp}) b_w * d$ (equation 6.2b) [20]

If the concrete has enough capacity, only a minimum amount of stirrup reinforcement is required. The requirements of steel reinforcement ratio and maximum spacing are given respectively as follows:

$\rho_w = A_{sw} / (s * bw * \sin \alpha)$ (equation 9.4) [20]

greater than: $\rho_{w,\,min} = (0.08 * f_{ck}^{½}) / f_{yk}$ (equation 9.5N) [20]

$s_{l,max} = 0.75 * d (1+\cot \alpha)$ (equation 9.6N) [20]

Only if the concrete itself does not have enough capacity does shear reinforcement need to be detailed. For this assessment, the maximum shear force has been established from the RAM Elements model. This maximum force occurs adjacent to the boundary support of the beam. However, the shear capacity analysis occurs in the locations where the beams were previously surveyed. This is often away from the support, closer to midspan. The beams typically haunch close to the support to provide additional shear capacity. Some of the beams analyzed do not have enough concrete shear capacity and detailed shear reinforcement locations are not available. These locations must be verified with additional onsite testing to provide the stirrup spacing.

Selected beams are subjected to torsion as will in the building. The torsional capacity of a beam is approximated as a “thin walled closed section, in which equilibrium is satisfied by a closed shear flow” (figure 8.2) [20]. The torsional capacity and shear capacity of the section are compared in an interaction equation to verify adequacy. The variables that make up the interaction equation are as shown here followed by the interaction equation:

$V_{Ed} = \tau_t * t_{ef} * z$ (equation 6.27) [20]

$V_{Rdc} = [C_{Rd,c} * k (100 * \rho_1 * f_{ck})^{1/3} + k1 * \sigma_{cp}] b_w * d$ (equation 6.2a) [20]

$T_{Rdc} = 2 * v * \alpha_{cw} * f_{cd} * A_k * t_{ef} * \sin \Theta * \cos \Theta$ (equation 6.30) [20]

$(T_{Ed} / T_{Rdc}) + (V_{Ed} / V_{Rdc}) \leq 1.0$ (equation 6.31) [20]

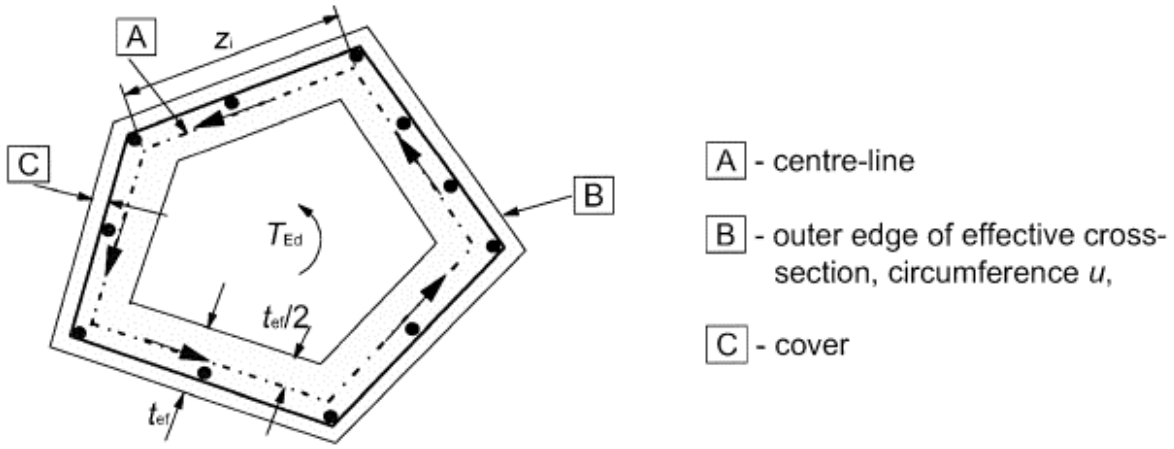

Figure 8.2: Eurocode 1992-1-1 Figure 6-11 - Concrete beam torsion distribution [20]

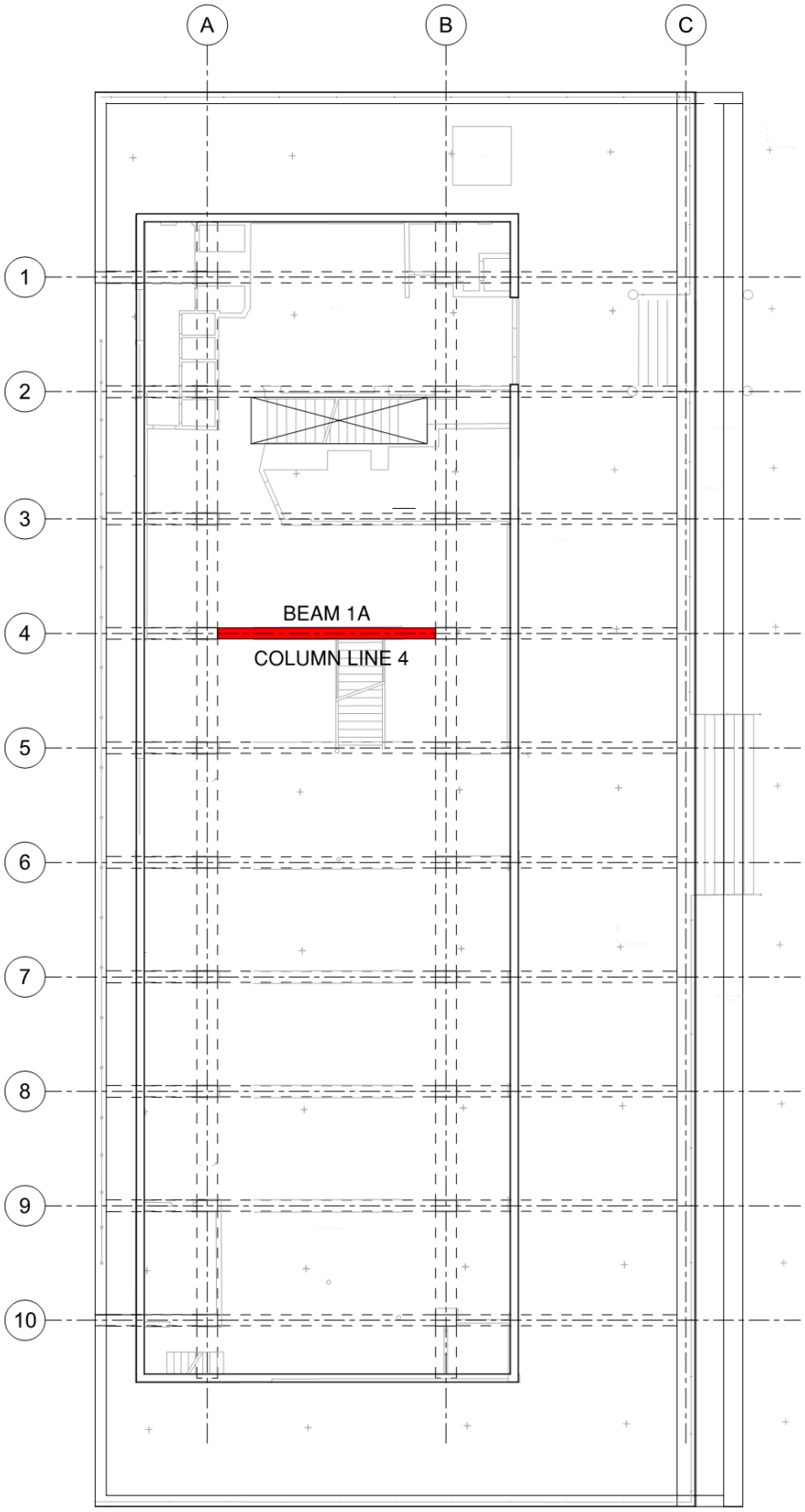

Figure 8.3: Level 1NP Framing Plan Showing Analysis Location

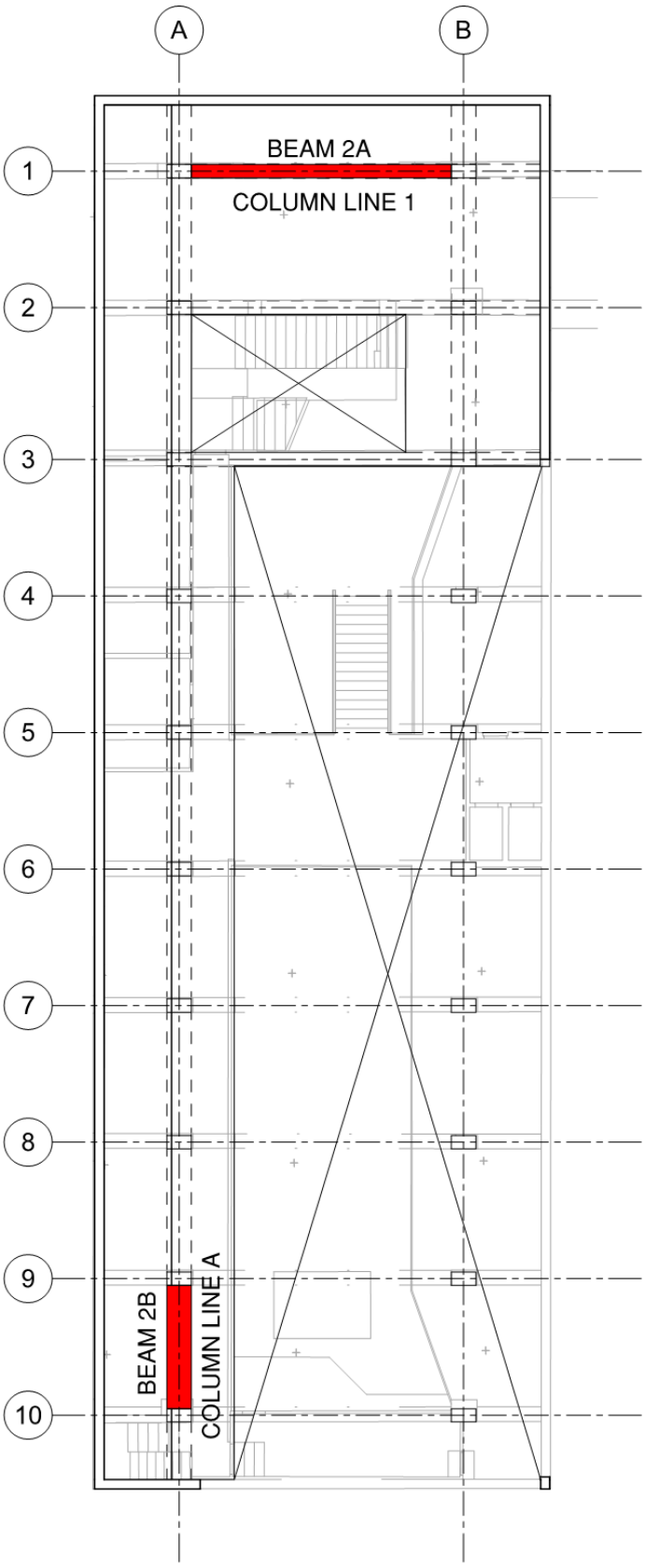

Figure 8.4: Level 2NP Framing Plan Showing Analysis Location

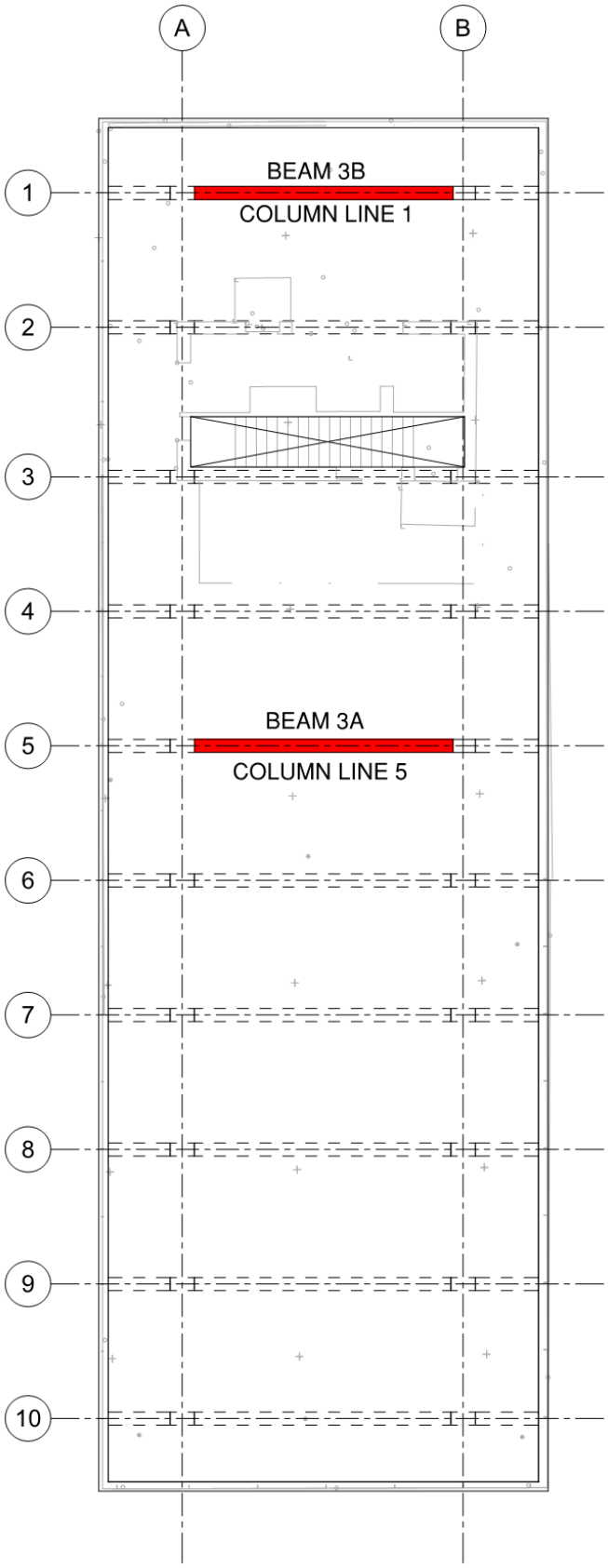

Figure 8.5: Level 3NP Framing Plan showing analysis location

8.2. Beam Analysis

8.2.1. Beam 1A Analysis

Beam 1A is a transverse beam on level 1NP at column line 4 as shown on figure 8.3. The beam is supporting the composite slab structure, which bears on top of the beam. It has five longitudinal bars and 7 mm diameter stirrups (figure 8.6). The beam is tension controlled because the steel reaches its yield point prior to the concrete (table 8.1).

The beam has sufficient bending capacity, however the shear check of the concrete strength fails (table 8.2). As previously discussed, the beam haunches at the support to provide additional shear capacity. If that added depth is estimated from the drawings and pictures, the new shear strength is adequate (table 8.3). With this assumption, the concrete by itself has enough strength to resist all the applied load. The stirrups, spaced at 20 cm, also fall within the maximum spacing limit. Therefore, with the previous assumptions, the beam is safe.

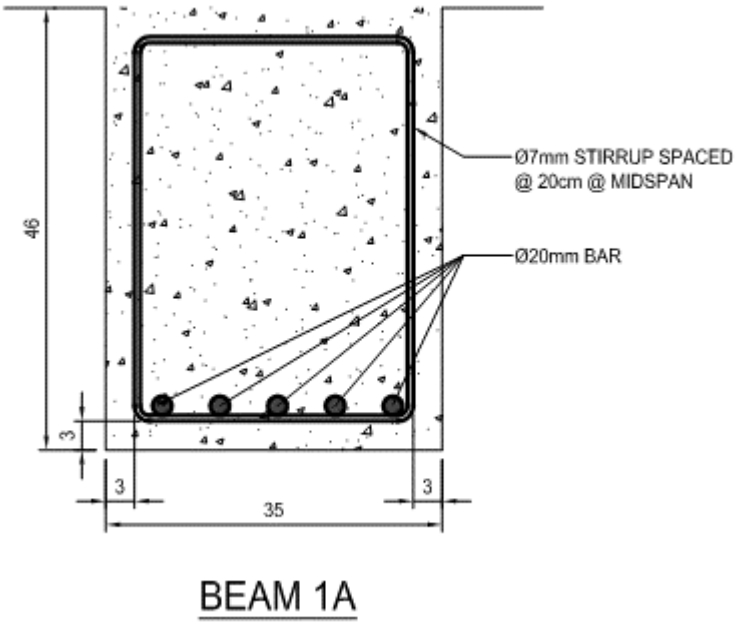

Figure 8.6: Beam 1A Cross Section with dimensions in centimeters [16]

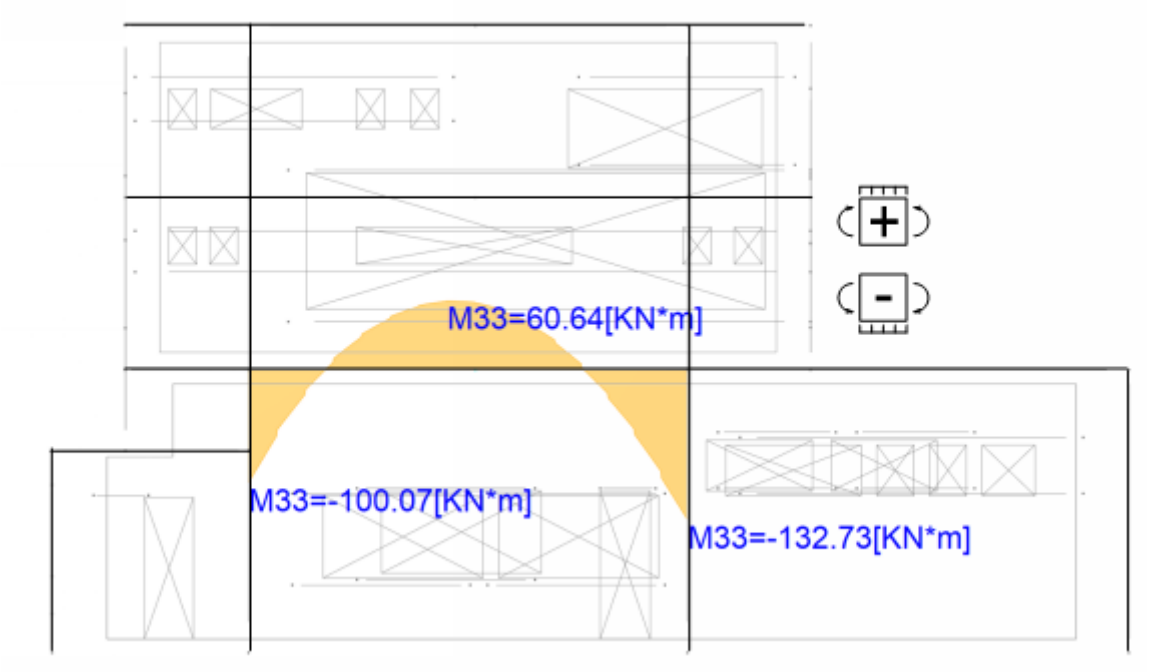

Figure 8.7: Beam 1A Moment Diagram from RAM Elements

Beam 1A (Transverse Beam 1NP) Concrete Capacity Check								
Thickness	t	460	mm	Concrete	Characteristic Strength	fck	12	MPa
Trans Bar Thk	d_t	6	mm		Partial Safety Factor	γc	1.5	
Cover	c	25	mm		Design Strength	fcd	8	MPa
Reinf Depth	d	429	mm		Youngs Modulus	Ec	21	GPa
Width	b	350	mm	Steel	Characteristic Strength	fyk	180	MPa
Area of Steel	As	1570	mm2		Partial Safety Factor	γs	1.15	
Comp Height	λ	0.8			Design Strength	fyd	157	MPa
Eff Strength	η	1			Youngs Modulus	Es	210	GPa

Set Internal Forces Equal at Steel Yield Point								
Conc Strain	ε_{cu3}	0.77	%	Internal Forces	Compression Force	Fc	246	kN
Steel Strain	ε_{ud}	2.25	%		Tension Force	Fs	246	kN
Neutral Axis	x	110	mm		Moment Arm	z	385	mm
Comp Block d	a	88	mm		Moment Capacity	MRd	95	kN*m
					Max Moment from Model	Med	60.6	kN*m
					Beam OK			

Table 8.1: Beam 1A Bending Capacity Check

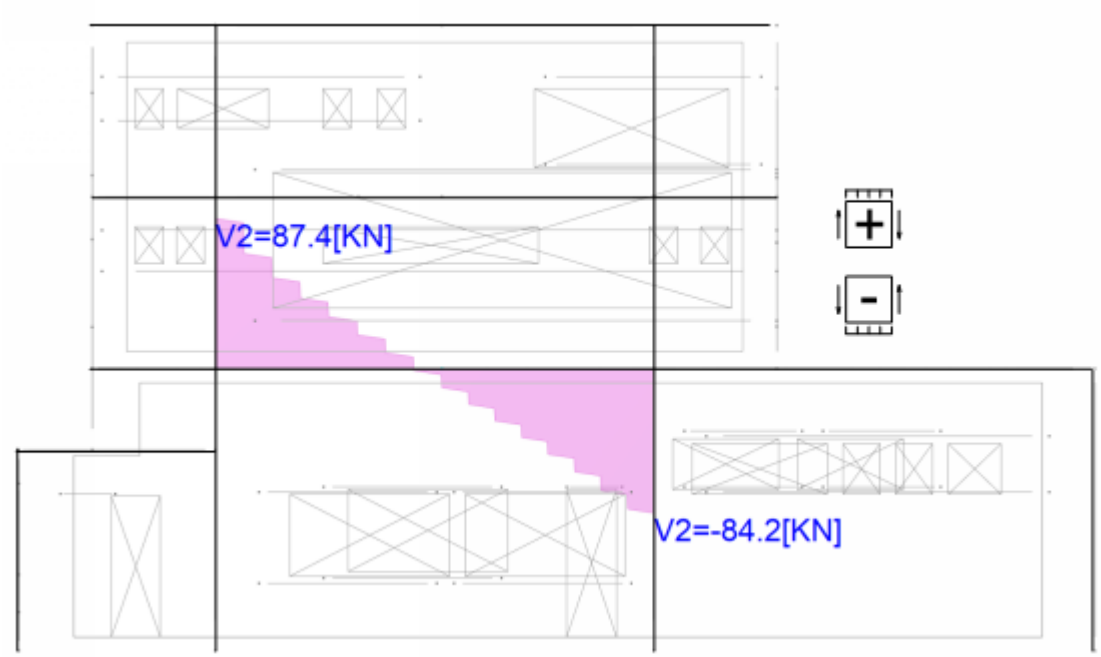

Figure 8.8: Beam 1A Shear Diagram from RAM Elements

Beam 1A Shear Capacity @ Midspan			
Factor	CRd,c	0.12	
Coefficient	k	1.68	
Reinf Ratio	rho	0.01	
Char Strength	Fck	12	Mpa
Eff Width	B	350	mm
Reinf Depth	d	429	mm
Shear Design	VRd,c	70.5	kN
Shear Effect	Ved,c	87.4	kN

Table 8.2: Beam 1A Shear Capacity Check at Midspan

Beam 1A Shear Capacity @ Haunch			
Factor	CRd,c	0.12	
Coefficient	k	1.59	
Reinf Ratio	rho	0.01	
Char Strength	Fck	12	Mpa
Eff Width	B	350	mm
Reinf Depth	d	569	mm
Shear Design	VRd,c	88.5	kN
Shear Effect	Ved,c	87.4	kN

Table 8.3: Beam 1A Shear Capacity Check at Haunch

8.2.2. Beam 2A Analysis

Beam 2A is a transverse beam on level 2NP at column line 1 as shown on figure 8.4. This beam is at the northern edge of the building so the slab south of the beam is composed of the composite slab structure, and the slab on the north side is solid reinforced concrete (figure 6.2). It has four longitudinal bars and 6 mm diameter stirrups (figure 8.9).

The exact bearing condition of the cantilevered slab is not known, but there are two possible outcomes. First, the composite slab and cantilevered slab are reinforced together in such a way that forces and moments are transferred between them and above the beam. If that is the case, Beam 2A will act as only a vertical support. However, the other possibility is that the composite slab structure is completely isolated from the beam and cantilevered reinforced slab. This could happen if the steel reinforcing in the cantilevered slab does not extend into the adjacent composite slab. The result of this is that Beam 2A would provide torsional restraint to the cantilevered slab. Based on material efficiency, it is assumed that the first condition exists. The reinforcing scenario that creates transfer between the two slab types would have been simple to implement during construction. Also, it would not make sense to unnecessarily subject a beam to torsion. Therefore, torsion will be neglected.

The beam is tension controlled because the steel reaches its yield point prior to the concrete (table 8.4). The beam has sufficient bending capacity but fails in shear capacity (table 8.5). There is currently no information about the stirrup reinforcing steel at the end of the beam where the shear force is the highest. The stirrups locations will need to be surveyed in the field to complete the beam analysis. The beam can be considered safe once the resulting shear reinforcing check is performed.

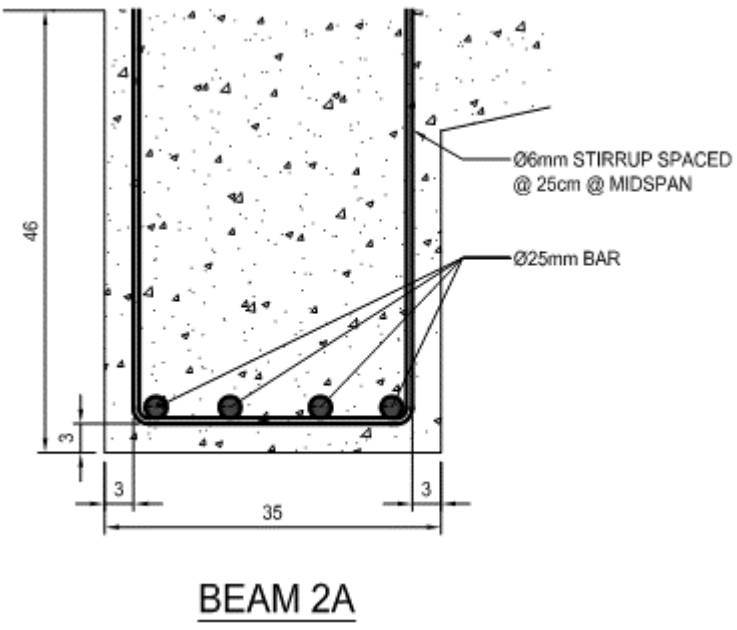

Figure 8.9: Beam 2A Cross Section with dimensions in centimeters [16]

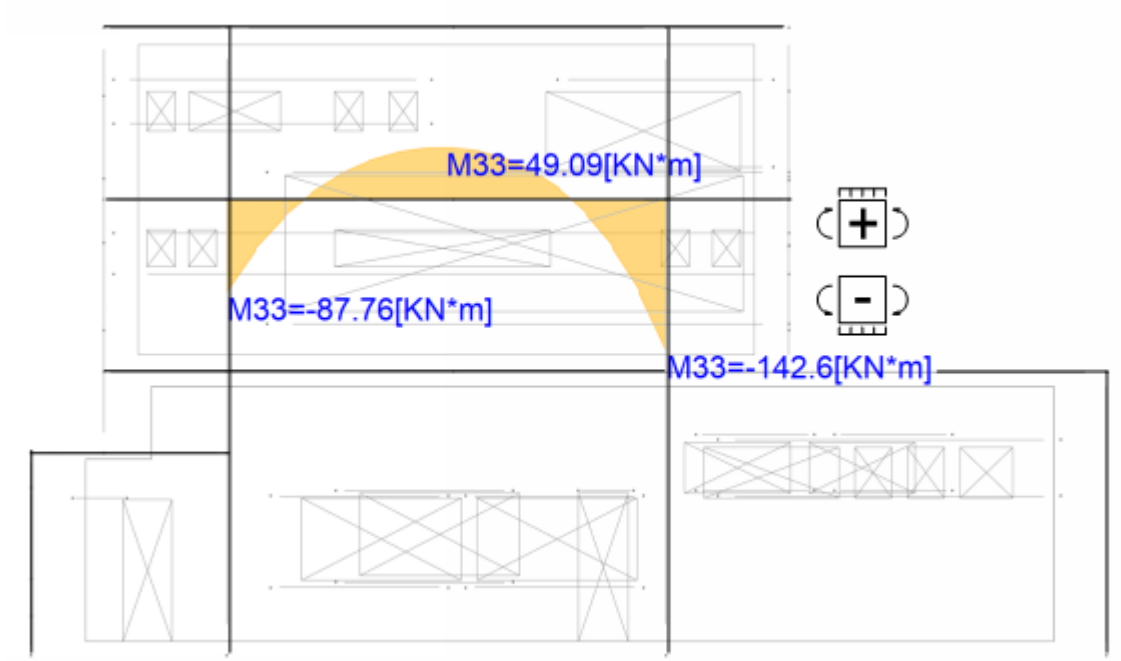

Figure 8.10: Beam 2A Moment Diagram from RAM Elements

Beam 2A (Transverse End Beam 2NP) Concrete Capacity Check								
Thickness	t	460	mm	Concrete	Characteristic Strength	fck	12	MPa
Trans Bar Thk	d_t	6	mm		Partial Safety Factor	γc	1.5	
Cover	c	30	mm		Design Strength	fcd	8	MPa
Reinf Depth	d	424	mm		Youngs Modulus	Ec	21	GPa
Width	b	350	mm	Steel	Characteristic Strength	fyk	180	MPa
Area of Steel	As	1964	mm2		Partial Safety Factor	γs	1.15	
Comp Height	λ	0.8			Design Strength	fyd	157	MPa
Eff Strength	η	1			Youngs Modulus	Es	210	GPa

Set Internal Forces Equal at Steel Yield Point								
Conc Strain	ε_{cu3}	0.82	%	Internal Forces	Compression Force	Fc	307	kN
Steel Strain	ε_{ud}	2.25	%		Tension Force	Fs	307	kN
Neutral Axis	x	113	mm		Moment Arm	z	379	mm
Comp Block d	a	91	mm		Moment Capacity	MRd	116	kN*m
					Max Moment from Model	Med	49.1	kN*m
					Beam OK			

Table 8.4: Beam 2A Bending Capacity Check

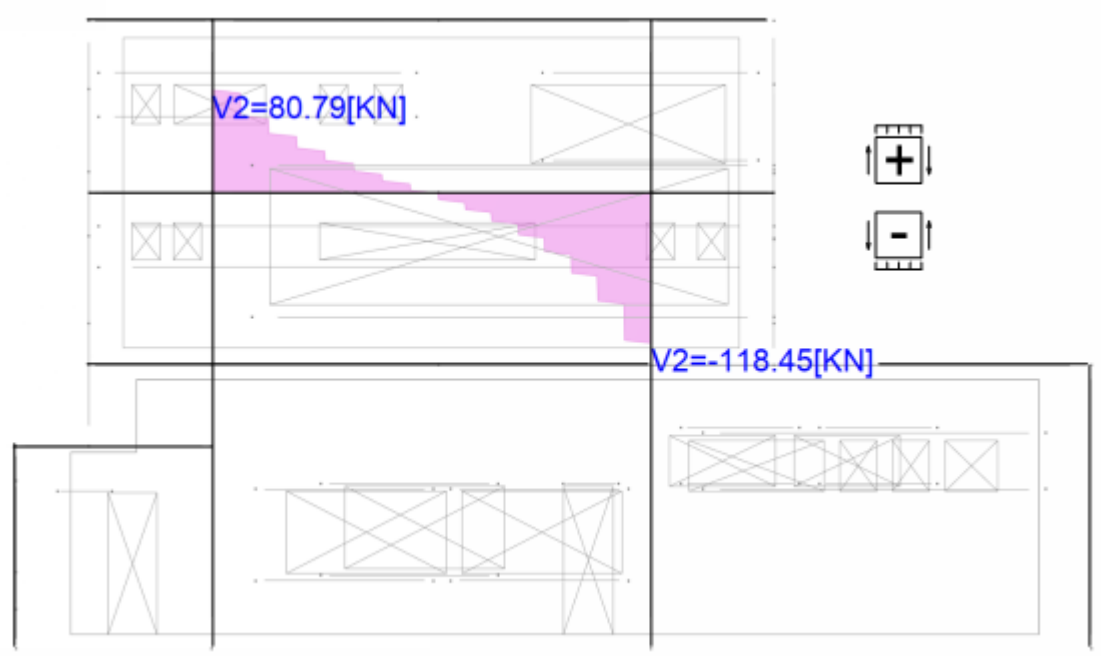

Figure 8.11: Beam 2A Shear Diagram from RAM Elements

Beam 2A Shear Capacity			
Factor	CRd,c	0.12	
Coefficient	k	1.69	
Reinf Ratio	rho	0.01	
Char Strength	Fck	12	Mpa
Eff Width	B	350	mm
Reinf Depth	d	424	mm
Shear Design	VRd,c	75.5	kN
Shear Effect	Ved,c	118	kN

Table 8.5: Beam 2A Shear Capacity Check

8.2.3. Beam 2B Analysis

Beam 2B is a longitudinal beam on level 2NP on the south side of the balcony area as shown on figure 8.4. The beam supports reinforced concrete slabs that cantilever from each side of the beam (figure 6.1). It has five longitudinal bars and 8 mm diameter stirrups (figure 8.12).

The beam is subjected to torsion as the beam is the only support for the slab on either side. The beam has a very large section, wider than it is deep, which helps provide better torsion resistance. Each cross-sectional dimension contributes to the torsional capacity; therefore, a square section provides the most economical torsional section for a beam. This beam, with a height to width ratio of 0.74, is the closest to 1.0 of all the beams investigated.

The beam is tension controlled because the steel reaches its yield point prior to the concrete (table 8.6). The beam has sufficient bending capacity and shear capacity (table 8.7). The concrete by itself has enough strength to resist all the applied load. The stirrups, spaced at 25 cm, also fall within the maximum spacing limit. In the torsional check, the beam is very close to the maximum capacity (table 8.8). Therefore, the beam is safe.

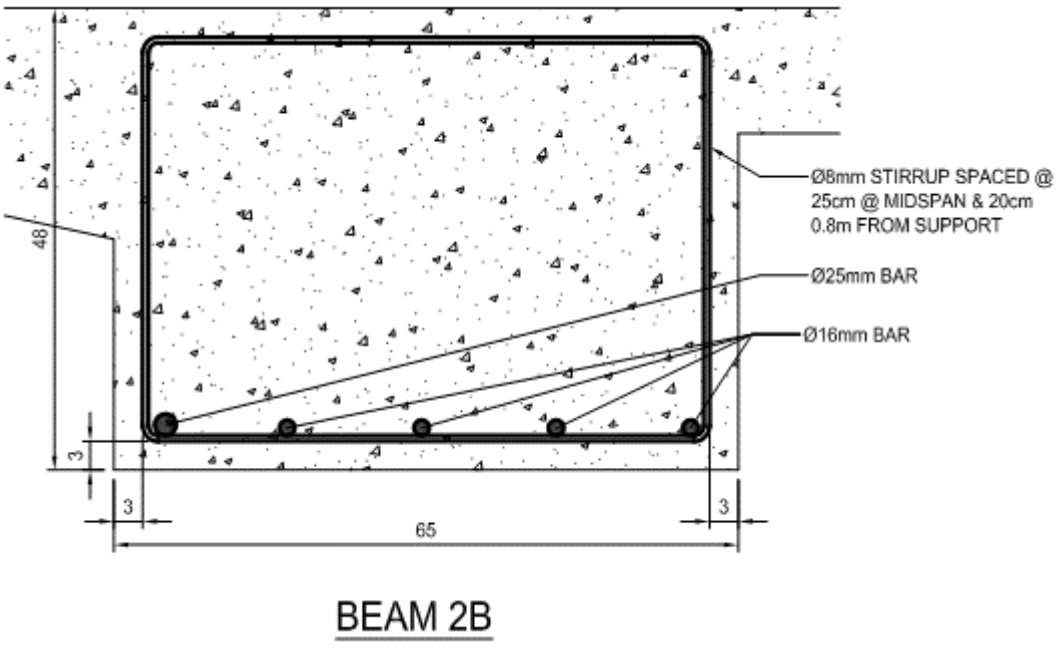

Figure 8.12: Beam 2B Cross Section with dimensions in centimeters [16]

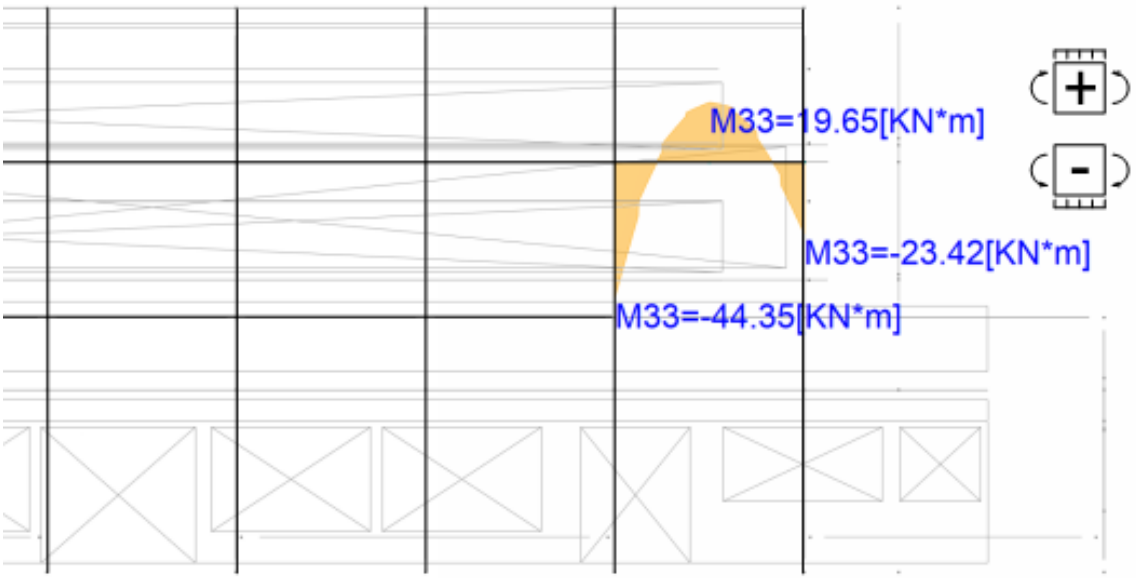

Figure 8.13: Beam 2B Moment Diagram from RAM Elements

Beam 2B (Longitudinal Beam 2NP) Concrete Capacity Check								
Thickness	t	480	mm	Concrete	Characteristic Strength	fck	12	MPa
Trans Bar Thk	d_t	8	mm		Partial Safety Factor	γc	1.5	
Cover	c	30	mm		Design Strength	fcd	8	MPa
Reinf Depth	d	442	mm		Youngs Modulus	Ec	21	GPa
Width	b	650	mm	Steel	Characteristic Strength	fyk	180	MPa
Area of Steel	As	1295	mm2		Partial Safety Factor	γs	1.15	
Comp Height	λ	0.8			Design Strength	fyd	157	MPa
Eff Strength	η	1			Youngs Modulus	Es	210	GPa

Set Internal Forces Equal at Steel Yield Point								
Conc Strain	ε_{cu3}	0.1318	%	Internal Forces	Compression Force	Fc	203	kN
Steel Strain	ε_{ud}	2.25	%		Tension Force	Fs	203	kN
Neutral Axis	x	24	mm		Moment Arm	z	432	mm
Comp Block d	a	20	mm		Moment Capacity	MRd	88	kN*m
					Max Moment from Model	Med	19.7	kN*m
					Beam OK			

Table 8.6: Beam 2B Bending Capacity Check

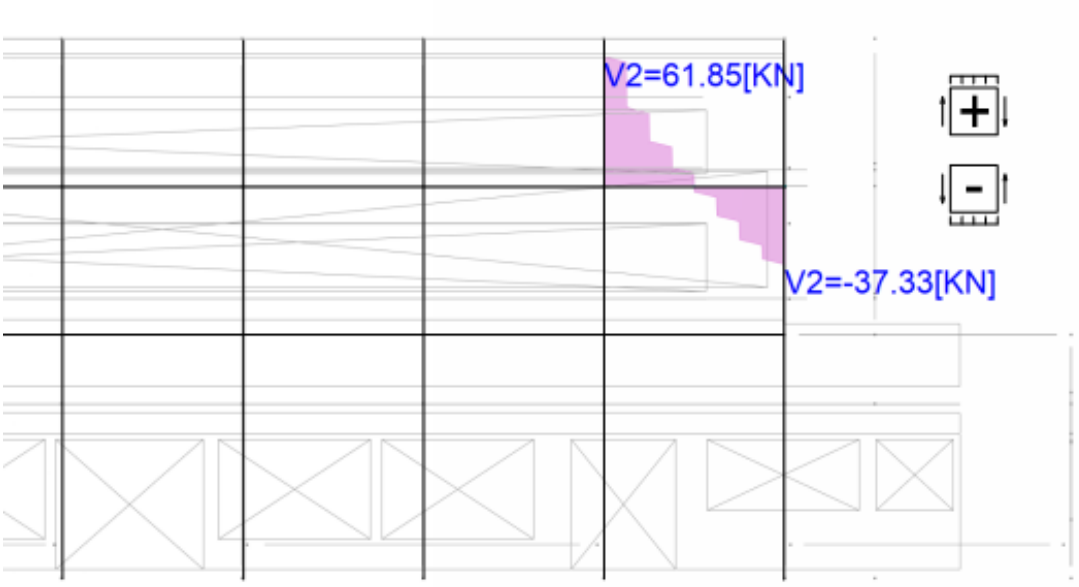

Figure 8.14: Beam 2B Shear Diagram from RAM Elements

Beam 2B Shear Capacity			
Factor	CRd,c	0.12	
Coefficient	k	1.67	
Reinf Ratio	rho	0.005	
Char Strength	Fck	12	Mpa
Eff Width	B	442	mm
Reinf Depth	d	650	mm
Shear Design	VRd,c	101.2	kN
Shear Effect	Ved	61.9	kN

Table 8.7: Beam 2B Shear Capacity Check

Beam 2B Torsion Capacity Check			
Cross Sec Area	A	0.312	m2
Circumfrance	u	2.26	m
Eff Wall Thick	t_{ef}	138	mm
Side Length	z_y	342	mm
Side Length	z_x	512	mm
Effective Area	A_k	0.175	m2
Applied torsion	T_{ed}	16.8	kN*m
Shear Force	V_{edy}	16.4	kN
Shear Force	V_{edx}	24.56	kN
Des Tor Res Mom	T_{rdc}	14770	kN*m
Coeff	v	0.571	
Alpha	α	1	
Strut Angle	Θ	0.78	°
Des Shear Res	V_{Rdc}	24.9	kN
Interaction Eq	<1	0.99	

Table 8.8: Beam 2B Torsion Capacity Check

8.2.4. Beam 3A Analysis

Beam 3A is a transverse beam on level 3NP at column line 5 as shown on figure 8.5. The beam is supporting the reinforced concrete slab structure. Because the slab above the beam is solid concrete and not the ceramic composite slab, for the purposes of bending and shear, the depth of the slab is included in the calculations. Therefore, the reinforcement depth of the beam (d) is increased by 13 centimeters. It has six longitudinal bars of different sizes and 6 mm diameter stirrups (figure 8.15).

The beam is tension controlled because the steel reaches its yield point prior to the concrete (table 8.9). The beam has sufficient bending capacity but fails in shear capacity (table 8.10). There is currently no information about the stirrup reinforcing steel at the end of the beam where the shear force is the highest. The stirrups locations will need to be surveyed in the field to complete the beam analysis. The beam can be considered safe once the resulting shear reinforcing check is performed.

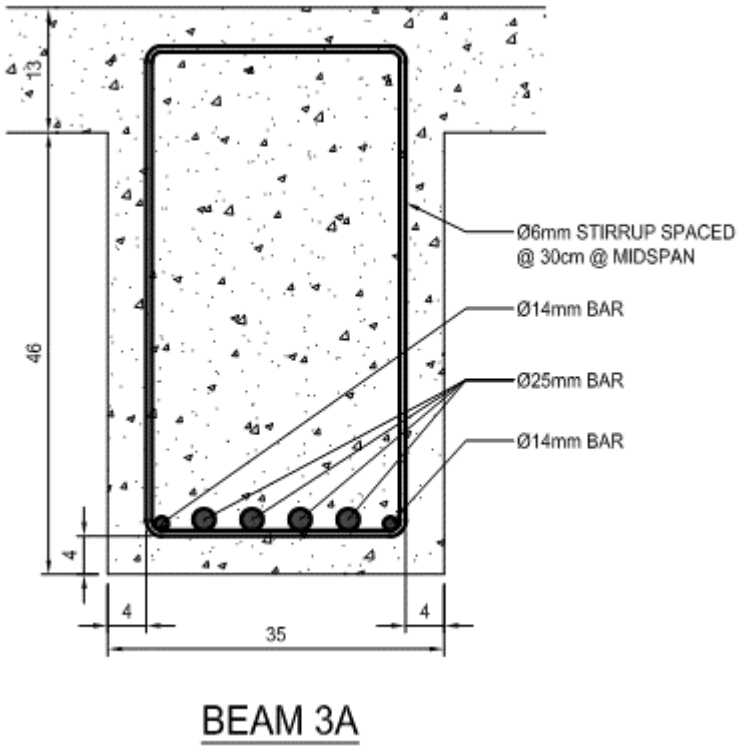

Figure 8.15: Beam 3A Cross Section with dimensions in centimeters [16]

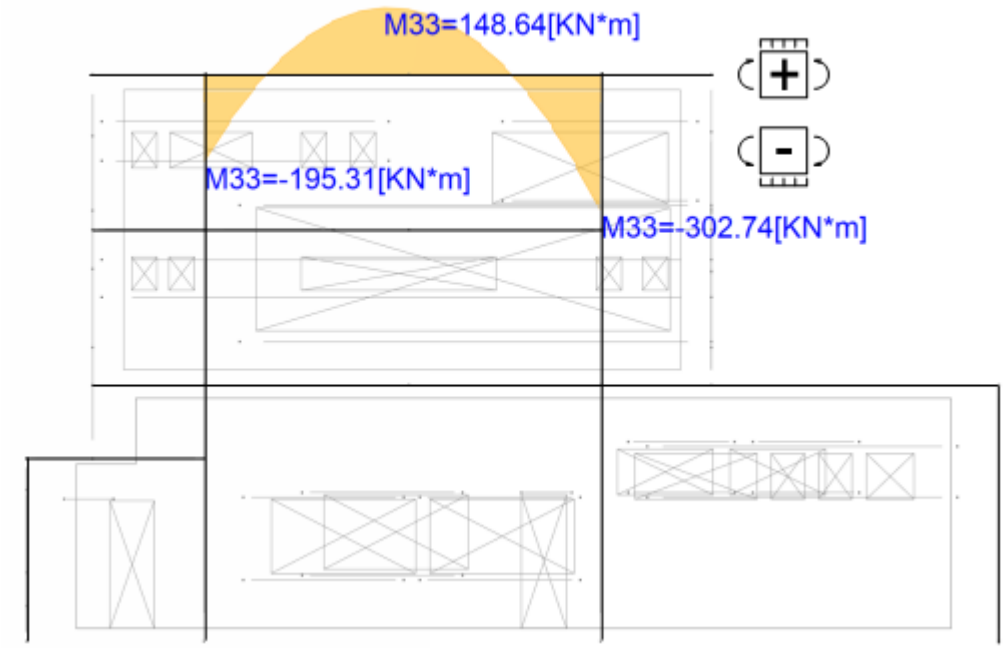

Figure 8.16: Beam 3A Moment Diagram from RAM Elements

Beam 3A (Transverse Beam 3NP) Concrete Capacity Check								
Thickness	t	590	mm	Concrete	Characteristic Strength	fck	12	MPa
Trans Bar Thk	d_t	6	mm		Partial Safety Factor	γc	1.5	
Cover	c	40	mm		Design Strength	fcd	8	MPa
Reinf Depth	d	544	mm		Youngs Modulus	Ec	21	GPa
Width	b	350	mm	Steel	Characteristic Strength	fyk	180	MPa
Area of Steel	As	2272	mm2		Partial Safety Factor	γs	1.15	
Comp Height	λ	0.8			Design Strength	fyd	157	MPa
Eff Strength	η	1			Youngs Modulus	Es	210	GPa

Set Internal Forces Equal at Steel Yield Point								
Conc Strain	ε_{cu3}	0.93	%	Internal Forces	Compression Force	Fc	356	kN
Steel Strain	ε_{ud}	2.25	%		Tension Force	Fs	356	kN
Neutral Axis	x	159	mm		Moment Arm	z	480	mm
Comp Block d	a	127	mm		Moment Capacity	MRd	171	kN*m
					Max Moment from Model	Med	148.6	kN*m
					Beam OK			

Table 8.9: Beam 3A Bending Capacity Check

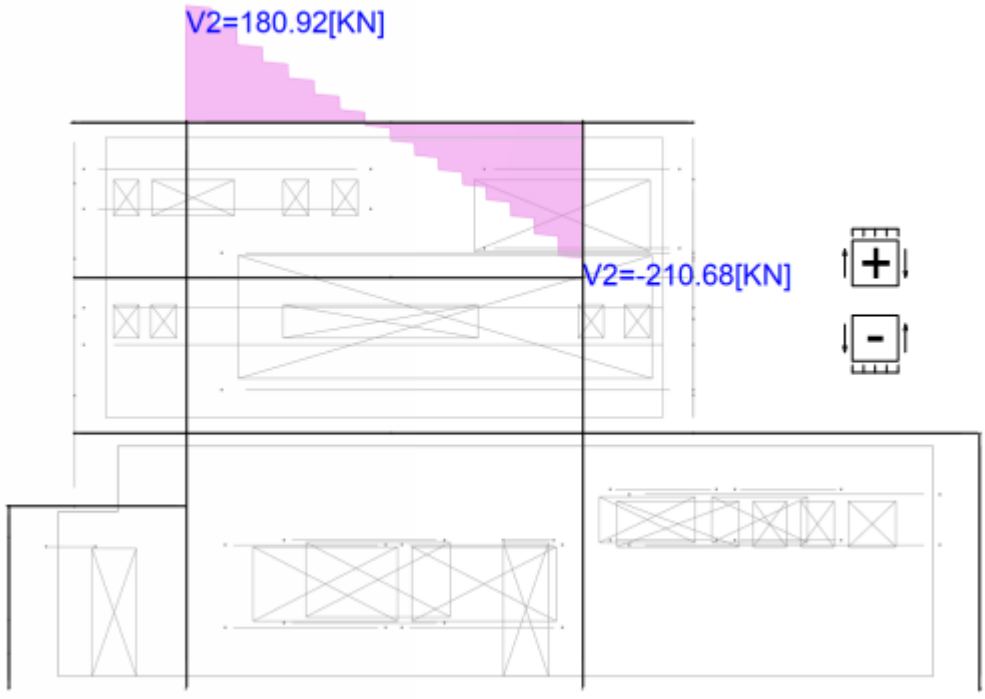

Figure 8.17: Beam 3A Shear Diagram from RAM Elements

Beam 3A Shear Capacity			
Factor	CRd,c	0.12	
Coefficient	k	1.61	
Reinf Ratio	rho	0.01	
Char Strength	Fck	12	Mpa
Width	B	350	mm
Reinf Depth	d	544	mm
Shear Design	VRd,c	89.1	kN
Shear Effect	Ved	211	kN

Table 8.10: Beam 3A Shear Capacity Check

8.2.5. Beam 3B Analysis

Beam 3B is a transverse beam on level 3NP at column line 1 as shown on figure 8.5. The beam is at the northern edge of the building supporting the reinforced concrete slab structure, which cantilevers to the north. This beam also has the extra help from the slab as this area was likely cast monolithically, increasing the depth of the slab. Therefore, the reinforcement depth of the beam (d) is increased by 13 centimeters. It has six longitudinal bars of different sizes and 7 mm diameter stirrups (figure 8.15).

Unlike the unknown of Beam 2A, with its cantilevered slab, it can safely be assumed that Beam 3B does not need to resist any torsion. Since there is a solid reinforced concrete slab on both side of the beam, it is expected that the steel reinforcement runs continuously between both sides of the beam.

The beam is tension controlled because the steel reaches its yield point prior to the concrete (table 8.11). The beam has sufficient bending capacity but fails in shear capacity (table 8.12). There is currently no information about the stirrup reinforcing steel at the end of the beam where the shear force is the highest. The stirrups locations will need to be surveyed in the field to complete the beam analysis. The beam can be considered safe once the resulting shear reinforcing check is performed.

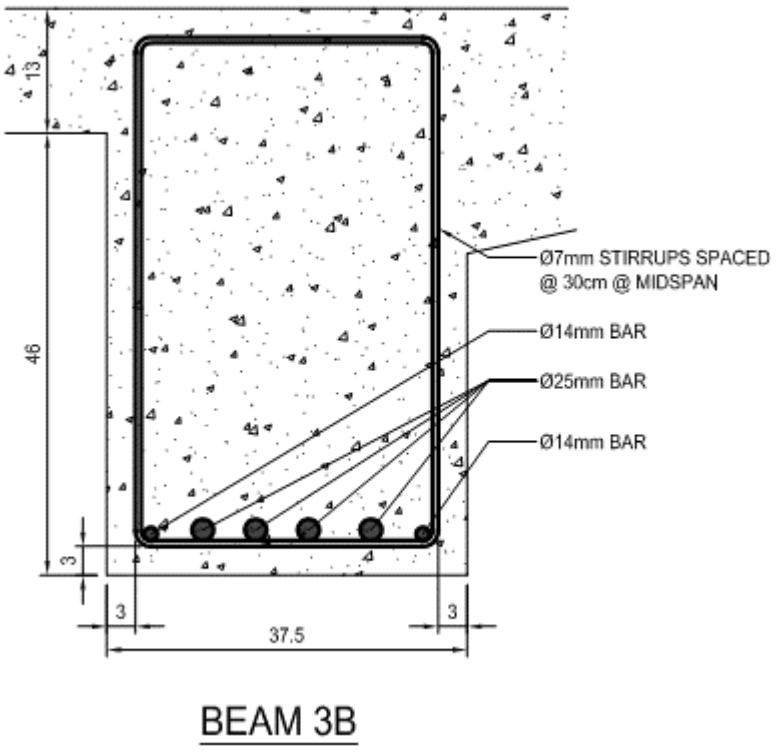

Figure 8.18: Beam 3B Cross Section with dimensions in centimeters [16]

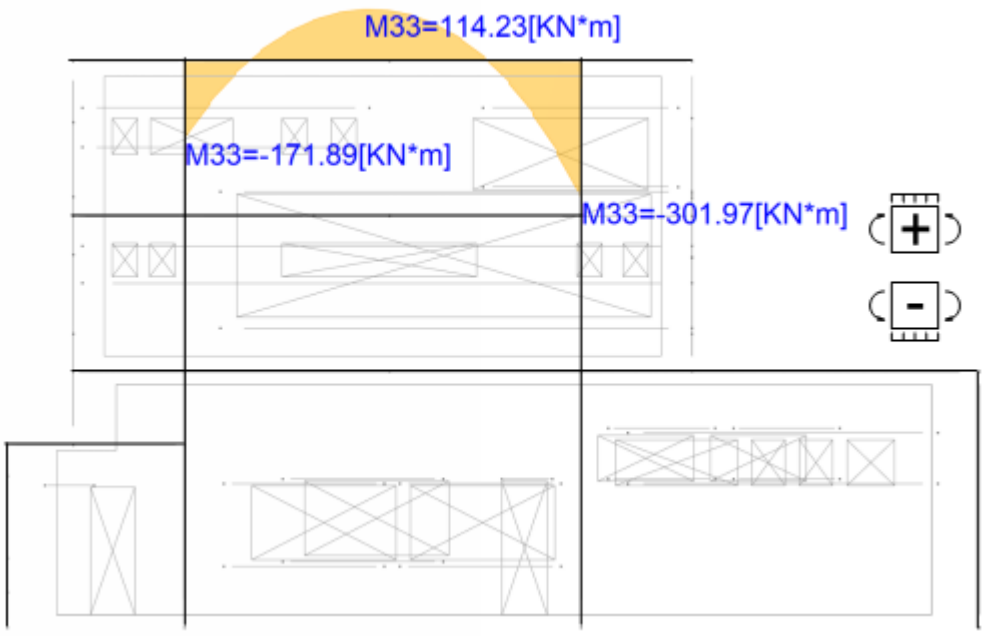

Figure 8.19: Beam 3B Moment Diagram from RAM Elements

Beam 3B (Transverse End Beam 3NP) Concrete Capacity Check								
Thickness	t	590	mm	Concrete	Characteristic Strength	fck	12	MPa
Trans Bar Thk	d_t	7	mm		Partial Safety Factor	γc	1.5	
Cover	c	30	mm		Design Strength	fcd	8	MPa
Reinf Depth	d	553	mm		Youngs Modulus	Ec	21	GPa
Width	b	375	mm	Steel	Characteristic Strength	fyk	180	MPa
Area of Steel	As	2272	mm2		Partial Safety Factor	γs	1.15	
Comp Height	λ	0.8			Design Strength	fyd	157	MPa
Eff Strength	η	1			Youngs Modulus	Es	210	GPa

Set Internal Forces Equal at Steel Yield Point								
Conc Strain	ε_{cu3}	0.82	%	Internal Forces	Compression Force	Fc	356	kN
Steel Strain	ε_{ud}	2.25	%		Tension Force	Fs	356	kN
Neutral Axis	x	148	mm		Moment Arm	z	494	mm
Comp Block d	a	119	mm		Moment Capacity	MRd	176	kN*m
					Max Moment from Model	Med	114	kN*m
					Beam OK			

Table 8.11: Beam 3B Bending Capacity Check

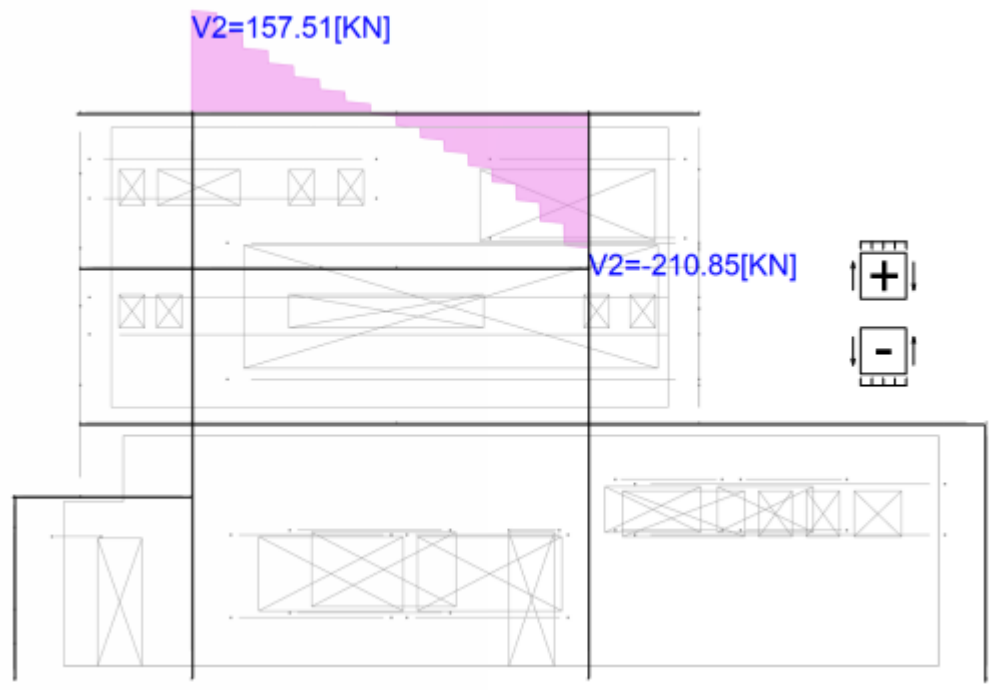

Figure 8.20: Beam 3B Shear Diagram from RAM Elements

Beam 3B Shear Capacity			
Factor	CRd,c	0.12	
Coefficient	k	1.6	
Reinf Ratio	rho	0.01	
Char Strength	Fck	12	Mpa
Eff Width	B	375	mm
Reinf Depth	d	553	mm
Shear Design	VRd,c	94.1	kN
Shear Effect	Ved,c	211	kN

Table 8.12: Beam 3A Shear Capacity Check

8.3. Beam SLS Results

The limits for deflection are based on occupant comfort as well as certain architectural finishes. The Eurocode dictates that any member that is subject to semi-permanent load is limited to a deflection of the span/250. All beam analyzed were well below this threshold with the SLS loads applied.

Beam	Deflection	Defl Limit
BM1A	3.6 mm	30 mm
BM2A	2.9 mm	30 mm
BM2B	1.2 mm	14 mm
BM3A	1.9 mm	30 mm
BM3B	2.2 mm	30 mm

Table 8.13: Concrete Beam Deflection Control

8.4. Composite Slab Analysis

As previously discussed, there is no information available regarding the reinforcing of the composite slabs. These elements are very important in the scope of the building, so the reinforcing must be estimated to set a baseline of the slab capacity. Relevant information is available in the form of historical documentation about similar types of slabs. The book “Železový beton v pozemním stavitelství II” by Jan Paul [17] discusses common techniques used in the era of this building. Included in this discussion are minimum reinforcing sizes and different detailing practices.

In the book, Paul indicates that typically two or three reinforcing bars are were typically placed between the ceramic ribs. The size of these bars ranged from 10 mm diameter to 16 mm diameter. Therefore, the minimum reinforcing possible for the slab would be two 10 mm diameter bars per rib. This configuration yields an area of steel of 156 mm^2, which will be used for this analysis.

Additionally, there were two typical ways of detailing the longitudinal reinforcement. The first assumed the slab was simply supported at the boundaries, meaning there was no rotational resistance at the supports. This means there was only positive moment on the beam and therefore, the beam only required bottom reinforcement. The book provides a typical detailing of a slab in this condition (figure 8.21). The two bars are run the length of the beam at the bottom. Then at the support, one of the bars is bent up to the beam top, which provides some shear strength. For all intents and purposes, the beam has no negative bending steel and resistance.

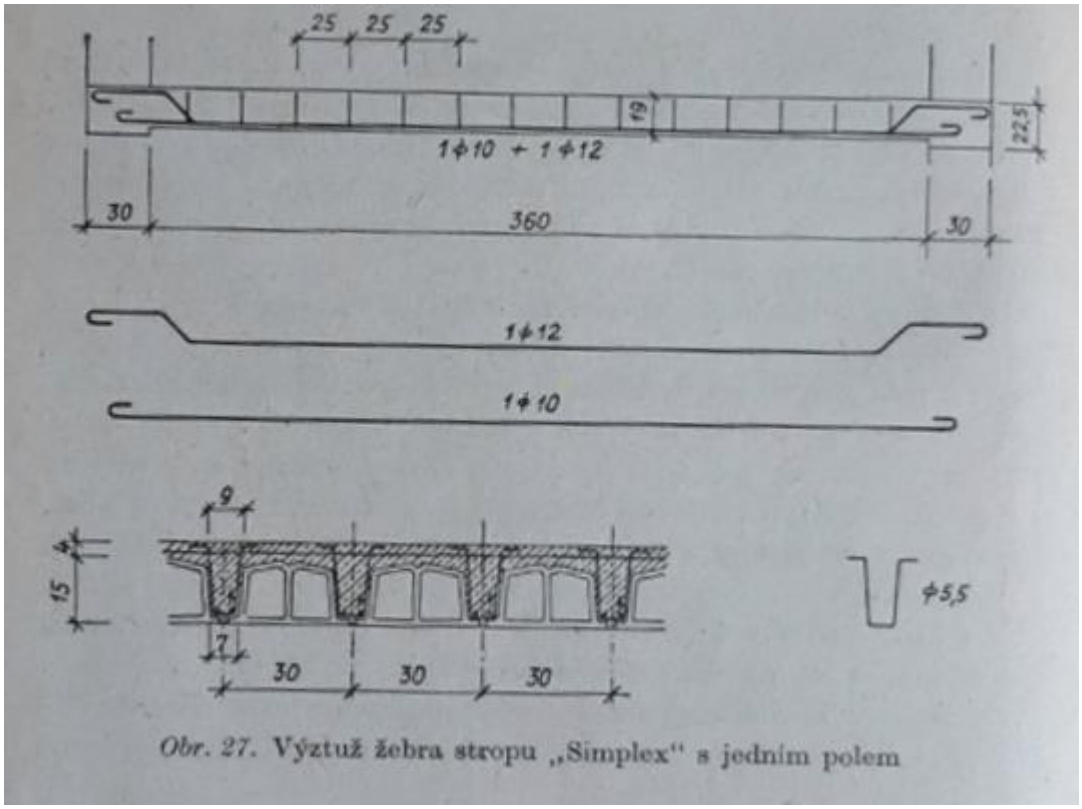

Figure 8.21: Typical composite slab reinforcing details in simple span condition [17]

Alternately, if the slab was designed to be continuous, additional top reinforcement would be detailed at the supports to resist the negative moment. An example of this is shown in figure 8.22. At the location of maximum negative moment, over the support, there are three bars shown.

For this analysis, the minimum bottom reinforcement has already been estimated, which is intended to resist the maximum positive moment. This minimum reinforcement would be the same for both possible detailing conditions. The reinforcement detail at the support is not known and would have to be verified in order to confirm these assumptions. The calculation of the applied moment on the beam will be checked in both conditions. Moment and shear diagrams have been created to compare the adequacy of the minimum reinforcement in each condition.

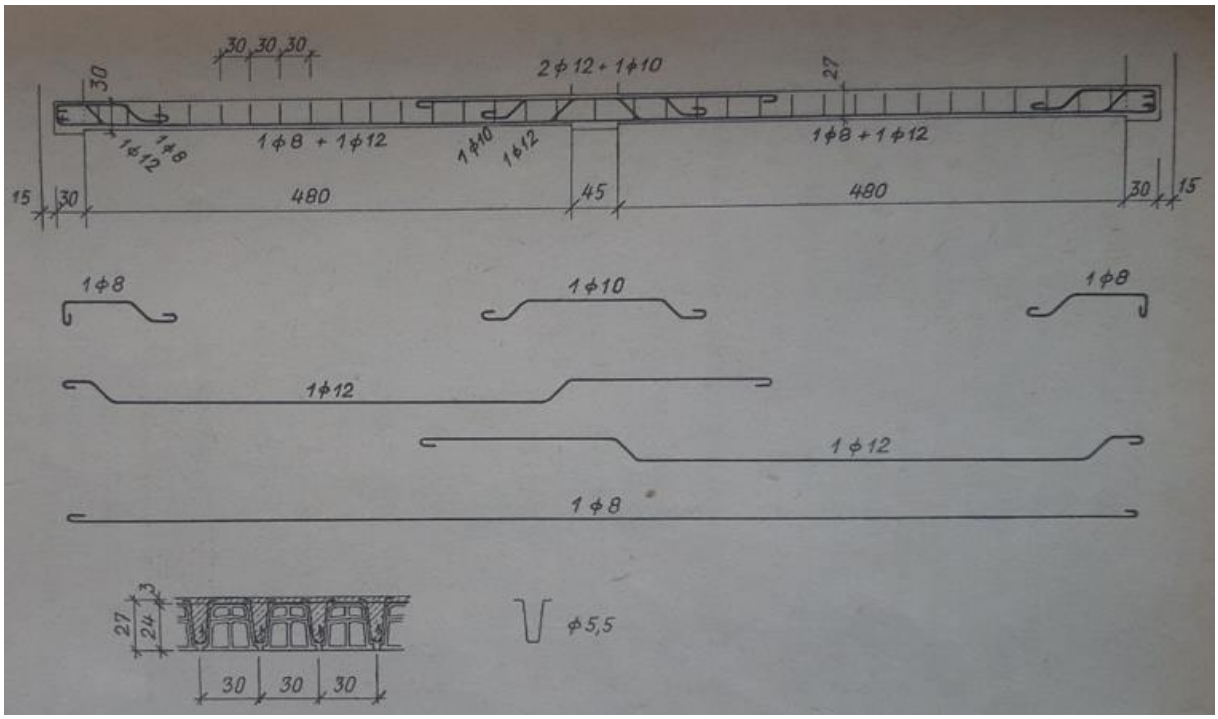

Figure 8.21: Typical composite slab reinforcing details in continuous span condition [17]

8.4.1. Slab 1NP Analysis

The slab at level 1NP is the thicker of the two composite slabs. The ceramic inserts are 30 centimeters wide and 15 centimeters deep (figure 22). Because of this, the analysis will be performed assuming that the structure is a 30 centimeter wide T-beam. For the bending of a T-beam, it needs to be verified whether the compression block of the slab is within the flange of the T. The slab is shown with two longitudinal bars and 5 mm diameter stirrups.

The moment diagrams in figure 8.23 and figure 8.24 show the bending moment intensity or moment per meter width in the continuous span condition and simple span condition, respectively. The maximum positive bending moment intensity from those diagrams is entered into table 8.14. Likewise, the shear diagrams of figure 8.25 and figure 8.26 express the shear force intensity or shear per meter width. The maximum shear is entered into table 8.15.

The slab is tension controlled because the steel reaches its yield point prior to the concrete and compression block does not extend into the stem of the T-beam (table 8.14). The slab has sufficient bending capacity and shear capacity (table 8.15). The concrete by itself has enough strength to resist all the applied load. Therefore, the slab is safe given the assumed minimum reinforcing parameters.

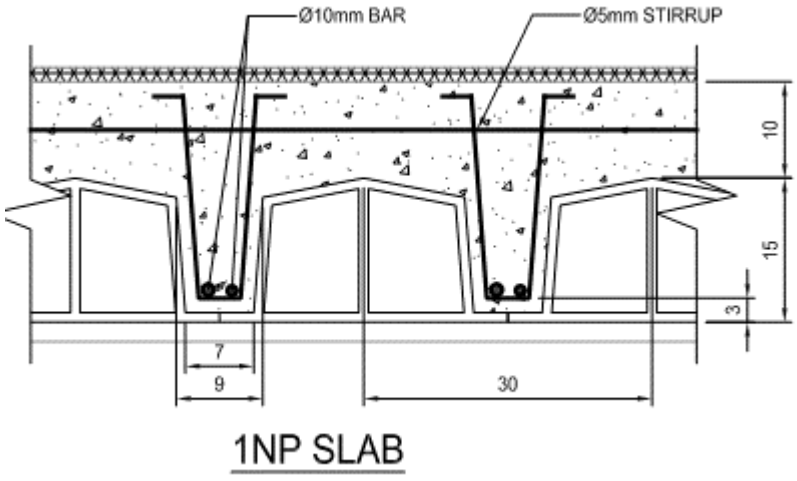

Figure 8.22: Level 1NP Slab Cross Section with dimensions in centimeters [16]

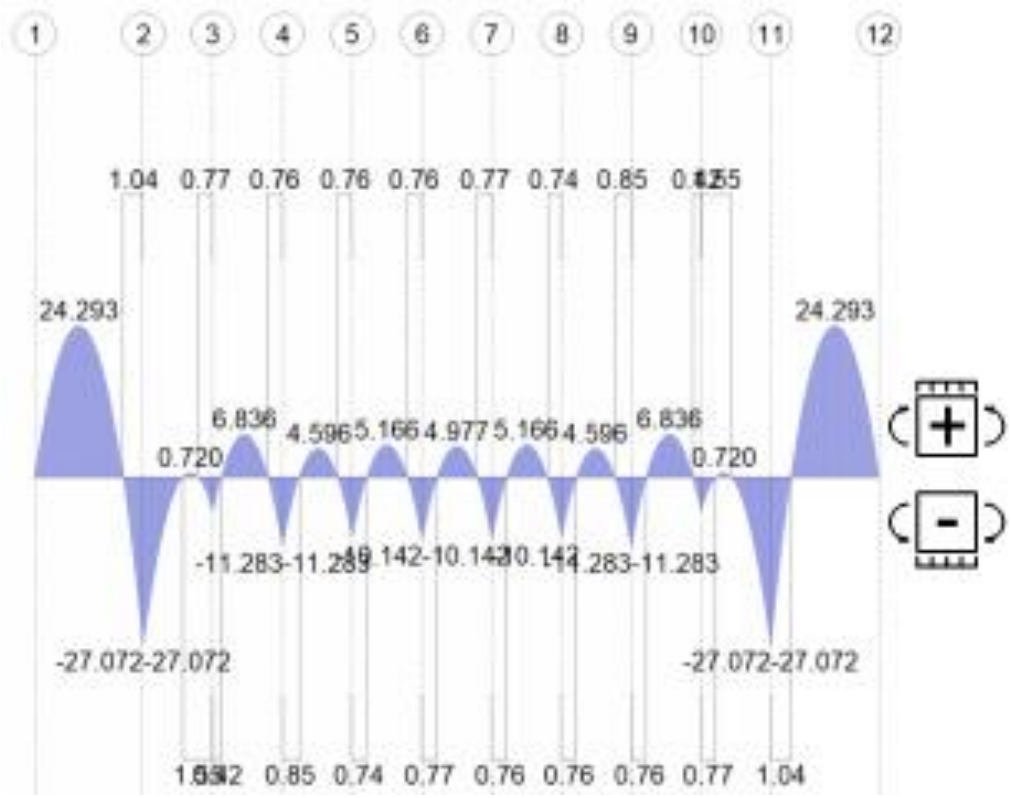

Figure 8.23: Level 1NP Moment Diagram from Continuous Reinforcement Condition (kN-m/m)

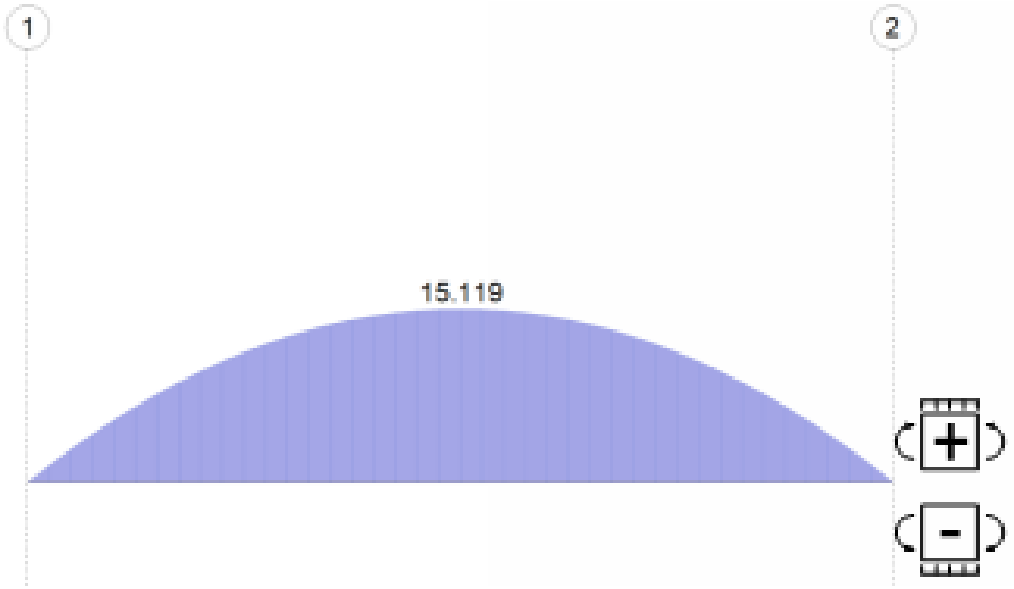

Figure 8.24: Level 1NP Moment Diagram from Simple Span Condition (kN-m/m)

Slab 1NP Concrete Reinforcement Capacity Check for 300 mm Section								
Thickness	t	250	mm	Concrete	Characteristic Strength	fck	12	MPa
Trans Bar Thk	d_t	6	mm		Partial Safety Factor	γc	1.5	
Cover	c	25	mm		Design Strength	fcd	8	MPa
Reinf Depth	d	219	mm		Youngs Modulus	Ec	21	GPa
Width	b	300	mm	Steel	Characteristic Strength	fyk	180	MPa
Area of Steel	As	157	mm2		Partial Safety Factor	γs	1.15	
Comp Height	λ	0.8			Design Strength	fyd	157	MPa
Eff Strength	η	1			Youngs Modulus	Es	210	GPa

Set Interior Forces Equal at Steel Yield Point								
Conc Strain	ε_{cu3}	0.14	%	Internal Forces	Compression Force	Fc	25	kN
Steel Strain	ε_{ud}	2.25	%		Tension Force	Fs	25	kN
Neutral Axis	x	13	mm		Moment Arm	z	214	mm
Comp Block d	a	10	mm		Moment Capacity	M	5	kN*m

Bending Moment Intensity (Per Meter)			
Unit Moment Capacity	M_{Rd}	17.52	kN*m
Max Moment Continuous	M_{ed}	6.8	kN*m
Max Moment Simple Span	M_{ed}	15.1	kN*m
Slab OK			

Table 8.14: Level 1NP Slab Bending Capacity Check

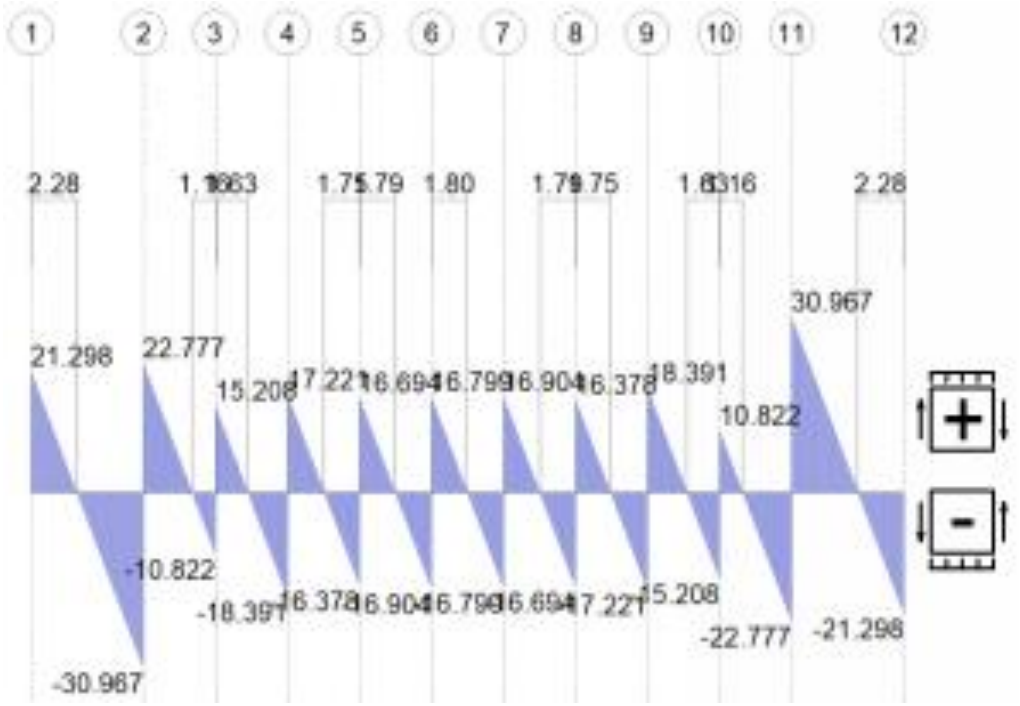

Figure 8.25: Level 1NP Shear Diagram from Continuous Reinforcement Condition (kN/m)

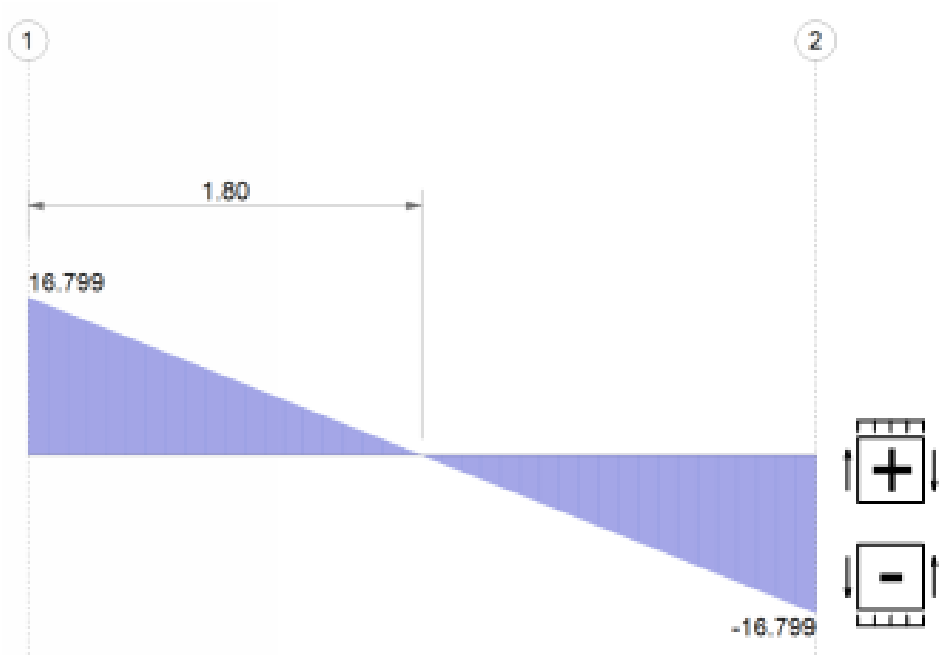

Figure 8.26: Level 1NP Shear Diagram from Simple Span Condition (kN/m)

Slab 1NP Shear Capacity Check			
Factor	$C_{Rd,c}$	0.12	
Coefficient	k	1.96	
Reinf Ratio	rho	0.02	
Char Strength	f_{ck}	12	Mpa
Eff Width	B	198	mm
Reinf Depth	d	219	mm

Shear Force Intensity (Per Meter)			
Shear Design	$V_{Rd,c}$	97.8	kN
Shear Effect	V_{ed}	22.8	kN
Slab OK			

Table 8.15: Level 1NP Slab Capacity Check

8.4.2. Slab 2NP Analysis

The slab at level 2NP is the thinner of the two composite slabs. The ceramic inserts are still 30 centimeters wide and 15 centimeters deep (figure 27) and the framing will be considered as a T-beam. The slab is shown with two longitudinal bars and 5 mm diameter stirrups.

The moment diagrams in figure 8.28 and figure 8.29 show the bending moment intensity or moment per meter width in the continuous span condition and simple span condition, respectively. The maximum positive bending moment intensity from those diagrams is entered into table 8.16. Likewise, the shear diagrams of figure 8.30 and figure 8.31 express the shear force intensity or shear per meter width. The maximum shear is entered into table 8.17.

The slab is tension controlled because the steel reaches its yield point prior to the concrete and compression block does not extend into the stem of the T-beam (table 8.16). The slab has sufficient bending capacity and shear capacity (table 8.15). The concrete by itself has enough strength to resist all the applied load. Therefore, the slab is safe given the assumed minimum reinforcing parameters.

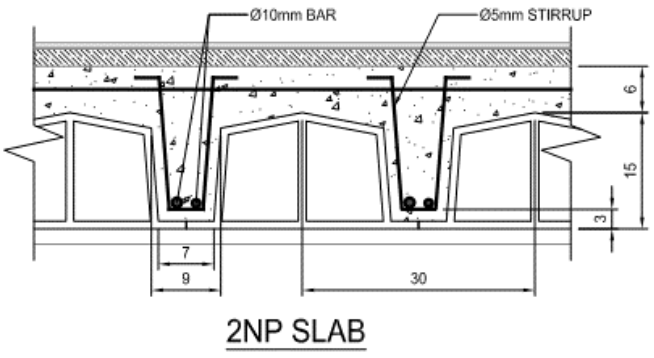

Figure 8.27: Level 2NP Slab Cross Section with dimensions in centimeters [16]

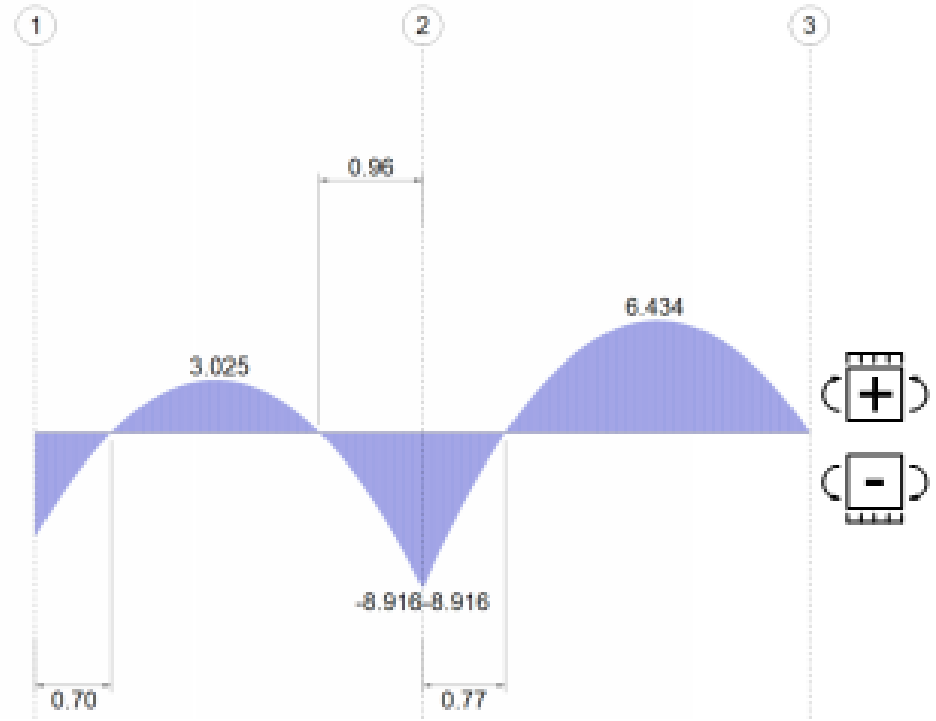

Figure 8.28: Level 2NP Moment Diagram from Continuous Reinforcement Condition (kN-m/m)

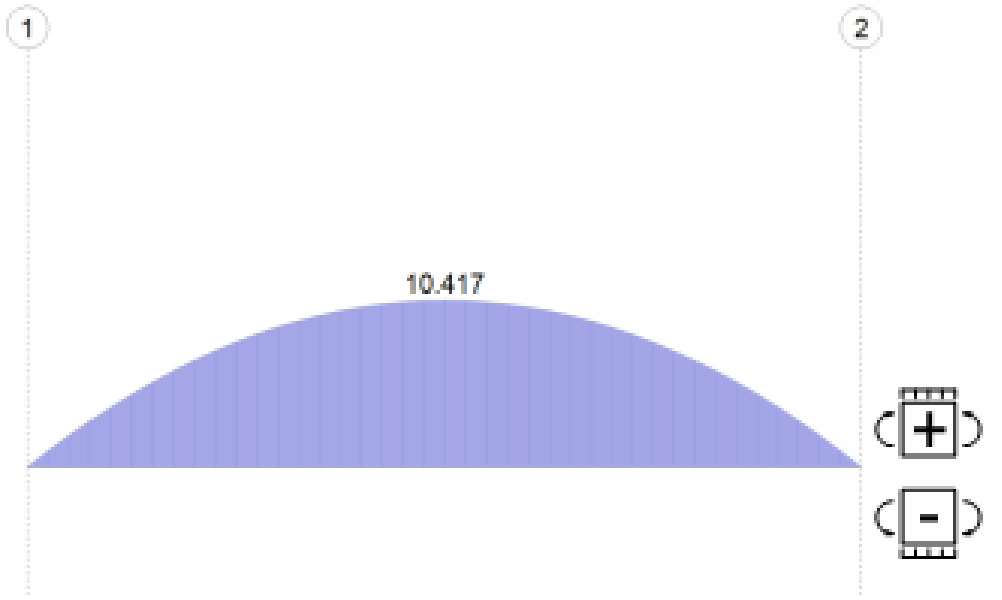

Figure 8.29: Level 2NP Moment Diagram from Simple Span Condition (kN-m/m)

Slab 2NP Concrete Reinforcement Capacity Check for 300 mm Section								
Thickness	t	210	mm	Concrete	Characteristic Strength	fck	12	MPa
Trans Bar Thk	d_t	6	mm		Partial Safety Factor	γc	1.5	
Cover	c	25	mm		Design Strength	fcd	8	MPa
Reinf Depth	d	179	mm		Youngs Modulus	Ec	21	GPa
Width	b	300	mm	Steel	Characteristic Strength	fyk	180	MPa
Area of Steel	As	157	mm2		Partial Safety Factor	γs	1.15	
Comp Height	λ	0.8			Design Strength	fyd	157	MPa
Eff Strength	η	1			Youngs Modulus	Es	210	GPa

Set Internal Forces Equal at Steel Yield Point								
Conc Strain	ε_{cu3}	0.17	%	Internal Forces	Compression Force	Fc	25	kN
Steel Strain	ε_{ud}	2.25	%		Tension Force	Fs	25	kN
Neutral Axis	x	13	mm		Moment Arm	z	174	mm
Comp Block d	a	10	mm		Moment Capacity	M	4	kN*m

Bending Moment Intensity (Per Meter)			
Unit Moment Capacity	M_{Rd}	14.24	kN*m
Max Moment Continuous	M_{ed}	6.43	kN*m
Max Moment Simple Span	M_{ed}	10.4	kN*m
Slab OK			

Table 8.16: Level 2NP Slab Bending Capacity Check

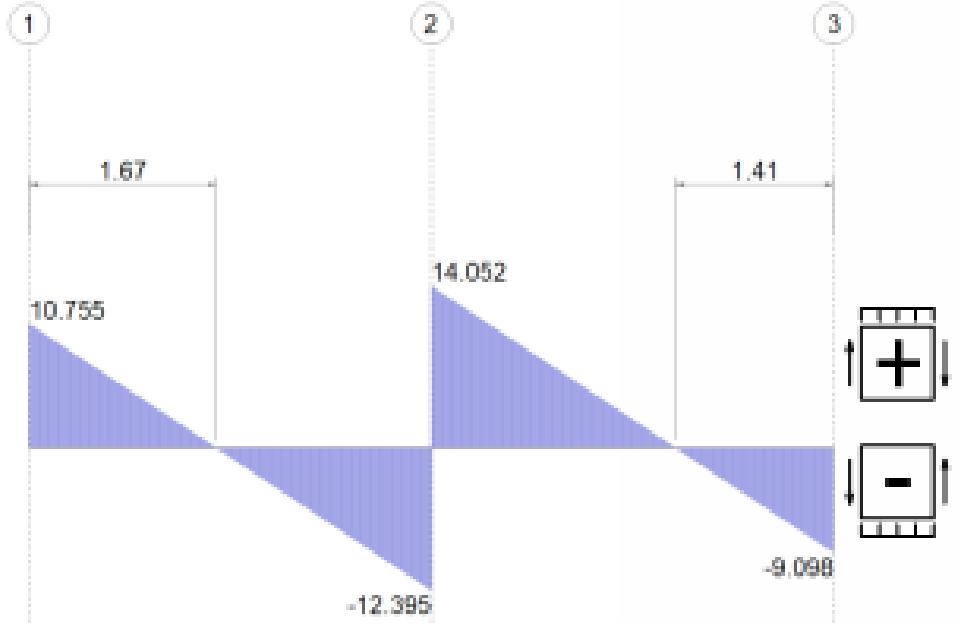

Figure 8.30: Level 2NP Shear Diagram from Continuous Reinforcement Condition (kN/m)

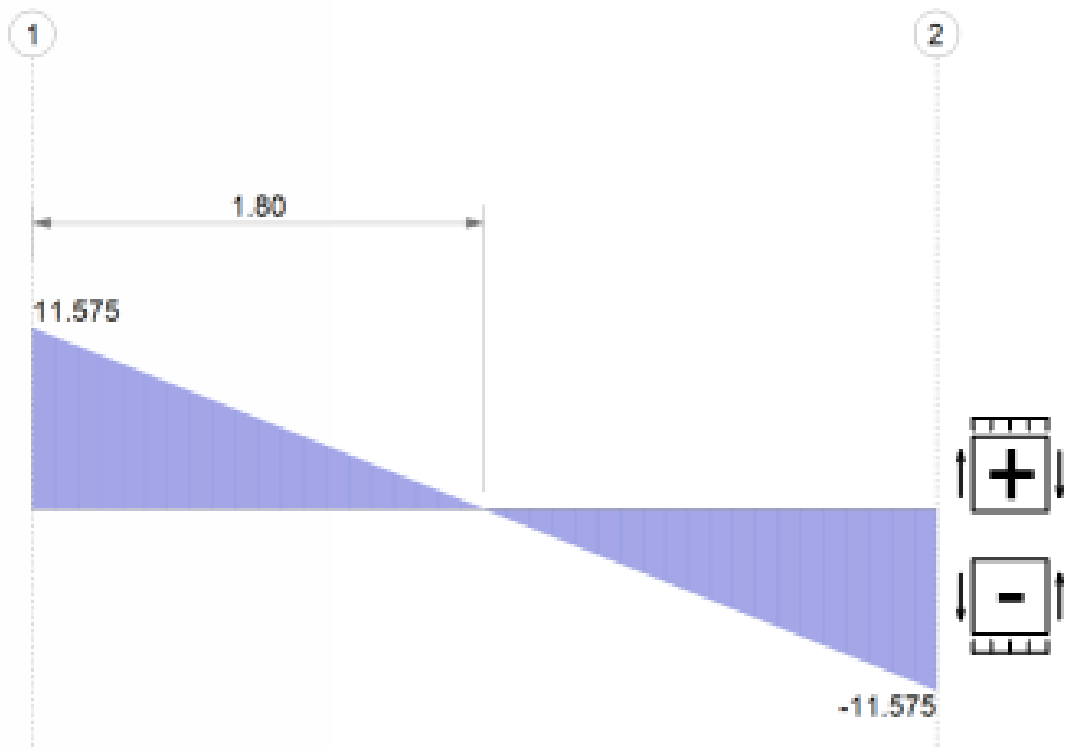

Figure 8.31: Level 2NP Shear Diagram from Simple Span Condition (kN/m)

Slab 2NP Shear Capacity Check			
Factor	$C_{Rd,c}$	0.12	
Coefficient	k	2.06	
Reinf Ratio	rho	0.02	
Char Strength	f_{ck}	12	Mpa
Eff Width	B	175	mm
Reinf Depth	d	179	mm

Shear Force Intensity (Per Meter)			
Shear Design	$V_{Rd,c}$	74.3	kN
Shear Effect	V_{ed}	14.1	kN
Slab OK			

Table 8.17: Level 2NP Slab Capacity Check

9. CONCLUSIONS AND RECOMMENDATIONS

9.1. Conclusions

As can best be determined from the evaluation completed, the fundamental structure of Fuchs Café building is adequate if all assumptions are validated. Pending further investigation and analysis, the building appears to be suitable for use in modern day. The building has some locations of moderate damage, but these tend to be localized and simple to resolve. In particular the a complete damage assessment but be completed on the shell of the building to identify all damage that is currently hidden.

This building and project is a good example of how if the different groups can come together and work towards a goal, the people can benefit. This building is an example of a distinctive architectural style that is hidden in plain view. It would be easy for someone to walk by it today and not have an appreciation for it. However, if the owner is willing to invest in it and conservationists are able to develop public support, it is up the conservation design team to thoroughly, affordably and creatively ensure the safety of the building.

If this project is completed, Fuchs' and Steigenhofer's legacy can live on the way they had intended, as a gathering place for the people of Prague.

9.2. Recommendations

The basis for these recommendations is that there are known and unknown inadequacies within the building that need to be addressed. The visible deterioration will have detailed solutions to directly address the damage. The second set of recommendations involve testing methods to be used to identify useful information for further evaluation. Maintenance recommendations will also be included.

9.2.1. Repairs

9.2.1.1. Level 1NP Slab Damage

There is clearly damage to the level 1NP slab north of column line 1, the full extent of which is not known at this time. The damage, likely due to water infiltration, is visible from below in the form of areas of missing ceiling plaster, areas of an apparent repair coating and temporary wood shoring supporting the slab. First, an assessment of the slab must be done to determine the severity of the damage. This can be done simply by using sonic testing to determine the depth of the concrete that is sound. Alternately, more advanced techniques such as x-rays or ground penetrating radar can be used to get a more detailed picture of the inside of the slab.

The first intervention that must be done is to provide a waterproof coating on the top of the concrete slab to prevent future water infiltration. This can be achieved by using a waterproof paint or by applying a membrane to the slab.

If from the testing, the concrete itself is sound, but the ceramic inserts are unstable, then a steel reinforced grout (SRG) system should be used to secure them in place. The ceramic inserts acted as a formwork while the concrete was poured. However, they were supported from below by temporary construction shoring, and once that shoring was removed, the bond between the concrete and ceramic is what holds the ceramic in place. If that bond is compromised by either water deteriorating the bond or by movement in the concrete, the ceramic inserts could collapse. To remedy that potential issue, a layer of SRG can be applied to the underside of the slab. The procedure would entail removing all ceiling plaster of the damaged area, about one meter beyond the at-risk inserts. Placing a sheet of steel mesh on the surface of the slab and then applying a layer of grout to the mesh. This would transfer support for the damaged tiles to a more sound portion of the slab.

If the testing confirms that the steel reinforcement is damaged, corroded or simply detached from the concrete, carbon fiber reinforced polymers (CFRP) can be applied to reinforce the slab (figure 9.1). Externally bonded CFRP strips can be a simple non-invasive way for the slab to regain its tensile strength. The reinforcing should be applied parallel to the slab span, at the joint between ceramic inserts, where the full depth concrete is, and along the entire span of the slab. Once again, the surface would need to be prepared by removing the plaster ceiling. Then a coating of adhesive must be applied and layers of CFRP strips added, adding more adhesive between each layer, ensuring the CFRP is hydrated [24].

Figure 9.1: Example of CFRP slab reinforcement [25]

If it is discovered that the damage is so severe, that the slab is at risk of collapse, immediate action must be taken to fully shore the structure. Then the recommended course of action would be to replace the slab. Czech companies like Heluz make modern versions of ceramic slabs (figure 9.2). The repair procedure would be to install temporary supportive shoring to all walls, above and below, that are connected to the slab. Then all existing concrete and ceramic will be demolished. The slab is to be demolished from the support on the exterior wall to the centerline of the concrete beam. Next, formwork shall be constructed to support the new ceramic. All connections between the slab and adjacent structural members need to be detailed and installed. This would entail drilling into the existing concrete and embedding new reinforcing bars from the existing concrete to the new slab. Longitudinal reinforcing steel and then concrete will be added. Once the concrete reaches a minimum strength, all formwork is well be removed.

Figure 9.2: Heluz Miako composite ceramic concrete slab schematic [26]

9.2.1.2. Damage from Previous Minor Destructive Testing

When the probe testing was conducted in 2015, concrete from 14 different structural elements was removed to expose the reinforcing steel within. These penetrations were never repaired, so now five years later, the rebar is still exposed. If left unprotected long term, the steel could corrode and then lose cross sectional area or begin to crack the nearby concrete. The procedure to repair would be to remove any remaining loose concrete in the area and thoroughly clean the steel. Then place new concrete in the area to fill the void, enabling the beam or column to return to its original geometry. It is recommended to use C16/20 concrete as it will have a similar compatibility with the existing concrete. If the new concrete is too strong, it could damage the adjacent historic concrete.

9.2.1.3. Shear Capacity Strengthening, If Necessary

In section 8.2, it was discovered that some of the beams analyzed fail the concrete shear capacity check and that size and spacing of the shear reinforcing was needed to complete the assessment. If the rebar is analyzed and the beam truly does fail the concrete shear capacity check, then the beam will need to be strengthened. This could be achieved by using externally bonded GFRP “stirrups” (figure 9.3). The installation procedure is similar to the GFRP installation in section 9.2.1.1.

Figure 9.3: GFRP shear beam reinforcing [26]

9.2.1.4. Exterior Wall Repair

The exterior walls have been extensively modified throughout the years and are currently covered. It is expected that the condition of the concrete within may be deficient. If that is the case, there are different levels of interventions that can be done.

If the damage is minor, like cracking or minor spalling, an SRG system can be put into place, in the location of the damage. The installation of which is discussed in section 9.2.1.1.

If the damage is moderate, like localized damage that extends the entire thickness of the wall, existing concrete can be removed while new concrete is put in its place, as described in section 9.2.1.2.

If the condition of the wall is severe, it would be necessary to remove the existing concrete wall and replace it with a new system. Depending the location, different systems could be used, ranging from cast-in-place concrete, precast concrete wall panels, or non-concrete system.

Regardless of the extent of damage and solution, the existing wall needs to be protected from the rain, snow and ice. It is imperative for the sustainability of the walls to keep water and moisture out.

9.2.2. Testing

As was mentioned previously, the lack of complete information about the building presents an obstacle to completing a full analysis. To rectify this, a full regimen of testing must be completed on the building. There are three areas of focus for the testing to be done including material testing, element composition and damage identification.

As previously discussed, the building was constructed in two phases with different concrete qualities. The objective of this testing is to determine where there is higher strength concrete and the locations of the lower quality concrete. This test can be performed using a Schmidt Hammer test. This method determines the hardness of the concrete and converts that, using previous testing data, to concrete strength. The test should be conducted in several locations and on several different types of element to find a pattern. The Schmidt Hammer test is a relative quick and simple test to conduct so the intention is to test 5-10 locations per level of the building.

For the element composition test, the goal is to find the precise element dimensions and reinforcing steel locations and sizes within. A probe test could be performed as a minor destructive test as has been used in the past. However, if available an X-ray test or ground penetrating radar examination could be conducted. These tests can identify the internal structure of a member in a non-destructive manner. The purpose of this test is to find complete data on currently unknown elements, like walls, slabs and beams. This data could also be used to validate assumptions made earlier like the slab reinforcement and to identify the shear reinforcement of the beams from section 8.2.

The damage identification testing is to determine further locations of unsound concrete. This test can be performed with sonic testing or by striking a member with a hammer and listening for different sounds if there is a crack or damage. The elements of particular interest are the building enclosure elements like the exterior walls and slabs. Therefore, most of the tests occur on level 1NP because that area of slab is the most vulnerable to damage.

To show the locations of interest for the testing, see figure 9.4, figure 9.5, figure 9.6 and figure 9.7 for the locations and types of tests to be performed.

9.2.3. Maintenance

The key to avoiding deterioration of a building is to perform proper maintenance. Maintenance is one of the more difficult procedures to convince an owner to perform on an ongoing basis as it requires funding when there are not typically major problems. Fixing a small issue now with a cheap repair could be preventing major reconstruction in the future if the damage is allowed to spread unmitigated.

Most of the issues found within Fuchs Café involve improper maintenance throughout the lifespan. The most visible damages are because of water damage to the shell of the building, the slabs and walls. It is important to ensure that the building remains waterproof. This means repairing the waterproofing system immediately if there is any damage. Any water the infiltrates the building will get exponentially worse when the temperatures freeze. The freeze thaw cycle can destroy concrete if the water gets within the concrete.

Furthermore, all renovations and repairs need to be done in a careful and legitimate way. Historic buildings are sensitive, so any alterations need to be studied carefully. All work performed on the building should be performed by people with expertise in historic concrete.

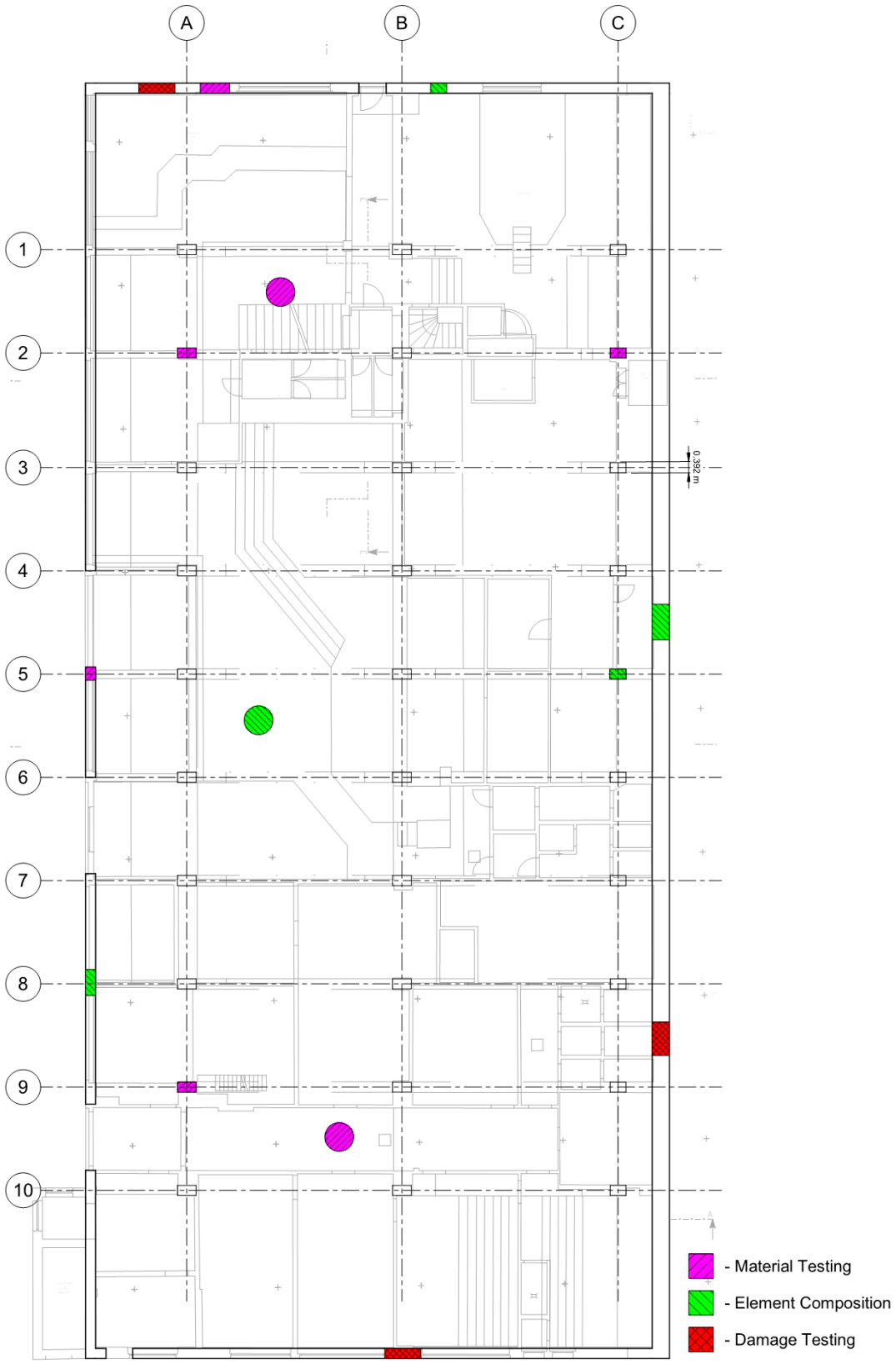

Figure 9.4: Level 1PP Testing Locations

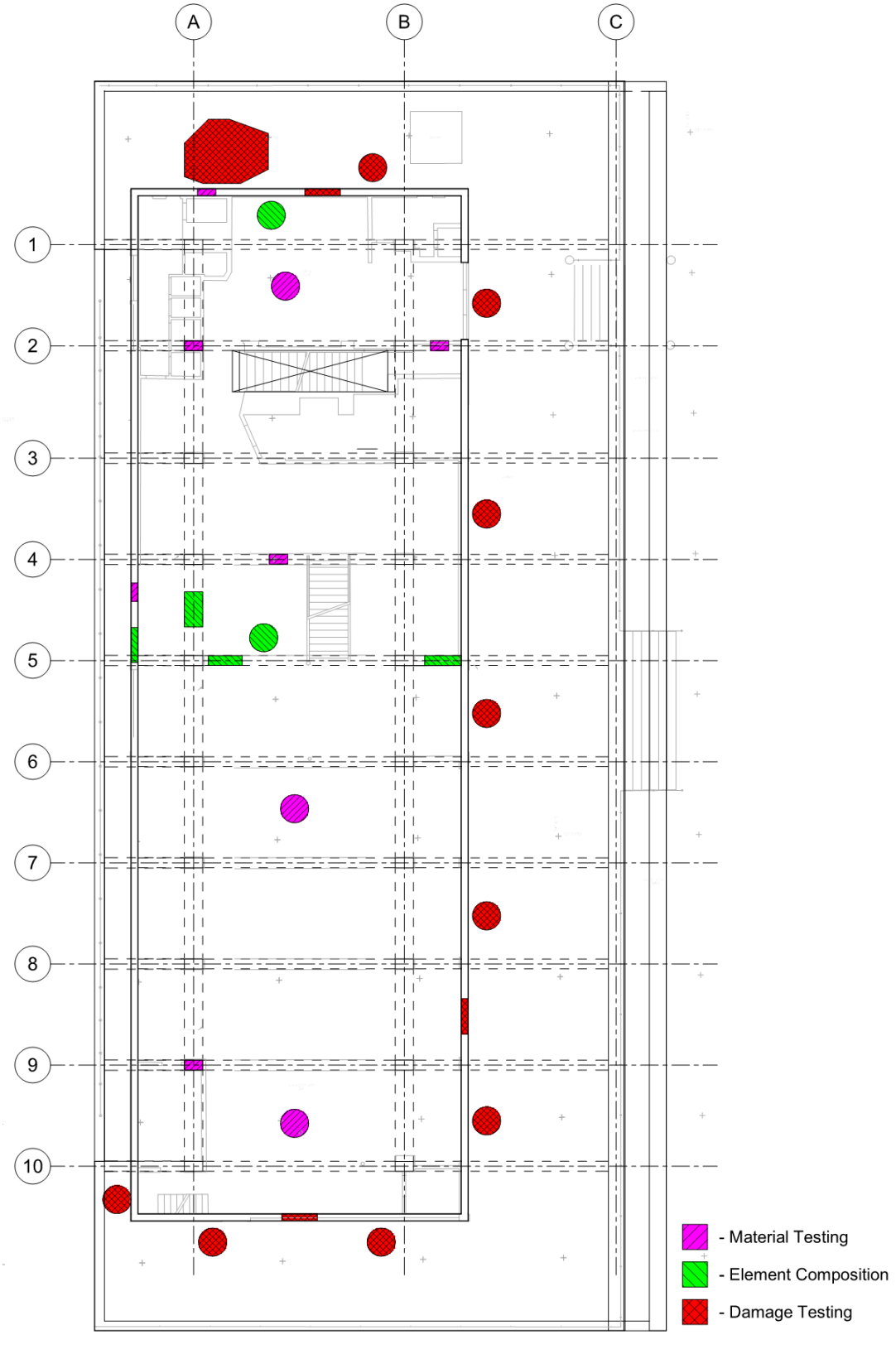

Figure 9.5: Level 1NP Testing Locations

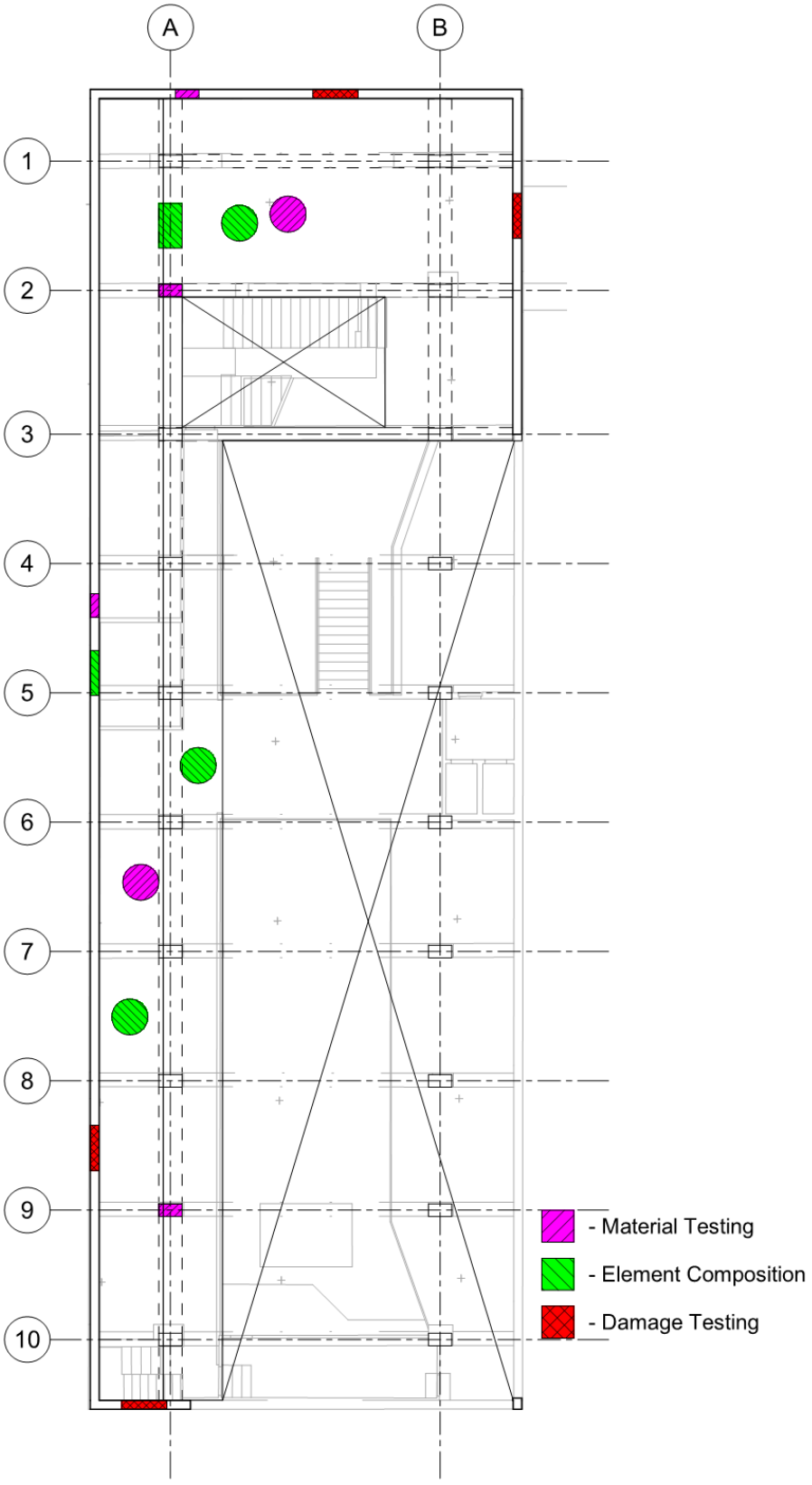

Figure 9.6: Level 2NP Testing Locations

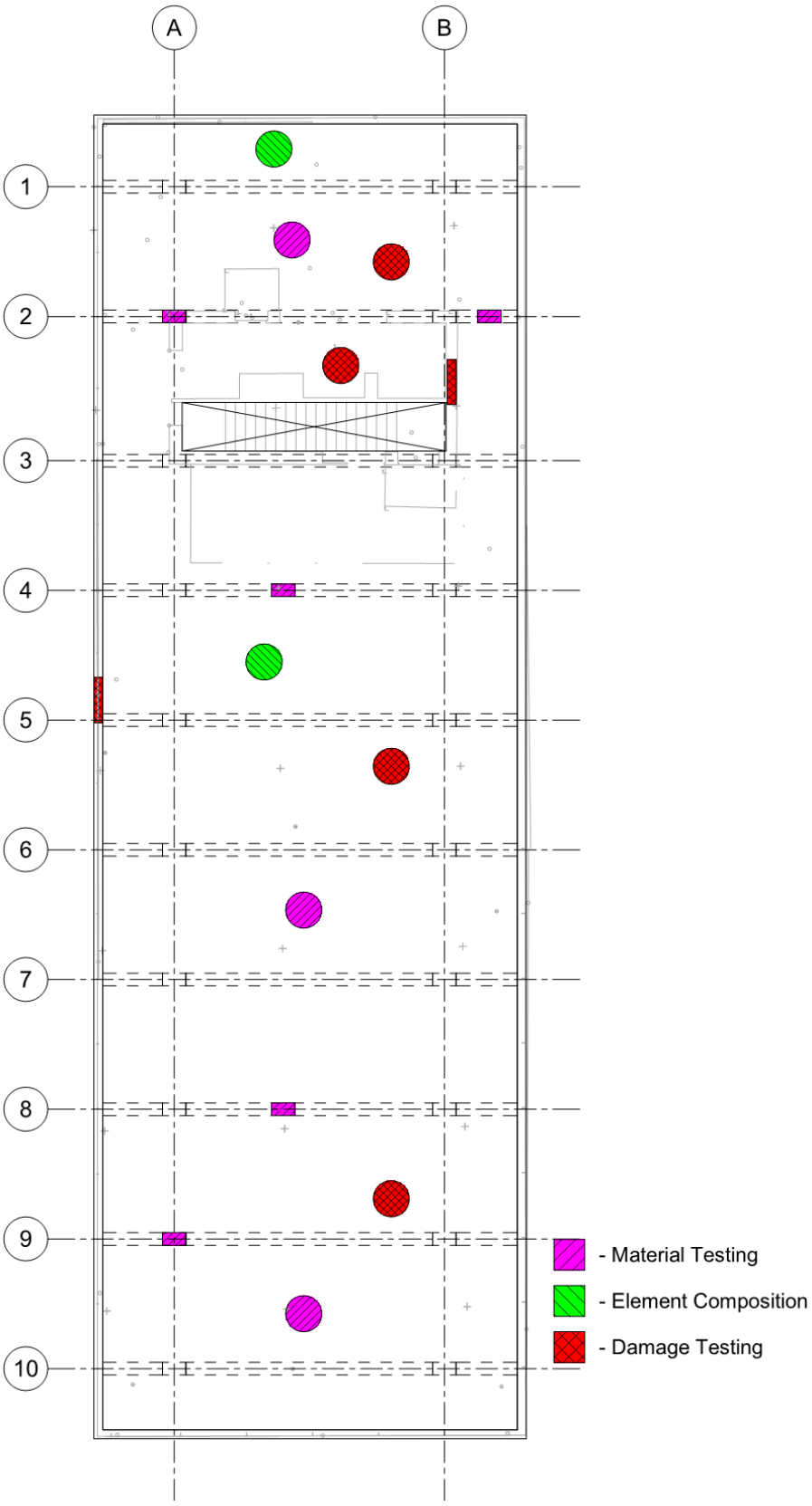

Figure 9.7: Level 3NP Testing Locations

10. BIBLIOGRPHY

[1] J. Kazimour and F. W. Carter, “Prague,” *Encyclopaedia Britannica*, 2020. https://www.britannica.com/place/Prague/Evolution-of-the-modern-city#accordion-article-contributors.

[2] T. Jirman and J. Stary, “Study of Technical of Construction and Parameters of Fuchs Cafe,” 2015.

[3] V. Neuberta, “Plán hlavního města Prahy,” *Municipal Library in Prague*, 1923. http://chartae-antiquae.cz/cs/maps/19887.

[4] K. Andre, “Viaduct Bei Prag,” 1854. https://en.wikipedia.org/wiki/Negrelli_Viaduct#/media/File:Negrelliho_viadukt_v_Karlíně,_lept,_1854.jpg.

[5] Unknown, “1920 Olympics Czechoslovakia Ice Hockey Team,” 1920. https://commons.wikimedia.org/wiki/File:1920_Olympics_Czechoslovakia_Ice_Hockey_Team.jpg.

[6] None, “Olympic Results,” *Olympics*, 2020. https://www.olympic.org/olympic-results.

[7] “1925 European Championships,” *Hockey Archives*, 1925. .

[8] O. Tyl and J. Fuchs, “Veletržní palác; Palace of the Prague Sample Fairs in Prague,” *ArchiWeb*, 1924. .

[9] J. JavĤrek, V. Thiele, and M. Nováková, “Usability Study of Fuchs’ Cafe,” 2015.

[10] J. K. Wight and J. G. MacGregor, *Reinforced Concrete; Mechannics and Design*, Fifh Editi. Pearson Prentice Hall, 2009.

[11] P.-C. Chang and A. Swenson, “Construction,” *Encyclopaedia Britannica*, 2020. https://www.britannica.com/technology/construction/Early-steel-frame-high-rises#ref60135 (accessed Jul. 02, 2020).

[12] E. Bajart, “Maison François Coignet,” *Wikipedia*, 2020. https://en.wikipedia.org/wiki/François_Coignet#/media/File:Maison_François_Coignet_2.jpg.

[13] Unknown, “Bohumil Steigenhofer,” *International Hockey Wiki*, 2020. https://internationalhockey.fandom.com/wiki/Bohumil_Steigenhofer.

[14] Unknown, “Latvia,” *International Hockey Wiki*, 2020. https://internationalhockey.fandom.com/wiki/1933_World_Ice_Hockey_Championships.

[15] Unknown, “1947 World Hockey Championships,” *International Hockey Wiki*. https://internationalhockey.fandom.com/wiki/1947_World_Ice_Hockey_Championships.

[16] L. Dostál and Z. Potužák, “Report on the Construction Technical Survey of Fuchs Cafe Building,” 2015.

[17] J. Paul, *Železový beton v pozemním stavitelství II*. 1958.

[18] W. H. Price, “Factors Influencing Concrete Strength,” *ACI J. , Proc.*, vol. 47, no. 6, pp. 417–432, 1951.

[19] P. Klieger, “Effect of Mixing and Curing Temperature on Concrete Strength,” *ACI J. , Proc.*, vol. 54, no. 12, pp. 1063–1081, 1958.

[20] European Committee for Standardization, *Eurocode 2: Design of Concrete Structures - Part 1-1: General Rules and Rules for Buildings; EN 1992-1-1*, vol. 1. 2004, p. 227.

[21] European Committee for Standardization, *Eurocode - Basis of Structural Design - EN 1990*. 2002.

[22] Z. Jechumtálová and J. Šílený, “Seismic loading of the Industrial Zone Triangle,” 2014.

[23] European Committee for Standardization, *Eurocode 1 - Actions on Structures - Part 1-3: General Actions - Snow Loads - EN 1991-1-3*. 2003.

[24] J. Sena Cruz, “Repair and Strengthening Techniques.” 2020.

[25] Sanax, “CarboLamela,” 2020. https://www.sanax.cz/produkt/carbolamela-s.

[26] Heluz, “Miako,” 2020. https://images.app.goo.gl/gUSnr3Cks27tumzs5.